

Functionalized Polymers and Surfaces via Ring-Opening Metathesis Polymerization

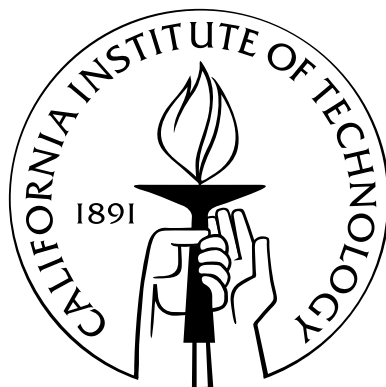
Thesis by

Isaac Michael Rutenberg

In Partial Fulfillment of the Requirements

for the Degree of

Doctor of Philosophy



California Institute of Technology

Pasadena, California

2005

(Submitted August 13th, 2004)

© 2005

Isaac Michael Rutenberg

All Rights Reserved

Acknowledgements

I would like to thank the following people, all of whom have played important roles in my journey through Caltech.

Professor Robert H. Grubbs (i.e., "Bob") has provided the opportunity and the support (moral and financial!) that have allowed me to pursue my own path in becoming a competent research chemist. I am also grateful to Bob for showing me that serious chemistry need not always be taken so, well, seriously. In addition to Bob, I thank the remaining members of my Committee - Prof. William A. Goddard III (Chairman), Prof. Dennis Dougherty, and Prof. James Heath.

Dr. (now Professor) Zhenan Bao and Professor Chad Mirkin have been extremely supportive, and have allowed me to gain experience in a variety of fields that may not have otherwise been accessible. Good luck to Prof. Bao with her new position on the faculty of Stanford.

For their invaluable friendship and generosity over the past four years, I would especially like to thank Oren A. Scherman and his wife, Cora Iberkleid.

Collaborating students have been particularly kind and helpful; many thanks to Tae-Lim Choi and Weirong Jiang. Xiaogang "Bruno" Liu has been very helpful in seeing that the collaboration with the Mirkin group at Northwestern University runs smoothly. I am grateful to have him as a colleague and for his continued updates on the SI-ROMP project!

The following people have been instrumental in helping me to learn "tools of the trade": Dr. Hyunjin Kim, Dr. Andreas Killbinger, Dr. Steve Goldberg, Dan Sanders, Dr. Stu Cantrill, Dr. Choon Woo Lee, Dr. Todd Younkin, Dr. J.P Morgan, Dr. Brian Connell, Mona Shahgholi, and Tom Dunn.

I thank many people for their thoughtful and insightful comments, and for proofreading my papers, proposals, and thesis. These people include Dr. Brian Connell, Andy Hejl, Dan Sanders, Dr. Anna Wenzel, and Dr. Anatoly Chlenov.

There are many other people with whom I've interacted over the past four years, and I would be remiss if I did not pay my respects to the Grubbs group at large. Thank you all for helping, being patient, and teaching me. I could not have asked for a more friendly environment in which to work, and this is in large part due to the students and postdocs. Logistical support provided by Dian Buchness, Anne Penney, Joe Drew, Steve Gould, and Larry Martinez is appreciated.

On a personal note, I would like to thank Bill and Delores Bing (Band and Chamber music directors, respectively), and Robert Dirks (for teaching me bridge, keeping me "well-rounded" with numerous game nights, and simply being a great friend). Special thanks to the Diener family for welcoming me into their lives without reservation. Having a surrogate family here has allowed California to become comfortable, as a home should be. Donna, Jim, Josh, Joe and the extended family have been simply amazing, and I would not have wanted to live here without them. Thank you, and may the future be bright for each of you! My sincere appreciation also goes to the Kamau family for welcoming me as a son.

My brother and sister, Ben and Naomi Rutenberg, and my soon-to-be sister-in-law, Nguyen Vu, each deserve many thanks for helping me to remember that I have a place, not too far from here, where I can always go and fit in just like a member of the family (because that's what I am!).

Most importantly, and in no particular order, I thank Wanjiru, whom I will marry on August 21st, my mother, who has become my best friend, my father, who has shaped me in so many ways, and Murray, who is all of the above in one amazing package. These individuals I thank for their unconditional love, support, and tolerance. Emphasis on the "tolerance" part.

Thanks, everyone!

Abstract

The research presented in this thesis focuses on the preparation of functionalized polymers using olefin metathesis polymerization methods. A portion of this research is also devoted to the development of applications for metathesis-derived polymers.

Three distinct types of olefin metathesis polymerizations can be recognized within this work. Ring-opening metathesis polymerization (ROMP) is the most prevalent type, followed by acyclic diene metathesis (ADMET) polymerization and a hybrid of the ROMP and ADMET mechanisms known as ring-opening-insertion metathesis polymerization (ROIMP).

Many of the concepts that appear throughout this thesis are introduced in Chapter 1. Olefin metathesis occupies a central role in each of the subsequent chapters; detailed descriptions of the mechanism and important olefin metathesis catalysts are provided. The chapter also includes background information regarding polymers, polymer properties and the application of ROMP in the construction of electronic devices.

Although the utility of ADMET does not yet seem to match that of ROMP, valuable information can be obtained from ADMET polymerizations. In an effort to elucidate catalytic activity, Chapter 2 details a comparison of the ADMET polymerizations of terminal and non-terminal dienes.

Experimental investigations involving ROIMP, a novel method for the production of A,B-alternating copolymers, is presented in Appendix A. The mechanism of ROIMP is conceptually very different from the mechanisms of either step growth

or chain growth polymerizations. Efforts toward understanding the mechanism of ROIMP using a mathematical model are discussed in Chapter 3.

Polymeric chain transfer agents (PCTAs) suitable for ROMP reactions are polymers that contain a single, metathesis-active olefin. These polymers are the focus of Chapter 4 and can be used in the preparation of novel block copolymers. As an example, Appendix B presents the preparation of block copolymers consisting of polyacetylene and various commodity polymers.

Finally, the development of applications for surface-initiated ROMP (SI-ROMP) is discussed in Chapter 5 and Appendix C. Polymer films prepared using SI-ROMP are shown to be viable dielectric layers in thin-film transistors, and research is presented involving microcontact printing and dip pen nanolithography as methods for forming patterned SI-ROMP polymer films.

Contents

Acknowledgements	iii
Abstract	v
1 Introduction	1
1.1 Polymers and Polymer Properties	2
1.2 Olefin Metathesis	3
1.3 Polymerizations	5
1.4 Electronic devices	8
References Cited	10
2 Acyclic Diene Metathesis (ADMET) Polymerization Using a Ruthenium Olefin Metathesis Catalyst Coordinated with a N-Heterocyclic Carbene Ligand	12
2.1 Abstract	13
2.2 Introduction	13
2.3 Experimental	15
2.4 Results and Discussion	16
2.5 Conclusion	19
References Cited	20
3 Understanding Ring-Opening-Insertion Metathesis Polymerization: Mathematical Models of Insertion Polymerizations	21
3.1 Abstract	22

3.2	Introduction	22
3.3	Results and Discussion	25
3.4	Conclusions	31
	References Cited	32
4	Development of Polymeric Chain Transfer Agents for Use in Ring-Opening Metathesis Polymerizations	33
4.1	Abstract	34
4.2	Introduction	34
4.3	Results and Discussion	37
4.3.1	Synthesis of Asymmetric PCTAs	37
4.3.2	Synthesis of Symmetric PCTAs	37
4.3.2.1	Coupling of Pre-formed Polymers	38
4.3.2.2	Generating Symmetric PCTAs in situ	40
4.3.3	The Use of PCTAs in ROMP	46
4.4	Conclusions	50
4.5	Experimental	51
	References Cited	53
5	Patterned Polymer Layers Using Surface-Initiated Ring-Opening Metathesis Polymerization	55
5.1	Abstract	56
5.2	Introduction	56
5.3	Results and Discussion	59
5.3.1	Electronic Devices Using SI-ROMP	59
5.3.2	Patterning of SI-ROMP Layers	66
5.4	Conclusions	71
5.5	Experimental Section	71
	References Cited	75
	Appendices	76

A Synthesis of A,B-Alternating Copolymers by Ring-Opening-Insertion Metathesis Polymerization	76
A.1 Abstract	77
A.2 Introduction	77
A.3 Results and Discussion	79
A.4 Conclusion	83
A.5 Experimental	83
References Cited	86
B Direct Synthesis of Soluble, End-Functionalized Polyenes and Polyacetylene Block Copolymers	87
B.1 Abstract	88
B.2 Introduction	88
B.3 Results and Discussion	91
B.3.1 Synthesis of Soluble Polyenes	91
B.3.1.1 Characterization of Soluble Polyenes	94
B.3.2 Synthesis of PA-containing Block Copolymers	98
B.3.2.1 Characterization of Block Copolymers	101
B.4 Conclusions	106
B.5 Experimental Section	107
B.6 Acknowledgements	110
References Cited	111
C Synthesis of Polymer Dielectric Layers for Organic Thin-Film Transistors via Surface-Initiated Ring-Opening Metathesis Polymerization	113
C.1 Abstract	114
C.2 Introduction	114
C.3 Acknowledgements	120
References Cited	121

List of Figures

1.1	Olefin metathesis – a carbon-carbon double bond shuffling reaction . .	3
1.2	Reactivity of metals used in olefin metathesis	4
1.3	Ruthenium olefin metathesis catalysts	4
1.4	Types of olefin metathesis reactions	5
1.5	Schematic diagrams of electronic devices	9
2.1	Ruthenium olefin metathesis catalysts	14
2.2	Plot of molecular weight vs. time	18
3.1	Definitions used for ROIMP model	26
3.2	Insertion polymerization mechanisms	26
3.3	Degree of polymerization vs. conversion for M1	27
3.4	Plots of molecular weight distribution at various conversions for mechanism M1	29
3.5	Important reactions for mechanism M2	30
4.1	Ruthenium olefin metathesis catalysts	36
4.2	Preparation of a symmetric polymer using ring-opening polymerization	38
4.3	Preparation of symmetric PCTA: coupling	39
4.4	Formation of polystyrene dimer	45
4.5	ROMP of cyclooctene with PCTA	46
4.6	ROMP of cyclooctadiene PCTA	47
5.1	Example I/V diagrams for an FET	58
5.2	Catalysts and linkers for SI-ROMP	58

5.3	Variation in polynorbornene film thickness with monomer solution concentration	61
5.4	Secondary metathesis reaction producing non-surface-bound polymer	62
5.5	Variation in poly(DCPD) film thickness with monomer solution concentration and polymerization time	63
5.6	Polynorbornene films as produced by SI-ROMP	64
5.7	Polynorbornene films after annealing	65
5.8	AFM images of patterned polynorbornene layers produced by μ CP . .	68
5.9	AFM images of polymer patterns produced by μ CP	69
5.10	AFM images of poly(COT) patterns produced by DPN	70
A.1	Ruthenium olefin metathesis catalyst	78
A.2	NMR data for a ROIMP product	81
B.1	Ruthenium olefin metathesis catalysts	90
B.2	Chain transfer agents	93
B.3	^1H NMR spectrum of telechelic polyene	95
B.4	UV-Vis spectrum of telechelic polyene	96
B.5	FT-IR of telechelic polyenes	97
B.6	MALDI-TOF MS spectrum of telechelic polyene	97
B.7	Olefin-terminated polymers	99
B.8	UV-vis spectra of PA-containing block copolymers in CH_2Cl_2 solution	102
B.9	FT-IR spectra PA- <i>b</i> -PMMA block copolymer and PMMA	103
B.10	Tapping Mode AFM images	106
C.1	Catalysts and linkers for SI-ROMP	115
C.2	Current-voltage characteristics of an FET produced by lamination . . .	118
C.3	Current-voltage characteristics of an FET produced by direct deposition	119

List of Schemes

1.1	Chauvin mechanism of olefin metathesis	4
2.1	ADMET polymerizations with a ruthenium olefin metathesis catalyst	15
4.1	Preparation of a symmetric PCTA using ATRP	41
4.2	Preparation of a symmetric polymer using LAP	42
4.3	Attempted preparation of a symmetric PCTA using LAP	42
4.4	Competing reaction in LAP of styrene using 1,1-diphenylethylene . .	43
A.1	Proposed mechanism for ROIMP	78
C.1	Construction of an FET using a SI-ROMP polymer dielectric layer . .	116

List of Tables

2.1	Comparison of ADMET results between catalysts 1 and 2	17
2.2	ADMET polymerizations for various catalyst loadings	17
2.3	Temperature effects in ADMET polymerizations	18
4.1	Symmetric polystyrene PCTAs	45
A.1	Examples of ROIMP products, their A,B-alternations, molecular weights, and distributions.	80
B.1	Polyene yields vs. monomer/CTA and monomer/catalyst ratios . . .	92
B.2	Variation in composition of PA block copolymers.	100

Chapter 1

Introduction

1.1 Polymers and Polymer Properties

Polymer science is a field of chemistry that has had significant influence on the development of humankind throughout the past century. Today, millions of tons of plastic materials are produced each year, and the number of applications suitable for polymers (and polymers suitable for applications) continues to increase at a high rate.

The enormous investments of time and money that are made each year in polymer materials research demonstrate the importance that is placed upon technological advancements. Emerging fields such as nanotechnology, bioengineering, and "green" manufacturing rely heavily on advancements in polymer science, and there is seemingly no end to the scope of applications for which polymers are being investigated. For example, throughout the first half of the twentieth century, polymers were thought to exist exclusively as electrical insulators. The development of conducting polymers such as polyacetylene proved this to be untrue, and conducting polymers are beginning to find widespread use in a variety of electronic applications. Such is the importance of electrically active polymers that the pioneers in the field were recently awarded a Nobel Prize for their work.¹

The unique material properties of polymers accounts for the widespread interest in their development and application. For structural applications, polymers are often attractive because they are lightweight, moldable, flexible, and recyclable. Although these characteristics can also be found individually in traditional materials such as metals and ceramics, polymers display them all in one material that can also be relatively inexpensive. For more specialized applications, such as drug delivery and food storage, polymers are attractive often for these same properties, as well as being non-toxic and chemically inert. The wide diversity of attractive properties, from the processability of thermoplastic elastomers to the light emissivity of poly(phenylene vinylene)s, stems from an ability to control and vary the chemical and architectural composition of polymeric materials. This control, in turn, is the result of previously-made advances in the synthetic methods

and materials that are used in the preparation of polymers. Further advances in the next decades will undoubtedly carry polymeric materials into a wide range of heretofore unimaginable applications.

1.2 Olefin Metathesis

Metal-catalyzed reactions constitute an important class of the large number of known organic chemical transformations. Many of these reactions were discovered within the last 50 years, and research into their development continues apace. Olefin metathesis reactions are an example of this, and substantial progress has been made since their first literature reports in the 1950s.^{2,3} The development and improvement of catalysts and substrates for olefin metathesis have resulted in many new scientific and industrial applications.



Figure 1.1: Olefin metathesis – a carbon-carbon double bond shuffling reaction.

Olefin metathesis,² simply a rearrangement of carbon-carbon double bonds, can be represented by Figure 1.1.³ Initially, metal catalysts for the reaction were poorly defined metal salts often combined with alkylating agents (e.g., $\text{WCl}_6/\text{Bu}_4\text{Sn}$ or $\text{MoO}_3/\text{SiO}_2$), and the mechanisms for reactions using these catalysts were not well understood. Furthermore, these systems often suffered from a limited substrate scope and the necessity of harsh reaction conditions.

The development of homogeneous, well-defined catalyst systems for olefin metathesis has been key to the popularity of the reaction. As shown in Figure 1.2, the reactivity of the metal strongly influences the characteristics of the catalyst. Although initial metathesis catalysts were highly active, the oxophilic, early transition metals utilized for these catalysts were again limiting due to their incompatibility with many chemical functionalities. Catalysts based on late transition metals, such as **1**,⁴ are more tolerant of heteroatoms, and show substantial

	Titanium	Tungsten	Molybdenum	Ruthenium
Increasing Reactivity ↑	Acids	Acids	Acids	Olefins
	Alcohols, Water	Alcohols, Water	Alcohols, Water	Acids
	Aldehydes	Aldehydes	Aldehydes	Alcohols, Water
	Ketones	Ketones	Olefins	Aldehydes
	Esters, Amides	Olefins	Ketones	Ketones
	Olefins	Esters, Amides	Esters, Amides	Esters, Amides
	← Increasing Catalyst Reactivity Increasing Functional Group Tolerance →			

Figure 1.2: Reactivity of metals used in olefin metathesis.

promise in promoting olefin metathesis reactions in the presence of a variety of functionalities. Unfortunately, catalyst **1** suffers from decreased reactivity relative to early-transition metal based systems. The lower reactivity of ruthenium based systems, however, has recently been addressed with the development of catalysts such as **2**, which utilize N-heterocyclic carbene ligands.⁵ In many cases, the activity of catalyst **2** rivals or exceeds that of catalysts based on early transition metals.⁶

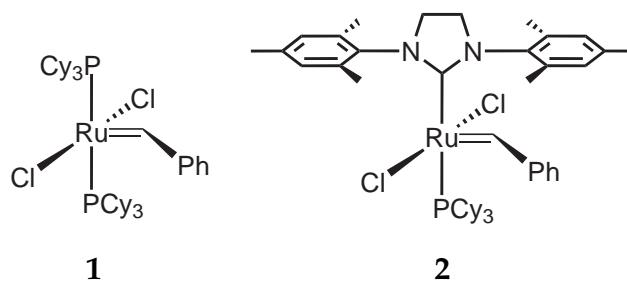
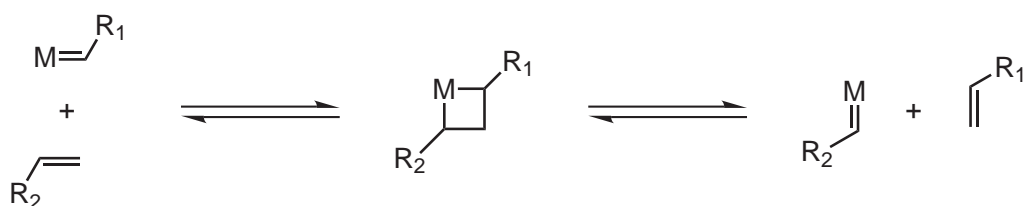


Figure 1.3: Ruthenium olefin metathesis catalysts.

Scheme 1.1: Chauvin mechanism of olefin metathesis.



The generally accepted mechanism for olefin metathesis is shown in Scheme 1.1.^{2,7} It is an equilibrium reaction, proceeding through a metallacyclobutane intermediate, that results in the interconversion of an olefin and a metal alkylidene. Through the use of different olefin geometries and reaction conditions, numerous olefin metathesis reactions are possible (Figure 1.4).⁸⁻¹³ For example, at low concentrations, α,ω -dienes can be used in ring-closing metathesis (RCM) reactions, while use of the same substrate in higher concentrations results in acyclic diene metathesis (ADMET) polymerization. The basis for much of the work reported in this thesis, ring-opening metathesis polymerization (ROMP) is a widely studied, highly versatile method of polymerization that utilizes strained, cyclic olefins.

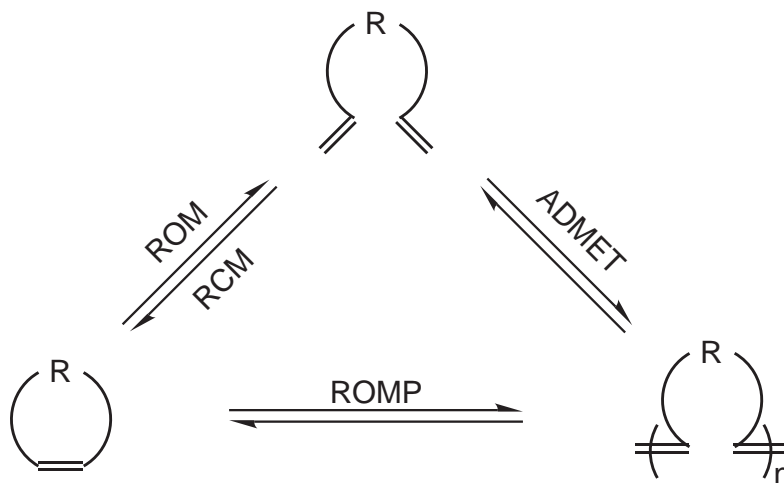


Figure 1.4: Types of olefin metathesis reactions.

1.3 Polymerizations

According to Gibbs Law (equation 1.1, where ΔH , ΔS , and ΔG are the changes in enthalpy, entropy, and Free Energy, respectively), a reaction will proceed only when ΔG is negative.

$$\Delta G = \Delta H - T\Delta S \quad (1.1)$$

Regardless of mechanism, all polymerization reactions link a large number of small molecules into a smaller number of larger molecules. This process is endoentropic ($\Delta S > 0$), because it decreases the number of degrees of freedom that are present in the system. Typically, the bond-forming reactions associated with a polymerization reaction are energetically favorable (i.e., exothermic, $\Delta H < 0$), and provide sufficient driving force to overcome the loss in entropy. Indeed, many polymerization reactions are so exothermic that heat dissipation becomes an important consideration upon scale-up of the reaction.

In the case of metathesis polymerizations, however, the polymerization reaction is simply an equilibrium-controlled rearrangement of carbon-carbon double bonds. The energy of the bonds that are formed in the polymerization is roughly equivalent to the energy of the bonds that are lost. As a result, released bond energy cannot account for the success of these polymerization. In the case of ROMP, the release of ring strain provides the driving force necessary to overcome the entropic barrier toward polymerization. This limits the monomer scope for ROMP reactions, as many cycloolefins (especially five-, six-, and seven-member rings) contain insufficient ring-strain to force the equilibrium of the reaction toward the ring-opened product.

Since ADMET polymerizations utilize cross-metathesis reactions between terminal olefins, the removal of the ethylene byproduct from the reaction vessel is typically used to shift the equilibrium of the reaction toward polymer product. This can be done via reduced pressure (i.e., the application of vacuum), which often precludes the use of solvent in the reaction. High viscosity due to the absence of solvent can be a limiting factor, as the efficiency of ethylene removal is critical toward the success and extent of polymerization. As a result, the products from ADMET polymerizations are typically limited to molecular weights of less than 30,000 g/mol, with corresponding limitations in their properties.

While ADMET polymerizations typically have physical limitations (e.g., viscosity and efficiency of ethylene removal), the success of ROMP reactions are more often determined by chemical limitations such as the compatibility of the

catalyst, monomer, and reaction conditions. Advancements in catalyst design, therefore, frequently result in corresponding advancements in the scope of ROMP with respect to new monomers or architectures. For example, catalyst **2** combines the functional group tolerance of other ruthenium-based metathesis catalysts with the high level of activity that is typified by early transition metal catalysts. As a result, the development of **2** not only allows, for example, the polymerization of cyclooctadiene at monomer:catalyst ratios of 100,000:1, but also allows such polymerizations to be carried out in the presence of numerous functional groups (present either in the monomer or in additives such as chain-transfer agents).⁶ Since it was first reported in 1999, numerous published journal articles indicate the wide variety of monomers and polymer architectures that can be produced with catalyst **2**.

The high activity of catalyst **2** toward propagation is unfortunately accompanied by relatively slow initiation.¹⁴ This is undesirable since control over the molecular weight distribution of the polymer product is best achieved by the reverse situation: fast initiation of the catalyst relative to the propagation step. Although there is little catalyst-derived control in polymerizations using **2**, the products from such reactions can be influenced by a number of other factors. For example, the addition of chain transfer agents allows for control over the molecular weight, as well as the endgroups of the polymer product.¹⁵ Such an approach has been used previously with small-molecule chain transfer agents to prepare potentially commercially important materials such as novel hydroxy-terminated poly(butadiene)s.¹⁶ This methodology is advanced further in Chapter 4, which describes recent efforts to develop polymeric analogues of traditional ROMP chain transfer agents, as well as in Appendix B, which describes a study into the synthesis of end-functionalized polyacetylene.

Exploitation of the activity and stability of **2** are further discussed in Chapter 3 and Appendix A, which describes the development of a highly generalized method for the preparation of alternating copolymers via ROMP. Unlike earlier catalysts, catalyst **2** was shown in previous reports to be reactive toward α,β -

unsaturated olefins. Furthermore, such olefins are able to insert into the olefins of certain cycloalkenes. By allowing this insertion reaction to occur between an α,ω -diene and a polyalkenamer (formed via ROMP either in situ or in a separate reaction), ring-opening-insertion metathesis polymerization (ROIMP) generates highly alternating copolymers in good yield. The mechanism of ROIMP is a unique hybrid of the more traditional step growth and chain growth polymerization methods. As such, it displays some of the advantages of each of these methods, and efforts to describe the ROIMP mechanism with a mathematical model are described in Chapter 3.

The decreased reactivity of the methylenide, relative to the benzylenide or alkylidene form of catalyst **2**, prompted a study into the ADMET polymerization of terminal and non-terminal dienes. The results of this study are presented in Chapter 2.

1.4 Electronic devices

Within the past 20 years, there has been rapid growth in both diversity and functionality of portable electronic devices. This growth has been supported by developments in the materials that are used in the electronics industry, and reciprocates by promoting further advancements in materials science. Although the size and material composition of electronic devices have changed considerably over the past several decades, the underlying principles of their operation have remained constant.

Perhaps the simplest of electronic devices, the parallel plate capacitor consists of two conductive plates separated by an insulating dielectric layer (Figure 1.5a). The device is used primarily for the storage of electrical charge; storage capacity (referred to as the device's capacitance) is determined by equation 1.2, where A represents the surface area of the plates, t represents their separation, k represents the dielectric constant of the dielectric material, and ϵ_0 represents a constant (permittivity of free space). When a voltage source is connected to the opposite

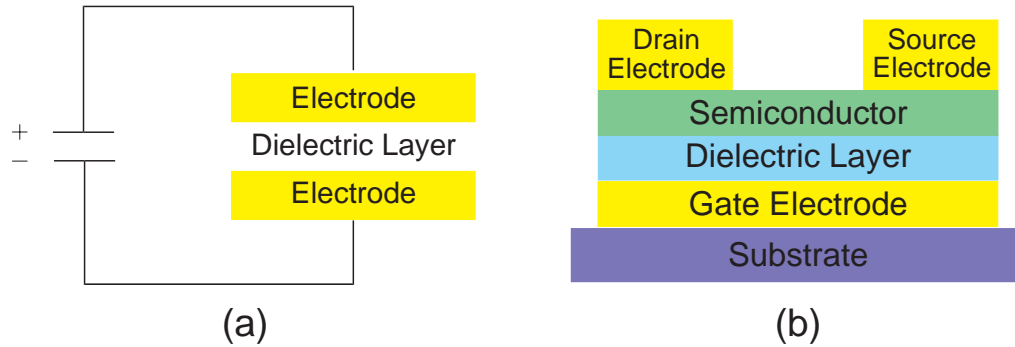


Figure 1.5: (a) Schematic diagram of a capacitor. (b) Schematic diagram of a top contact field-effect transistor.

plates of a capacitor, charges accumulate on the plates until the bias between them is equal to the applied voltage. After removing the voltage source, the capacitor can be discharged by placing a load across the plates. Conduction through the dielectric layer (a process known as "breakdown") occurs if the voltage between the capacitor plates exceeds the breakdown voltage of the dielectric material. To avoid this scenario, it is important for the breakdown voltage of a dielectric material to be higher than the working voltage of the capacitor.

$$\text{Capacitance} = \frac{\epsilon_0 * k * A}{t} \quad (1.2)$$

Equation 1.2 implies that a larger capacitance can be obtained by increasing the surface area of the plates, or by decreasing their separation. In cases where device geometry is constrained, however, capacitance can be affected only by changing the dielectric constant of the dielectric layer. This is typically done by changing the material itself; a wide range of dielectric materials are available, including metal oxides, organic polymers, paper, and air.

Transistors are solid-state devices that were first developed in 1947 at Bell Laboratories. Although a number of different transistor geometries are known, they are all primarily used to regulate or modify current flows in electronic circuits. Field-effect transistors (FETs) accomplish this task using an electric field to modify the conductivity of a semiconducting layer. The geometry of a top contact FET is

shown in Figure 1.5b.* In the operation of an FET, a voltage is applied between the gate and source electrodes. The dielectric layer allows transmission of the electric field that results from this voltage, while preventing electrical conduction between the electrodes. The electric field increases the charge density at the top and bottom of the (doped) semiconducting layer, and it is this concentration of charges that allows conduction between the drain and source electrodes.

In thin-film transistors (TFTs), each component layer is present as a thin layer of material. Most commonly used in flat-panel displays, TFTs can be constructed using a variety of conducting, semiconducting, and insulating materials. Recent research has allowed the preparation of transparent TFTs.¹⁷

Frequently, polymers are used as the dielectric layer in electronic devices such as capacitors and TFTs.¹⁸ Materials including polymethacrylates and polyimides have been incorporated and characterized. Relative to inorganic materials such as silicon dioxide, polymers are superior for their mechanical flexibility, low weight, and low cost. The standard approach for depositing polymer dielectric layers is by spin-coating a solution of the polymer in an organic solvent.

Chapter 5 and Appendix C are concerned mainly with the development of ROMP reactions using surface-bound catalyst. These surface-initiated ring-opening metathesis polymerization (SI-ROMP) reactions allow for the formation of polymer layers that are covalently tethered to surfaces. The covalent attachment methodology produces more robust films in comparison to film-forming processes that rely on polymer adsorption through weaker bonding schemes. Advantages of the SI-ROMP polymer films include stability toward temperature and solvent; these properties will be discussed as they relate to the use of the films as component layers in electronic devices.

*The bottom contact FET geometry is similar except that the semiconducting layer is deposited on top of the drain and source electrodes.

References Cited

- [1] Shirakawa, H. *Angew. Chem.-Int. Edit.*, **2001**, *40*, 2575–2580.
- [2] Trnka, T. M.; Grubbs, R. H. *Acc. Chem. Res.*, **2001**, *34*, 18–29.
- [3] Anderson, A.W.; Merkling, N.G. *Chem. Abstr.*, **1955**, *50*, 3008.
- [4] Schwab, P.; Grubbs, R. H.; Ziller, J. W. *J. Am. Chem. Soc.*, **1996**, *118*, 100–110.
- [5] Scholl, M.; Ding, S.; Lee, C. W.; Grubbs, R. H. *Org. Lett.*, **1999**, *1*, 953–956.
- [6] Bielawski, C. W.; Grubbs, R. H. *Angew. Chem.-Int. Edit.*, **2000**, *39*, 2903–2906.
- [7] Herisson, J. L.; Chauvin, Y. *Makromol. Chem.*, **1971**, *141*, 161–167.
- [8] Grubbs, R. H., Ed. *Handbook of Metathesis*. Wiley, Weinheim, 2003.
- [9] Ivin, K.J.; Mol, J.C. *Olefin Metathesis and Metathesis Polymerization*. Academic Press, London, 1997.
- [10] Ivin, K.J. *NATO Science Series, II: Mathematics, Physics and Chemistry*, **2002**, *56*, 1–15.
- [11] Tindall, D.; Pawlow, J.H.; Wagener, K.B. *Top. Organomet. Chem.*, **1998**, *1*, 183–198.
- [12] Morgan, J. P.; Morrill, C.; Grubbs, R. H. *Org. Lett.*, **2002**, *4*, 67–70.
- [13] Connon, S. J.; Blechert, S. *Angew. Chem.-Int. Edit.*, **2003**, *42*, 1900–1923.
- [14] Sanford, M. S.; Love, J. A.; Grubbs, R. H. *J. Am. Chem. Soc.*, **2001**, *123*, 6543–6554.
- [15] Benedicto, A. D.; Claverie, J. P.; Grubbs, R. H. *Macromolecules*, **1995**, *28*, 500–511.
- [16] Bielawski, C. W.; Scherman, O. A.; Grubbs, R. H. *Polymer*, **2001**, *42*, 4939–4945.
- [17] Masuda, S.; Kitamura, K.; Okumura, Y.; Miyatake, S.; Tabata, H.; Kawai, T. *J. Appl. Phys.*, **2003**, *93*, 1624–1630.
- [18] Katz, H. E.; Bao, Z. *J. Phys. Chem. B*, **2000**, *104*, 671–678.

Chapter 2

Acyclic Diene Metathesis (ADMET) Polymerization Using a Ruthenium Olefin Metathesis Catalyst Coordinated with a N-Heterocyclic Carbene Ligand

2.1 Abstract

The use of non-terminal dienes in acyclic diene metathesis (ADMET) polymerizations is investigated. In terms of the maximum attainable molecular weight and the overall rate of reaction, non-terminal dienes are found to impart no advantages over terminal dienes. In addition, the general reactivity of the well-defined ruthenium olefin metathesis catalyst (1,3-dimesityl-4,5-dihydroimidazol-2-ylidene)(PCy₃)Cl₂Ru=CHPh (**2**) in ADMET polymerizations is investigated. With catalyst **2**, very low catalyst loadings (up to monomer:catalyst ratios of 10,000:1), and short reaction times (ca. 24 hours) are possible. Compared with standard ADMET conditions for previous ruthenium catalysts (monomer:catalyst ratios of 400:1, and reaction times of 48-72 hours), these findings demonstrate the high level of activity of catalyst **2**.

2.2 Introduction

Acyclic diene metathesis (ADMET) is a step-growth polycondensation reaction that has attracted considerable attention in recent years.¹ High molecular weight, unsaturated polymers that contain various functional groups in the backbone are accessible via ADMET.² Synthesis of low molecular weight telechelic polymers³⁻⁵ as well as fully conjugated oligomers⁶ have further shown the versatility of the reaction.

A variety of olefin metathesis catalysts have been shown to facilitate ADMET polymerization. In particular, molybdenum- and tungsten-based catalysts^{7, 8} have been of interest for their high levels of activity and ability to produce polymers of high molecular weight, and the ruthenium catalyst **1** has been investigated for its tolerance of functional groups.⁹⁻¹¹ However, these catalysts have significant drawbacks. Early transition metal catalysts require stringent reaction conditions, and suffer from a lack of functional group tolerance, while late transition metal catalysts, such as **1**, are relatively inactive toward a variety of substrates such

as disubstituted olefins¹² and conjugated monomers.* Furthermore, ADMET polymerizations using these catalysts typically require long reaction times (48-72 hours) and high temperatures to yield high molecular weight polymers.

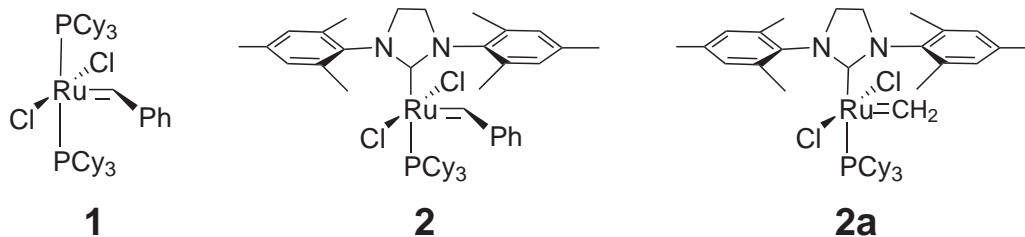


Figure 2.1: Ruthenium olefin metathesis catalysts.

Recently, the development of catalyst **2** has been reported, substituting an N-heterocyclic carbene for a phosphine ligand in **1**.¹³ The high level of activity, as well as functional group tolerance of **2**, has been documented.^{14,15} The first reported use of catalyst **2** in ADMET polymerizations demonstrated its ability to form well-defined graft copolymers.¹⁶ An increase in the rate of ADMET depolymerization has also been found using catalyst **2**.^{†18} Considering the advantages of **2** over previous metathesis catalysts, further investigations into the use of **2** in ADMET polymerizations are warranted, and are discussed herein.

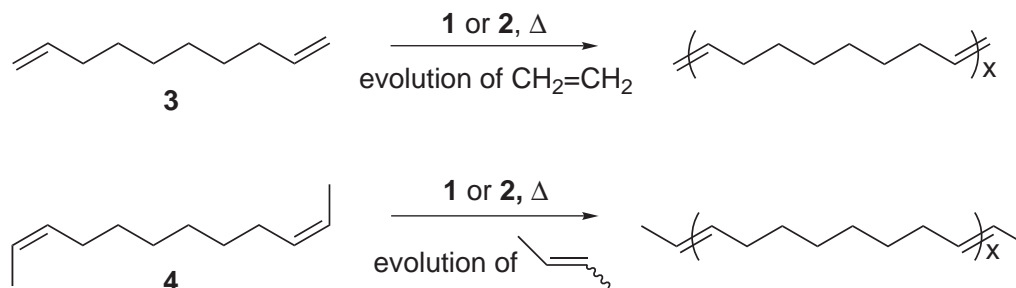
At ambient temperature, previous investigations have shown that **2a**, the phosphine-bound, methyldiene form of **2**, is a poor catalytic species for olefin metathesis.¹⁵ For ADMET polymerizations of monomers with terminal olefins, each turnover in the catalytic cycle has the potential to form **2a**.^{1,15} If **2a** is unable or slow to re-enter the catalytic cycle, the amount of active catalyst would decrease as conversion increases. ADMET has been shown to follow typical polycondensation-type kinetics,¹ yielding high molecular weight polymer only at high conversion. This suggested to us that monomers with non-terminal olefins may be better substrates for ADMET using catalyst **2**. We report here a comparison

*Unpublished results from this lab

†After completion of this work, Lehman and Wagener measured and reported the rate of oligomerization of 1,9-decadiene with catalyst **2**, finding it to be greater than that of catalyst **1**.¹⁷

of ADMET polymerizations between 1,9-decadiene (**3**) and 2,10-dodecadiene (**4**) to form polyoctenylene (Scheme 2.1).

Scheme 2.1: ADMET of **3** and **4** with a ruthenium olefin metathesis catalyst.



2.3 Experimental

Materials and characterization. 1,9-decadiene (98%) (**3**) was purchased from TCI and used as received. 2,10-dodecadiene (**4**) was prepared by a modified literature procedure.¹⁹ Toluene, methanol, diethyl ether, and hexane were obtained from EM Science and used as received. $(\text{PCy}_3)_2(\text{Cl})_2\text{Ru}=\text{CHPh}$ (**1**)²⁰ was prepared according to literature procedures. $(\text{IMesH}_2)(\text{PCy}_3)(\text{Cl})_2\text{Ru}=\text{CHPh}$ (**2**)²¹ was prepared according to literature procedures, and further purified to remove residual **1** by flash column chromatography on silica gel 60 (230–400 mesh) from TSI Scientific, eluting with 9:1 hexane/diethyl ether.

NMR spectra were recorded on a Varian Mercury 300 (299.817 MHz for ^1H and 74.45 MHz for ^{13}C). All NMR spectra were recorded in CDCl_3 and referenced to residual protio species. Gel permeation chromatography (GPC) was carried out on two PLgel 5mm Mixed-C columns connected in series with a DAWN EOS multi angle laser light scattering (MALLS) detector and an Optilab DSP differential refractometer (both from Wyatt Technology). No calibration standards were used and dn/dc values were obtained for each injection assuming 100% mass elution from the columns.

Polymerizations. All manipulations were performed under argon using standard Schlenk techniques. A typical polymerization (i.e., reaction 6, Table 2.2)

would proceed as follows: a dry Schlenk tube, purged with argon, was charged with 0.2184 g (1.580 mmol) monomer **3** and a magnetic stir bar. Three freeze-pump-thaw cycles were carried out to degas the monomer. Under an argon atmosphere, 1.4 mg (0.0017 mmol) of catalyst **2** was then added. The tube was heated to 50 °C, and pulsed with high vacuum (approximately 60 mTorr) every 10-15 minutes to remove volatiles. The reaction mixture solidified after approximately one hour, at which time dynamic vacuum was applied for the remainder of the reaction. For reactions done at 70 or 95 °C, the temperature was increased from 50 °C upon solidification of the reaction mixture. After the prescribed reaction time, heat was removed and the reaction exposed to air. The product was dissolved in a minimal amount of boiling toluene, precipitated into an excess of ice-cold methanol, filtered and dried under high vacuum overnight.

2.4 Results and Discussion

ADMET with catalysts 1 and 2. Table 2.1 displays a comparison between ADMET polymerizations using catalysts **1** and **2**. With **1** as catalyst, monomer **3** polymerizes to much higher molecular weight than does monomer **4**. This result is expected, considering the lower reactivity of **1** for this type of disubstituted olefin.¹² However, catalyst **2** does not appear to favor **4** over **3**, as had been expected. Under typical ADMET conditions (i.e., 50-70 °C in the bulk), **3** polymerizes at least as well as **4**. It is likely that the high concentration of monomer relative to phosphine precludes large-scale formation of phosphine-bound **2a**, or that **2a** is in fact an active catalytic species under ADMET conditions. We speculate that the improbability of forming **2a** under ADMET conditions allows the terminal olefin monomer to polymerize to high molecular weight.

Furthermore, the cis/trans ratios for polyoctenylene obtained with **1** and **2** are comparable. Catalyst **1** is known to favor the formation of trans over cis olefins under thermodynamic conditions.⁹ Similarly, polyoctenylene obtained

rxn	monomer	catalyst	[M]/[C]	time (hrs)	M_n (10^3) (GPC)	PDI
1	3	1	480	69	11.5	2.1
2	4	1	340	69	2.6	1.5
3	3	2	400	71	14.8	2.0
4	4	2	410	71	14.4	1.7

Table 2.1: Comparison of ADMET results between catalysts 1 and 2.

from polymerizing monomer 3 with catalyst 2 was found to have a high *trans* content of 80% by ^{13}C NMR.

Activity of catalyst 2. Having shown that the reactivity of the terminal diene monomer is comparable to that of the non-terminal diene monomer with catalyst 2, commercially available 3 was chosen to investigate the reactivity of 2 under ADMET conditions. Table 2.2 shows that the molecular weight of the resulting polymer is virtually independent of monomer:catalyst ratios, unlike ADMET of monomer 3 with catalyst 1.⁹ In addition, lower catalyst loadings do not require longer reaction times as is evident by rxn 9 (monomer:catalyst of 10000:1).

rxn	[3]/[2]	time (hrs)	yield (%) ^a	M_n (10^3) (GPC)	PDI
5	420	26	36	11.3	1.8
6	960	23	27	14.7	1.4
7	2600	23	42	10.2	1.6
8	4700	23	47	12.9	1.6
9	10000	23	60	13.4	2.0

Table 2.2: ADMET of 3 with catalyst 2; ^areported yields are based on mass of recovered product, and do not account for the lost mass of condensation byproducts.

Previously, reaction times of 2-3 days have been standard for ADMET polymerizations.^{9,16} Figure 2.2 shows that long reaction times are unnecessary with catalyst 2. The maximum number average molecular weight for a given set of conditions (i.e., temperature and monomer:catalyst ratio) is reached within 24 hours; polydispersity remains fairly constant throughout this time ($M_w/M_n = 1.6-2.1$). Thus, given sufficient reaction time of approximately 24 hours, molecular weight for bulk polymerizations seems to be most influenced by changes in temperature. Given the high viscosity of the reaction mixture after a few hours,

the maximum percent conversion is apparently limited by diffusion of monomer or oligomer to the active catalyst end of a growing polymer chain. Accordingly, Table 2.3 shows that higher temperatures allow polymerization to proceed to higher molecular weight.

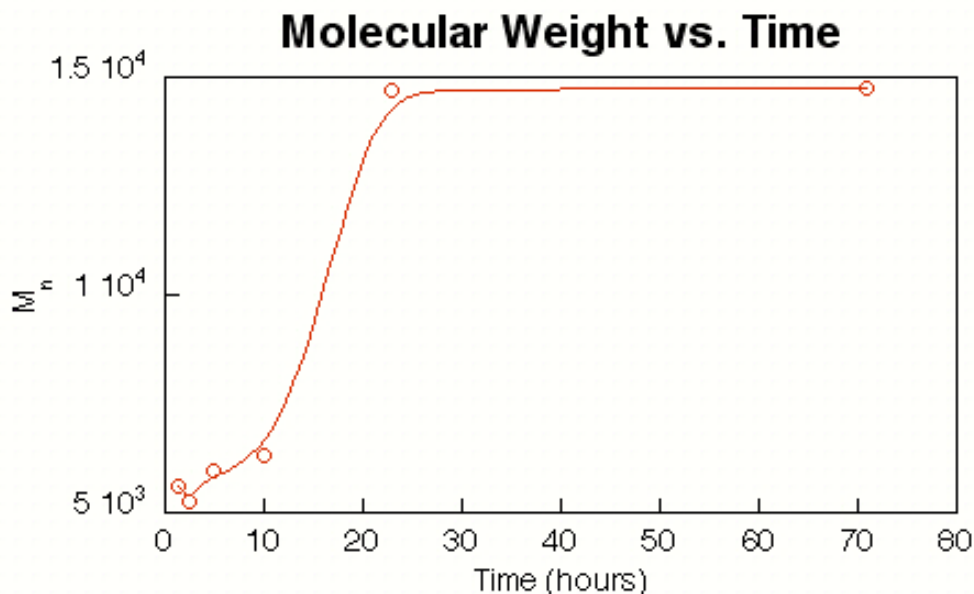


Figure 2.2: Plot of molecular weight vs. time for ADMET of **3** with catalyst **2**. Reaction conditions: $[3]/[2] = 1000$, $50\text{ }^\circ\text{C}$, 50 mTorr .

rxn	$[3]/[2]$	time (hrs)	Temp ($^\circ\text{C}$)	yield (%) ^a	M_n (10^3) (GPC)	PDI
10	960	23	50	60	2.9	1.7
11 ^b	960	23	70	27	14.7	1.4
12	990	23	95	22	23.7	1.6
13	2500	23	50	57	4.3	1.7
14 ^c	2600	23	70	42	10.2	1.6
15	2600	23	95	46	27.8	1.8

Table 2.3: Temperature effects in ADMET polymerizations of **3** with catalyst **2**; ^asee Table 2.2, ^bsame as reaction 6; ^csame as reaction 7.

Finally, given that backbiting^{22, 23} and depolymerization²⁴ reactions are known to occur with catalyst **2**, and that monomer **4** is fairly volatile under ADMET conditions, it is conceivable that “chain clipping” (i.e., depolymerization of the terminal monomer unit from a polymer chain) is responsible for the low yields shown in

the tables.[‡] However, only 2-butene was found in the volatile materials lost during polymerization of **4**. The lack of monomer suggests both that dimerization of the monomer (forming less volatile species) is rapid, and that chain clipping is not occurring to any appreciable extent. The low reported yields probably result from the small scale of the reactions, and inefficient workup procedures.

2.5 Conclusion

We have demonstrated that, with the highly-active catalyst **2**, ADMET polymerizations produce high molecular weight polymer with shorter reaction times relative to standard ADMET conditions. Catalyst **2** rapidly polymerizes terminal dienes, even with very low catalyst loadings. In terms of molecular weight and rate of polymerization, no significant advantage is gained by using non-terminal olefins over terminal olefins. The ability of **2** to polymerize disubstituted olefins as readily as terminal olefins suggests that high molecular weight, telechelic polymers may be accessible using **2**. Studies are currently under way to investigate the ability of **2** to form high molecular weight telechelic polymers under ADMET conditions.

[‡]For a reaction that goes to complete conversion, a recovered mass of 79% would correspond to 100% yield.

References Cited

- [1] Tindall, D.; Pawlow, J. H.; Wagener, K. B. *Top. Organomet. Chem.*, **1998**, *1*, 183–198.
- [2] Wagener, K. B.; Brzezinska, K.; Anderson, J. D.; Younkin, T. R.; Steppe, K.; DeBoer, W. *Macromolecules*, **1997**, *30*, 7363–7369.
- [3] Brzezinska, K.; Deming, T. J. *Macromolecules*, **2001**, *34*, 4348–4354.
- [4] Brzezinska, K. R.; Wagener, K. B.; Burns, G. T. *J. Polym. Sci. Pol. Chem.*, **1999**, *37*, 849–856.
- [5] Tamura, H.; Maeda, N.; Matsumoto, R.; Nakayama, A.; Hayashi, H.; Ikushima, K.; Kuraya, M. *J. Macromol. Sci. Pure Appl. Chem.*, **1999**, *36*, 1153–1170.
- [6] Tao, D.; Wagener, K. B. *Macromolecules*, **1994**, *27*, 1281–1283.
- [7] Patton, J. T.; Boncella, J. M.; Wagener, K. B. *Macromolecules*, **1992**, *25*, 3862–7.
- [8] Bloesch, L. L.; Gamble, A. S.; Boncella, J. M. *J. Mol. Catal.*, **1992**, *76*, 229–37.
- [9] Brzezinska, K.; Wolfe, P. S.; Watson, M. D.; Wagener, K. B. *Macromol. Chem. Phys.*, **1996**, *197*, 2065–2074.
- [10] Valenti, D. J.; Wagener, K. B. *Macromolecules*, **1998**, *31*, 2764–2773.
- [11] Wolfe, P. S.; Wagener, K. B. *Macromolecules*, **1999**, *32*, 7961–7967.
- [12] Blackwell, H. E.; O’Leary, D. J.; Chatterjee, A. K.; Washenfelder, R. A.; Bussmann, D. A.; Grubbs, R. H. *J. Am. Chem. Soc.*, **2000**, *122*, 58–71.
- [13] Scholl, M.; Ding, S.; Lee, C. W.; Grubbs, R. H. *Org. Lett.*, **1999**, *1*, 953–956.
- [14] Bielawski, C. W.; Grubbs, R. H. *Angew. Chem.-Int. Edit.*, **2000**, *39*, 2903–2906.
- [15] Sanford, M. S.; Love, J. A.; Grubbs, R. H. *J. Am. Chem. Soc.*, **2001**, *123*, 6543–6554.
- [16] O’Donnell, P. M.; Brzezinska, K.; Powell, D.; Wagener, K. B. *Macromolecules*, **2001**, *34*, 6845–6849.
- [17] Lehman, S. E. Jr.; Wagener, K. B. *Macromolecules*, **2002**, *35*, 48–53.
- [18] Craig, S. W.; Manzer, J. A.; Coughlin, E. B. *Macromolecules*, **2001**, ASAP.
- [19] Moeller, K. D.; Tino, L. V. *J. Am. Chem. Soc.*, **1992**, *114*, 1033–41.
- [20] Schwab, P.; Grubbs, R. H.; Ziller, J. W. *J. Am. Chem. Soc.*, **1996**, *118*, 100–110.
- [21] Sanford, M. S.; Ulman, M.; Grubbs, R. H. *J. Am. Chem. Soc.*, **2001**, *123*, 749–750.
- [22] Bielawski, C. W.; Grubbs, R. H. *Macromolecules*, **2001**, *34*, 8838–8840.
- [23] Bielawski, C. W.; Benitez, D.; Morita, T.; Grubbs, R. H. *Macromolecules*, **2001**, *34*, 8610–8618.
- [24] Marmo, J. C.; Wagener, K. B. *Macromolecules*, **1995**, *28*, 2602–2606.

Chapter 3

Understanding Ring-Opening-Insertion Metathesis Polymerization: Mathematical Models of Insertion Polymerizations

3.1 Abstract

Initial results toward the development of a mathematical model for ring-opening-insertion metathesis polymerization (ROIMP) are reported. Two approaches at simplifying the mathematical description of the ROIMP mechanism are discussed. The first approach involves the one-step insertion of monomer units into polymer chains that contain a specified number of insertion sites. The second approach is more representative of the ROIMP mechanism, separating the insertion process into two steps.

3.2 Introduction

Beginning in the 1920s, statistical treatments of polymerization reactions were developed. These mathematical models describe the progression of the reaction, taking into account the mechanism of polymerization, and the presence of various reacting species. Equations have been derived that describe changes in the average degree of polymerization and molecular weight distribution, as well as the effects of relative reaction rates and the inclusion of various additives. Theoretical treatments have proven valuable in helping to understand and control various polymerization systems upon scale-up and commercialization. This is particularly true for two types of polymerizations: step growth and chain growth.^{1,2}

Step growth polymerizations involve repeated coupling reactions of α,ω -difunctionalized monomers. The coupling reaction often involves the loss of a small molecule such as H₂O or HCl, and so the process is historically (and still frequently) referred to as condensation polymerization.³ The extent of reaction conversion is typically defined as the proportion of chain ends that remain. Because of this definition, and since each coupling reaction forms a product species containing two reactive chain ends, it is possible to observe complete consumption of *monomer* at less than 100% conversion. In step growth polymerizations, however, monomer typically remains the most numerous species until very high

conversions are reached. As a result, it is statistically most likely for reactions to occur between monomers, or at least between a monomer and a species of higher order.

In 1936, Carothers determined that the average degree of polymerization (\overline{DP}) is an inverse function of the reaction conversion, p (equation 3.1).⁴

$$\overline{DP} = \frac{1}{1 - p} \quad (3.1)$$

The average degree of polymerization of the reactants increases very slowly until the reaction has reached well over 90% conversion. This approach is therefore only useful for polymerization reactions that are extremely high yielding, such as condensation type reactions where the equilibrium can be driven toward the formation of polymer by the removal of condensation byproducts.

As opposed to the geometric growth observed for step growth polymerizations, chain growth mechanisms involve the sequential, linear addition of monomers to a growing polymer chain. Three (and sometimes four) separate reactions can typically be recognized in the chain growth process: initiation, propagation, chain transfer (in some systems), and termination. The extent of conversion of the reaction is directly related to the consumption of monomer. However, polymer chains initiate, propagate, and are terminated throughout the reaction. Therefore, to a first approximation, initiation, propagation, and termination occur independently of monomer conversion. Polymer chain length is determined largely by the relative rates of propagation and termination, and is largely unaffected by reaction conversion.

A number of disadvantages limit the applicability of these methods. In particular, for step growth polymerizations, extremely pure reagents, high monomer concentration, and high-yielding coupling reactions are required to form high molecular weight polymer. Side reactions must be suppressed, and it is often necessary to remove and dispose of condensation byproducts. In addition, control over molecular weight and molecular weight distribution is often very difficult.

Chain growth polymerizations suffer less from these drawbacks, although many polymer compositions and architectures are most easily accessed by step growth methods. Both processes, therefore, remain important for many commercial applications.

The unique mechanism of ring-opening-insertion metathesis polymerization (ROIMP) combines many of the aspects of step growth and chain growth polymerizations (see Appendix A). Ring-opening metathesis polymerization (ROMP) of the cycloolefin, a chain growth process, is very quick and occurs almost entirely uninterrupted. The diene subsequently inserts into the olefins in the backbone of the polycycloolefin. Normally, terminal dienes (although not α,β -unsaturated terminal dienes) polymerize via ADMET, a step growth polymerization process. The insertion portion of ROIMP, however, displays marked differences from a normal step growth mechanism. In particular, a driving force for the insertion step is the thermodynamically favored formation of α,β -unsaturated internal olefins. This driving force is strong, and as a result, ROIMP can be carried out in solvent and without the need for rigorously purifying the reagents.

Another consequence of the combination of different polymerization mechanisms in ROIMP is that the overall reaction likely does not conform to the mathematical models that have been developed for either step growth or chain growth polymerizations. During the ROMP portion of the reaction, molecular weight distribution and degree of polymerization most likely behave as for normal ROMP reactions. However, the insertion portion of the reaction also affects these variables. Conversion cannot be measured by monomer consumption, as there are typically two monomers which are consumed at drastically different rates. Average degree of polymerization most likely is not monotonically increasing, but rather decreases in the early stages of the insertion portion of the reaction. The relative rates of various reactions, including ring-opening and cross metathesis between the numerous species present must certainly play a role in the molecular weight distribution at different stages of the reaction. Experimental work involving ROIMP is presented in Appendix A. A mathematical model of the ROIMP

reaction would be useful for understanding the influence of variables such as monomer identity, monomer ratio and extent of reaction. Initial work toward the development of such a model is presented here.

3.3 Results and Discussion

In a ROIMP reaction involving a cycloolefin and an α,β -unsaturated terminal diene, nearly 30 different reactions are possible between reactants and catalyst. This necessitates a number of simplifying assumptions. The experimental data indicates that the ROMP portion of the reaction occurs much faster than the insertion portion (see Appendix A). It seems reasonable, therefore, to ignore the ROMP portion of the reaction, and assume that the insertion of the diene monomer occurs with a pre-formed polyalkenamer.

For simplicity in the following discussion, a terminal olefin (which is defined to be equivalent to one-half of an internal olefin) will be referred to as "A," so that an internal olefin can be represented by "AA." In addition, a terminal α,β -unsaturated olefin will be referred to as "B," and a diacrylate monomer will thus be represented by B-B. An internal α,β -unsaturated olefin will be referred to as "C," although note that it is equivalent to "AB." See Figure 3.1 for clarification of this nomenclature.

Each metathesis reaction must be facilitated by the ruthenium catalyst. This adds a further level of complication, since each metathesis reaction involving the catalyst can lead to two distinct products (depending upon the connectivity of the metallacyclobutane). Certain connectivities are more likely than others, depending upon the sterics and electronics of the reactants and resulting products. In this initial treatment of the ROIMP reaction, the action of the catalyst has been completely ignored. Coupling of A and B groups occurs without consideration of the orientation of the reactants or the catalyst.

Although terminal acrylates are observed to dimerize during ROIMP reactions, the extent of this unwanted side reaction is typically very small (1–2%). Reactions

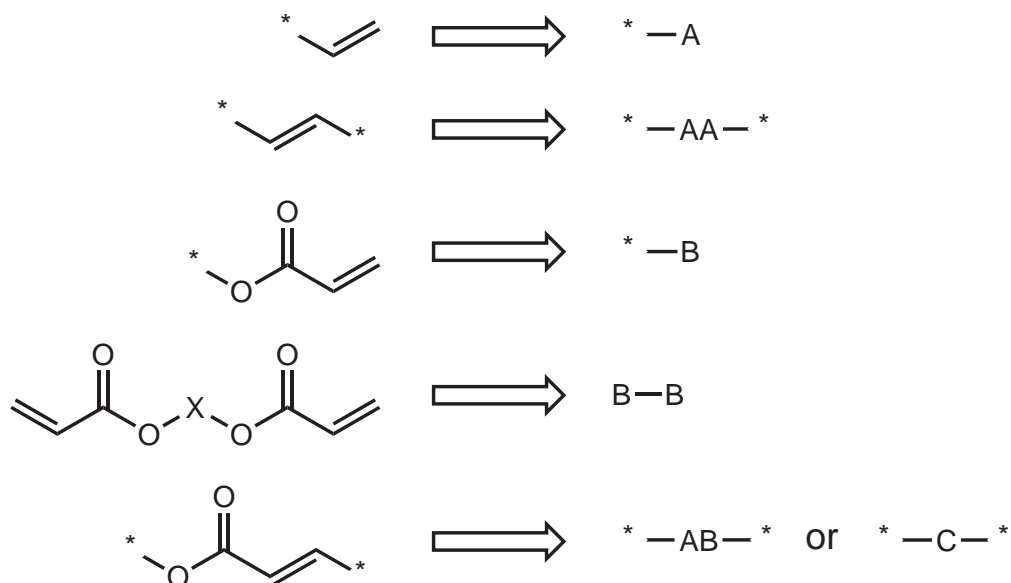
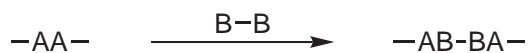


Figure 3.1: Definitions used for ROIMP model.

involving two B groups are therefore ignored in order to further simplify the calculations.

Figure 3.2 shows M1 and M2, the different mechanisms by which an insertion polymerization can occur. In the simplest mechanism, M1, each BB monomer is inserted in one step into an AA group. Although this mechanism is not realistic for ROIMP, it represents a simplified version of insertion polymerizations from which to begin the development of a mathematical model. The end product is identical to that of the more complicated mechanism, M2, in which each B group must react individually with an A group. Initial calculations were therefore performed using the simplified insertion mechanism, M1.

M1: Concerted Mechanism



M2: Step-Wise Mechanism



Figure 3.2: Insertion polymerization mechanisms.

In calculating the average degree of polymerization (\overline{DP}), it was decided to first consider only polymer molecules present in the reaction. Given NAA (the number of AA groups initially present) and NP (the number of initial polymer chains), the initial \overline{DP} is NAA/NP. Then, defining NBB as the number of B-B monomer units initially present, and p as the fractional conversion of B-B monomer units at any point in the reaction, \overline{DP} is defined by

$$\overline{DP} = \frac{(NAA + p * NBB)}{NP}$$

This indicates that, for mechanism M1, \overline{DP} increases linearly with conversion when conversion is defined as the number of reacted B-B monomers units (or, equivalently, the number of reacted AA groups).

An alternative method for calculating \overline{DP} is to consider all species present in the reaction. Degree of polymerization is then given by equation 3.2.

$$\overline{DP} = \frac{(NAA + NBB)}{(NP + NBB - p * NBB)} \quad (3.2)$$

Note that, because of the definition used for p, equation 3.2 is applicable under conditions where $NAA \geq NBB$, but not when $NBB > NAA$. As with traditional step growth polymerizations, \overline{DP} as defined by equation 3.2 increases very rapidly only at high values of conversion (Figure 3.3).

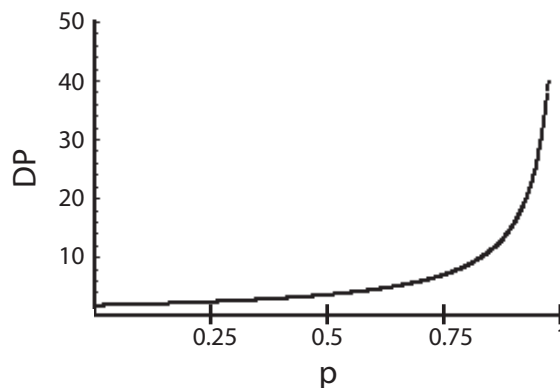


Figure 3.3: Degree of polymerization vs. conversion for M1, considering all species present (equation 3.2). Values of constants: NAA = NBB = 1000, NP = 50.

Determination of molecular weight distribution as a function of conversion of B-B units (p) for mechanism M1 requires the initial distribution of polymer chains to be defined. Let $g_p(y)$ be a function that defines the number of polymer chains with y repeat units (i.e., either AA groups or C groups) at p conversion. For example, $g_p(10)$ represents the number of chains containing a total of 10 AA and/or C groups. Then, $g_0(y)$ represents the initial distribution of chains. Although any distribution can be chosen for $g_0(y)$, a normal distribution is used in the present study. Therefore, by the definition of the normal distribution,

$$g_0(y) = num * (2 * pi * s^2)^{(-1/2)} * e^{\frac{-(y-m)^2}{(2*s^2)}}$$

where m represents the mean, s represents the standard deviation, and num is a scaling factor that accounts for the number of initial polymer chains. For the calculations performed here, $m = 50$, $s = 5$, and $num = 500$.

The probability of a B-B unit inserting into a given polymer chain is determined by the number of unreacted AA units that are present in that chain relative to the total number of unreacted AA units left in the reaction. This is determined by the chain's initial number of AA units as well as the number of insertion reactions that have occurred for that chain. Furthermore, the number of polymer chains of overall length y (i.e., with the sum of the number of AA units and the number of inserted B-B units equal to y) is equal to the sum of chains where the initial number of AA groups and the number of insertion reactions sum to equal y . For example, at any conversion p , $g_p(4)$ is equal to the number of chains that initially contained two AA groups and have undergone two insertion reactions, plus the number of chains that initially contained three AA groups and have undergone one insertion reaction, plus the number of chains that initially contained four AA groups and have undergone no insertion reactions. This summation can be represented by equation 3.3, given that p is also equal to the probability that an insertion reaction has occurred at any randomly selected AA group.

$$g_p(y) = \sum_{y=l/2}^l g_0[y] * p^{(l-y)} * (1-p)^{(2*y-l)} \quad (3.3)$$

Plots of $g_p(y)$ for various values of $p < 0.5$ are given in figure 3.4. Interestingly, the original distribution is distorted as conversion nears 50%. It appears that polyolefins with larger numbers of initial AA groups are more prone to insertion reactions, and thereby increase their molecular weight faster than polyolefins with fewer initial AA groups. This seems reasonable, as the probability of a B-B unit inserting into a chain is directly related to the number of AA groups that are present in that chain.

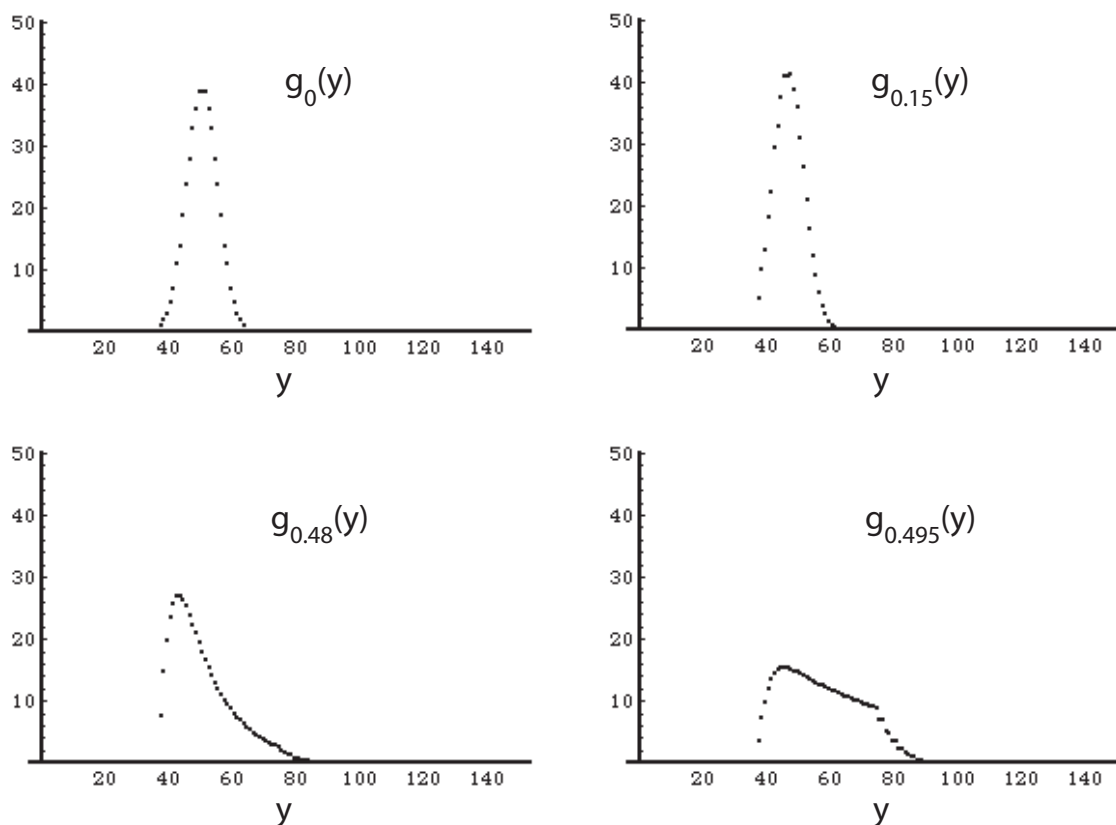


Figure 3.4: Plots of $g_p(y)$ vs. y for mechanism M1 at various levels of reaction conversion (vertical axes units represent an arbitrary number of chains).

Currently, due to problems in rounding and the handling of even/odd integers, implementations of equation 3.3 using Mathematica (Wolfram Research, version

5.0.0.0) are invalid for conversions greater than 50%. One would expect, however, that the evolution of the distribution for values of $p > 0.5$ would be similar to the evolution for values of $p < 0.5$. Indeed, by modifying the equation to calculate $g_p(y)$ only for even values of y , this behaviour is observed for values of $p > 0.5$.

A mathematical model for mechanism M2 is far more complex than the model for mechanism M1. The significant difference between the two mechanisms is that the molecular weight of a polymer chain can decrease for M2, whereas it is strictly increasing for M1. Therefore, for M2, the number of polymer chains containing a given number of monomer units is dependent not only upon the number of insertion reactions that have occurred, but also upon the location within the polyolefins that those insertions occur.

For the M2 mechanism, three key reactions can be identified: R1, R2, and R3 (Figure 3.5). At any given conversion p , the molecular weight distribution and \overline{DP} will be dependent upon the number of each of these reactions that have occurred. For example, since the number of molecules remains constant, reactions of type R1 do not change \overline{DP} (assuming that \overline{DP} is defined to include all species present in the reaction). In addition, the molecular weight of a chain can either increase or decrease upon undergoing an R1 reaction, whereas it can only increase as a result of R2 and R3 reactions.

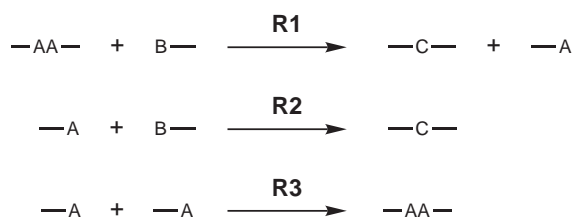


Figure 3.5: Important reactions for mechanism M2.

As a further complicating factor, the order in which reactions occur must also be considered. In achieving 100% conversion, the fewest number of overall reactions will occur if R3 reactions are completely suppressed. However, every two reactions of type R1 that occur produce the reactants necessary for an R3 reaction. Therefore,

if R1 reactions occur much faster than R2 reactions, there will be a buildup of terminal A groups and R3 reactions will become more probable.

Due to the complexity of the M2 mechanism, suitable equations for calculating the molecular weight distribution and \overline{DP} of the reaction as a function of conversion have yet to be derived. However, it may be possible to simplify the model using statistical distributions of chain fragments, with the number of fragments determined by the conversion. This, and other possible simplifying methods, await further investigation.

3.4 Conclusions

Initial attempts to model the ROIMP reaction have been successful only using highly simplified models. Further work is necessary in order to extend this work to more realistic models.

References Cited

- [1] Flory, P. J. *Principles of Polymer Chemistry*. Cornell University Press, Ithaca, N.Y., 2nd edition, 1953.
- [2] Odian, G. *Principles of Polymerization*. Wiley, Hoboken, NJ, 4th edition, 2004.
- [3] Carothers, W. H. *J. Am. Chem. Soc.*, **1929**, 51, 2548–2559.
- [4] Carothers, W. H. *Trans. Faraday Soc.*, **1936**, 32, 39–49.

Chapter 4

Development of Polymeric Chain Transfer Agents for Use in Ring-Opening Metathesis Polymerizations

4.1 Abstract

Ring-opening metathesis polymerization (ROMP) of cyclic olefins in the presence of polymeric chain transfer agents (PCTAs) resulted in the formation of block copolymers. Suitable PCTAs include a variety of commodity polymers, although chain transfer is most effective for PCTAs with low molecular weight (below 10,000 g/mol). For well-defined block copolymers products, the PCTA must contain only a single olefin. Reactivity of the PCTA is influenced by the substitution and location of the olefin; PCTAs containing terminal olefins are more highly active than those containing internal olefins. Herein is reported the synthesis of symmetric PCTAs containing an internal olefin, as well as the use of symmetric PCTAs in controlling molecular weight in ROMP reactions.

4.2 Introduction

Numerous advances over the past century have aided the development of chain growth polymerization processes. The highly reactive nature of the active species in some chain growth polymerizations (particularly those involving free radicals) necessitates the use of methods for controlling polymer growth. One approach to limiting polymer molecular weight is through the use of chain transfer agents (CTAs). A propagating polymer chain reacts with a CTA by transferring the active species. The original polymer chain is terminated (either reversibly or irreversibly) and a new polymer chain begins to propagate. By adjusting the ratio of CTA to monomer or initiator, the frequency of chain transfer can be affected. Alternatively, the relative activity of the chain transfer agent can be modified. Through the manipulation of these variables polymer molecular weight and structure can often be finely controlled.

Ring-opening metathesis polymerization (ROMP) is a chain growth polymerization process that has benefited from the development of chain transfer agents.¹⁻⁴ In the absence of CTAs, many ROMP systems exhibit relatively uncontrolled

propagation characteristics. The use of CTAs has afforded control in both polymer molecular weight and endgroups. Molecular weight, which in the absence of a CTA is influenced mostly by the nature of the catalyst and by the ratio of monomer to catalyst, is determined by the ratio of monomer to CTA. Typically a linear relationship is observed between the amount of added CTA and the molecular weight of the resulting polymer. Such systems are limited, however, by the reactivity of the catalyst and the identity of the CTA.

In general, CTAs for ROMP reactions are small organic molecules containing acyclic olefins. Both symmetric and asymmetric olefins have been employed, and the resulting polymer products are influenced by the structure of the CTA. Given sufficient reaction time and temperature, the chain transfer process results in a statistical distribution of CTA groups and catalyst initiator fragments at the polymer chain ends. Thus, telechelic polymers (i.e., polymers that are functionalized at the chain ends) can be produced using symmetric CTAs if the CTA is present in significantly greater quantities than the catalyst. For example, if 200 equivalents (relative to catalyst **1** or **2**) of a symmetric CTA are used, phenyl endgroups from the catalyst will statistically be present on only 0.25% of polymer chain ends, with the remaining 99.75% of polymer endgroups originating from the CTA.

The formation of telechelic polymers using a chain transfer process in ROMP reactions can be aided if the catalyst is able to undergo secondary metathesis reactions with the backbone olefins of the polymer. These “backbiting” reactions work best for polymers containing metathesis-active olefins. Thus, chain transfer is most effective with monomers such as cyclooctadiene and cyclooctene, which generate less bulky backbone olefins. In addition, the functionality of the CTA is limited to groups that are not reactive with the metathesis catalyst. For these reasons, much recent attention has been focused in the employment of catalyst **2** in ROMP reactions using CTAs. The high level of activity of catalyst **2** has been documented, and allows chain transfer reactions with more sterically demanding olefins.^{5,6} In addition, the functional group tolerance of ruthenium catalysts enable the use of CTAs containing a wide variety of functionalities.

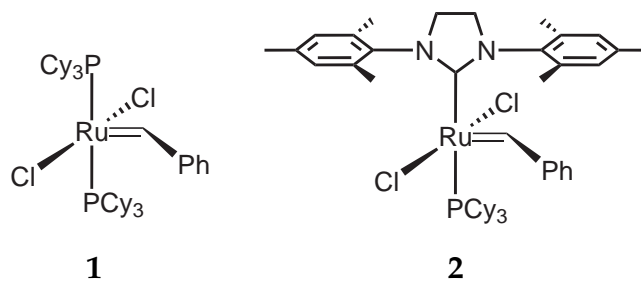


Figure 4.1: Ruthenium olefin metathesis catalysts.

Although in the majority of cases, CTAs are well-defined, small organic molecules, the use of *polymers* as CTAs has been documented in a few cases.⁷⁻⁹ For example, thiol-containing polymers function as CTAs in radical polymerizations. This method results in grafted, comb-type polymer architectures. In general, polymeric chain transfer agents (PCTAs) remain an underdeveloped method for controlling chain growth polymerizations.

A suitable PCTA for ROMP reactions must contain an acyclic olefin. As with traditional CTAs, the olefin can be either symmetric or asymmetric. The former is necessarily an internal olefin, while the latter is most conveniently (but not necessarily) a terminal olefin. The active portion of the PCTA is then a single olefin that may be extensively surrounded by the inert polymer portion of the molecule. It is expected, therefore, that effective reaction conditions and PCTA compositions will be different from those that have been developed for small molecule CTAs.

The first report of the use of PCTAs in ROMP reactions is reproduced as Appendix B of this thesis. Recently, Emrick and coworkers published the first reported use of a symmetric PCTA.¹⁰ In Emrick's work, the PCTA was composed of a pair of benzyl ether dendrons connected by a short, olefin-containing linear segment. Cyclooctadiene was used as monomer, and triblock copolymers with end-functionalization in excess of 95% were obtained. These examples of the use of PCTAs in ROMP reactions begin to demonstrate the utility, but fail to address the scope of the method. In addition, an understanding of the variables that are influential in ROMP reactions involving PCTAs, both symmetric and

asymmetric, would aid in the development of suitable applications. Herein is reported preliminary work toward expanding the scope and understanding of metathesis-active PCTAs.

4.3 Results and Discussion

4.3.1 Synthesis of Asymmetric PCTAs

Asymmetric PCTAs (i.e., polymers containing terminal olefins) can be easily synthesized using a variety of polymerization methods. Indeed, many examples of polymers containing an olefin as one of the endgroups are sold commercially. These polymers are likely synthesized via living anionic polymerization, with an alkenyllithium as the initiating species. Alternatively, Zeigler Natta catalysts yield olefin-terminated polymers when β -hydride elimination is the method of termination.^{11, 12}

The preparation of olefin-terminated, asymmetric PCTAs via atom transfer radical polymerization (ATRP) is described in Appendix B. The synthetic simplicity of ATRP is virtually unmatched compared with other methods for controlled polymerization. Reagents are commercially available and do not require rigorous purification. In addition, acceptable reaction conditions are easily achieved, and the resulting polymers are well-defined. The main difficulty with this method is the residual metal contaminants that are present in the product polymer. This contamination has prevented us from characterizing the polymers by multi-angle laser light scattering (MALLS); alternative methods for the preparation of asymmetric PCTAs await further investigation.

4.3.2 Synthesis of Symmetric PCTAs

The synthesis of polymers containing a single olefin in the backbone is, in itself, a challenging problem. One method has been reported in the literature, whereby a cyclic tin oxide was used to initiate the ring-opening polymerization of various

monomers (Figure 4.2, lactic acid shown as example monomer).¹³⁻¹⁵ Insertion reactions on either side of the olefin lead to expansion of the tin macrocycle, and hydrolysis yields the final, hydroxy-terminated, symmetric polymer. The presence of an olefin in the backbone of the polymer was confirmed by ¹H NMR spectroscopy, and the reactivity of that olefin was demonstrated by its ability to undergo epoxidation with mCPBA. This method is currently under investigation as a means of producing symmetric PCTAs suitable for ROMP. The approach is particularly interesting for its ability to use lactic acid and ϵ -caprolactam as monomers, thereby creating polymers with numerous heteroatoms in the backbone. In addition, molecular weight is easily controlled, and the method is able to form polymers with a low polydispersity index (PDI).

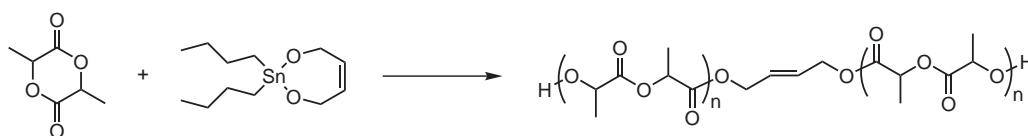


Figure 4.2: Preparation of a symmetric polymer using ring-opening polymerization.

Symmetric PCTAs should be highly uniform and well defined. If the method for their synthesis is less than quantitative, a portion of the polymer product will be asymmetric. The asymmetric polymer molecules may contain an olefin near the chain end; the reactivity of such olefins could be substantially different from the reactivity of olefins located at the center of PCTA chains. Since mixtures of polymers are typically very difficult to separate into their constituent components, a method for quantitatively producing symmetric, olefin-containing PCTAs is desirable.

4.3.2.1 Coupling of Pre-formed Polymers

Well-defined polymers with differing moieties at opposite chain ends (i.e., heterotelechelic polymers) are commercially available. This includes a variety of molecular weights of poly(ethylene oxide) (PEO) that contain hydroxy and

methoxy chain ends. Two methods for coupling hydroxy-terminated PEO, as shown in Figure 4.3, were attempted in an effort to form symmetric PCTAs (preparation of the coupling agents is discussed below). Analysis of the products by MALDI-TOF MS, unfortunately, showed a mixture of the desired product, unreacted PEO, and in many cases, undesirable products from side reactions. Attempts to isolate the bis-coupled PEO by dialysis or fractional precipitation were unsuccessful.

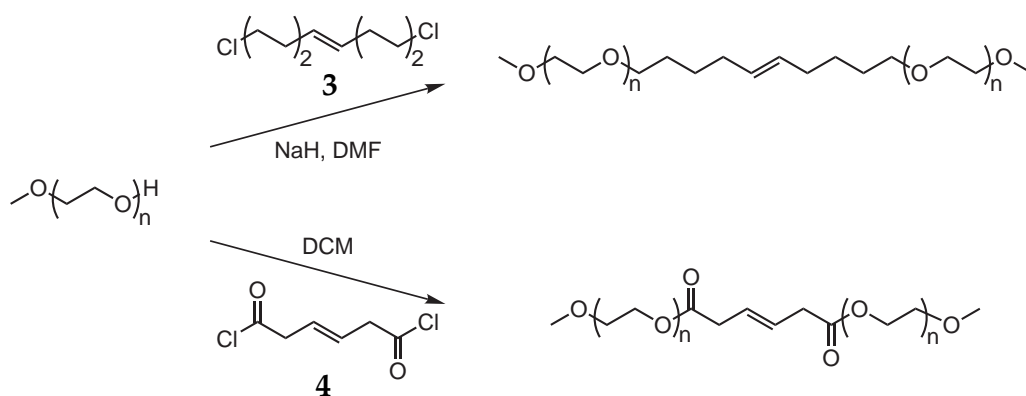


Figure 4.3: Preparation of symmetric PCTA: coupling of heterotelechelic PEO.

Polystyrene (PS) terminated with an acid chloride group is also commercially available. Reaction of this polymer with 2-butene-1,4-diol afforded a mixture of both mono-coupled (asymmetric) and bis-coupled (symmetric) PS. Fractional precipitation was found to be an effective method of separation; the overall yield of the desired product, however, was only 17%. Considering the expense of the functionalized PS starting material, this method is not practical on a larger scale.

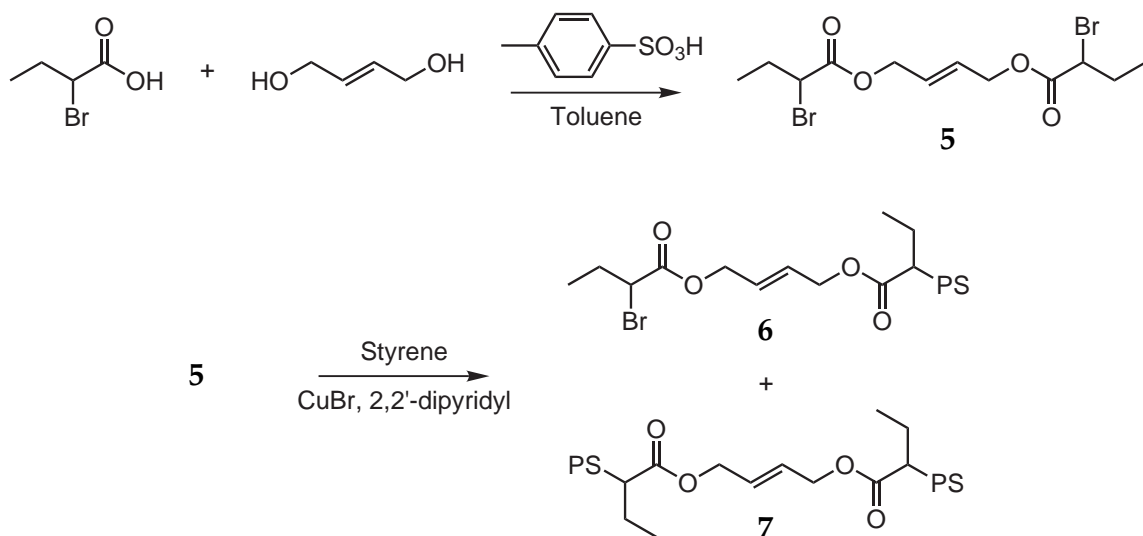
Another approach toward coupling heterotelechelic polymers utilizes cross metathesis as the coupling reaction. Unfortunately, cross metathesis reactions using olefin-terminated polymers (such as the asymmetric PCTAs described earlier) and catalyst **2** failed to reach 100% conversion. In addition, as in the previous cases, isolation of the desired product from uncoupled polymer proved unsuccessful by the attempted methods. Due to the inherent limitations presented by these methods (e.g., the tedious separation processes required after the coupling

reaction), alternative methods for the preparation of symmetric PCTAs were investigated.

4.3.2.2 Generating Symmetric PCTAs in situ

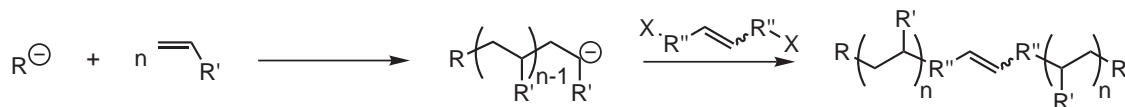
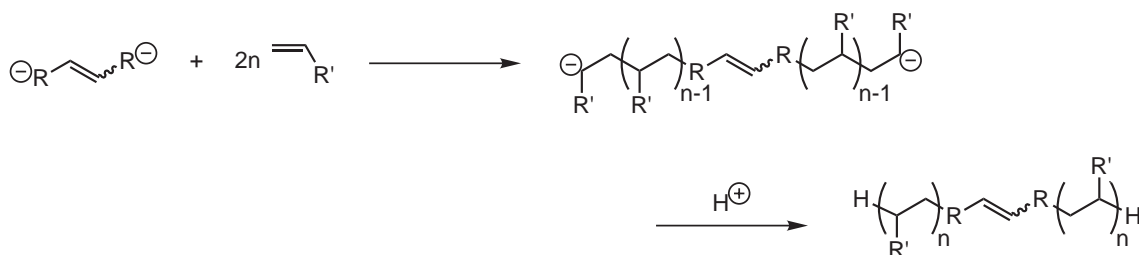
Extension of the ATRP method used to prepare asymmetric PCTAs was expected to be straightforward, as a similar system was reported by Yuan and coworkers.¹⁶ Unfortunately, the dual site ATRP initiator **5** shown in Scheme 4.1 suffered from unsatisfactory efficiency. As a result, the polymer product was a mixture of structure **6** and the desired structure **7**, as shown by ¹H NMR spectroscopy. The olefin in **6** is very near the polymer chain end, and is thus possibly closer in reactivity to a terminal olefin than to the internal olefin of the desired product. It is therefore likely that a mixture containing compounds **7** and **6** would not be characteristic of a well-defined, symmetric PCTA. Incomplete initiation has been observed previously in ATRP reactions, and studies have been performed in an attempt to find more efficient initiating systems.¹⁷ From these studies, it seems likely that substituting one or two methyl groups for the ethyl substituents next to the halogen atoms would provide better initiation. However, considering limitations inherent in ATRP, this modification may not be sufficient to provide the uniformity that is desired for symmetric PCTAs.

The ability to precisely control polymer architecture and composition is perhaps the most attractive advantage of living anionic polymerization (LAP).¹⁸ Although it requires rigorously controlled reaction conditions, LAP remains a popular technique for producing well-defined functionalized polymers. Initiators in LAP are typically highly reactive carbanions such as butyllithium. For monomers such as styrene and methacrylates, the resulting propagating species are relatively stable. This ensures that initiation occurs much more rapidly than propagation, which leads to the high degree of control afforded by LAP. If reactive impurities are excluded from the reaction, termination with functionalized reagents allows for further control over the composition of the final product.

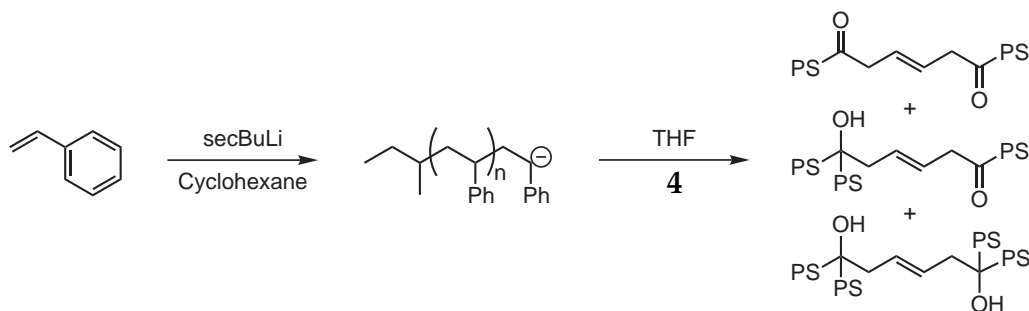
Scheme 4.1: Preparation of a symmetric PCTA using ATRP.

Considering these aspects of LAP, the method was targeted for the synthesis of symmetric PCTAs. Two approaches are possible: polymerizing in two directions from a bifunctional initiator, and using a bifunctional terminating agent. Preparation of symmetric, olefin-containing polymers using these methods is shown in Scheme 4.2. The bifunctional initiator approach involves generation of a biscarbanion containing an internal olefin, and seems synthetically challenging. As a result, only the bifunctional termination approach has been investigated to date. Nevertheless, if a bifunctional initiator can be prepared (by the reaction of lithium metal with compound **3**, for example), the method would be well suited for the unambiguous preparation of symmetric PCTAs.

Functionalization of polymer chain ends in LAP is conveniently accomplished via addition/elimination reactions between the growing polymer chain and an appropriate electrophile. Side reactions, however, often produce unwanted results. Scheme 4.3 shows our first attempt to produce symmetric PCTAs using LAP. The bis(acid chloride) **4** was easily prepared by the reaction of 3-hexenedioic acid with thionyl chloride. Unfortunately, the reaction between polystyrenyllithium and an acid chloride generates a ketone, which is prone to further nucleophilic attack by a second polystyrenyllithium. Indeed, regardless of stoichiometry, termination

Scheme 4.2: Preparation of a symmetric polymer using LAP.**Bifunctional Terminator****Bifunctional Initiator**

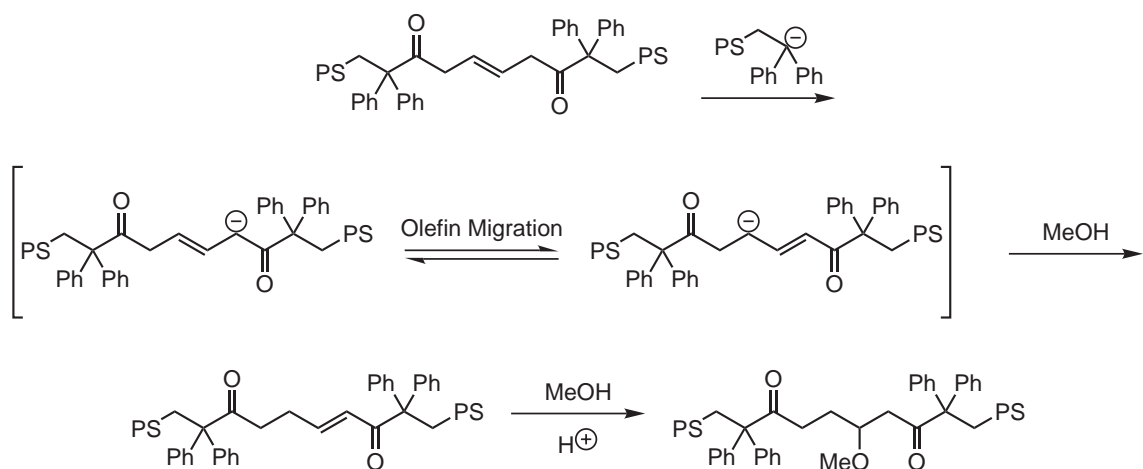
of the LAP of styrene with **4** led in all cases to polymer products in which two, three, and in some cases four polymer chains were attached to each terminating molecule. This result was clearly shown by MALDI-TOF and GPC analyses of the products.

Scheme 4.3: Attempted preparation of a symmetric PCTA using LAP.

Because of steric constraints, 1,1-diphenylethylene (DPE) is reactive toward polystyryl anions, but does not homopolymerize via anionic polymerization.^{19,20} As a result, the addition of a single unit of DPE to the end of a growing polymer chain has been used to moderate the reactivity of polystyrenyl anions. For example, DPE end-capped polystyryl anions were reacted with polymers containing pendant alkylhalide groups in order to create branched and comb-like polymers.²¹ In the current work, it was thought that the steric bulk of DPE

end-capped polystyryl anions would prevent multiple reactions with each acid chloride group in **4**. This proved to be the case, and MALDI-TOF analysis of the product indicated the presence of the desired bis-coupled product. A new series of peaks, however, were also detectable by MALDI-TOF. The mass differential of the new series may indicate the presence of a side reaction involving hydrogen-abstraction by the anionic polymer, migration of the olefin, and addition across the olefin upon quenching the reaction in acidic methanol (Scheme 4.4).*

Scheme 4.4: Competing reaction in LAP of styrene using 1,1-diphenylethylene.

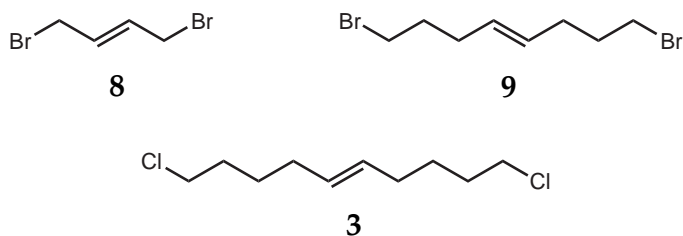


Having deemed acid chlorides (and other carbonyl-based terminating agents) as inappropriate for the current investigations, our attention was shifted toward terminating agents containing alkyl halides.²² Such molecules should undergo S_n2 reactions with polymer anions, generating products which are inert toward reaction with additional anions.

Suitable, symmetric bis(alkylhalide) coupling agents are not commonly commercially available, with the exception of 1,4-dibromo-2-butene (**8**). However, a wide range of alkyl halides containing a terminal olefin are available. Unlike the difficulties that are encountered in cross metathesis reactions involving olefin-terminated polymers, cross metathesis involving alkenylhalides is suitable for

*Olefin migration likely also occurs when neutral methanol is used; the resulting olefin-containing polymer would be relatively inactive toward metathesis.

producing fairly pure symmetric terminating agents. The difference lies in the ability to efficiently isolate (by column chromatography or distillation) the homocoupled product from the uncoupled starting material. This approach has the potential to yield symmetrical, difunctional terminating agents displaying a wide variety of steric and electronic environments.



For the current research, 1,10-dichloro-5-decene (**3**) and 1,8-dibromo-4-octene (**9**) were prepared in 76% and 56% yield, respectively, using catalyst **1**. With strong nucleophiles, the β -hydrogens of these linking agents are highly susceptible to elimination-type reactions. Quirk and coworkers reported, however, that the addition of LiCl is effective in suppressing this competing reaction, presumably by moderating the reactivity of the anions through the formation of aggregates.²³ Indeed, in LAP reactions of styrene with cyclohexane as solvent and *sec*-BuLi as initiator, elimination reactions were substantially suppressed by the addition of LiCl. Unfortunately, the desired doubly-coupled product was never observed in appreciable amounts. Aggregation of the polystyryl anions likely increased the steric barrier toward the coupling of two polymer chains to a molecule of **3**.

Rather than moderating the reactivity of the polystyryl anions through the use of LiCl, a second approach toward suppressing elimination reactions is to increase the reactivity of the alkylhalide. Indeed, using the alkylbromides **8** and **9**, elimination reactions were not observed. In cyclohexane solvent at room temperature, however, the reactivity of **8** was sufficient to allow lithium-halogen exchange followed by Wurtz coupling (Figure 4.4).^{23, 24} The major product, although symmetric, contained no olefin units. This competing reaction can be avoided by lowering the reaction temperature. Thus, in THF solvent at $-98\text{ }^{\circ}\text{C}$, the desired product was obtained in good yield. It is important to note that

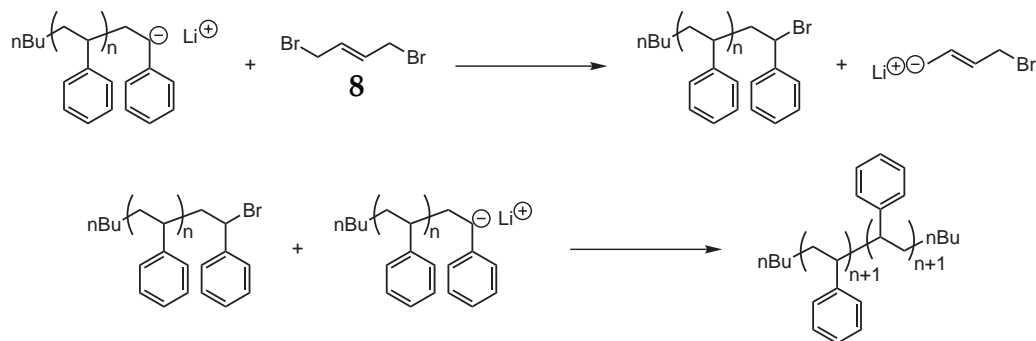


Figure 4.4: Formation of polystyrene dimer by lithium-halogen exchange and Wurtz coupling.

the terminating agent must be added to the solution of polystyryl anions *slowly* in order to ensure that the polystyryl anions are always present in excess. A small amount of H-terminated polystyrene, presumably resulting from water that was present in the solution of terminating agent, was observed by GPC and MALDI-TOF. This contaminant polystyrene fraction is expected to be inert toward metathesis reactions, and should therefore not affect the activity of the PCTA.[†] Polystyrene CTAs with a variety of molecular weights and compositions were prepared (see Table 4.1).

Table 4.1: Symmetric polystyrene PCTAs

Compound	Product Structure	Terminating Molecule	Molecular Weight ^a (g mol ⁻¹)	PDI
10		8	10,000	1.13
11		8	4,600	1.15
12		8	2,500	1.08
13		9	2,100	1.06

^a Average value as determined by ¹H NMR and MALLS GPC, when available.

[†] More rigorous drying of the terminating agent using CaH_2 should eliminate the formation of this contaminant.

4.3.3 The Use of PCTAs in ROMP

With the symmetric PCTAs **10–13**, effective molecular weight control was observed for cyclooctene and cyclooctadiene monomers (Figures 4.5 and 4.6). The success of the reactions could be qualitatively determined by GPC. For example, two peaks were observed in the MALLS detector signal of an unsuccessful reaction. These two peaks corresponded to the molecular weights of the unmodified PCTA and the polymer that is formed in a control reaction in which the PCTA is excluded. In addition, only one peak, corresponding to the molecular weight of the unmodified PCTA, was observed in the UV detector signal of the same sample. This is notable since the monomer (by itself) produces a polymer that is transparent to UV light ($\lambda = 254$ nm), while the PCTA (or any fragments of the PCTA) is strongly absorbent at this frequency. These data indicated that the polymerization of the monomer was unaffected by the presence of the PCTA, and that the resulting polymer did not contain any portion of the PCTA.

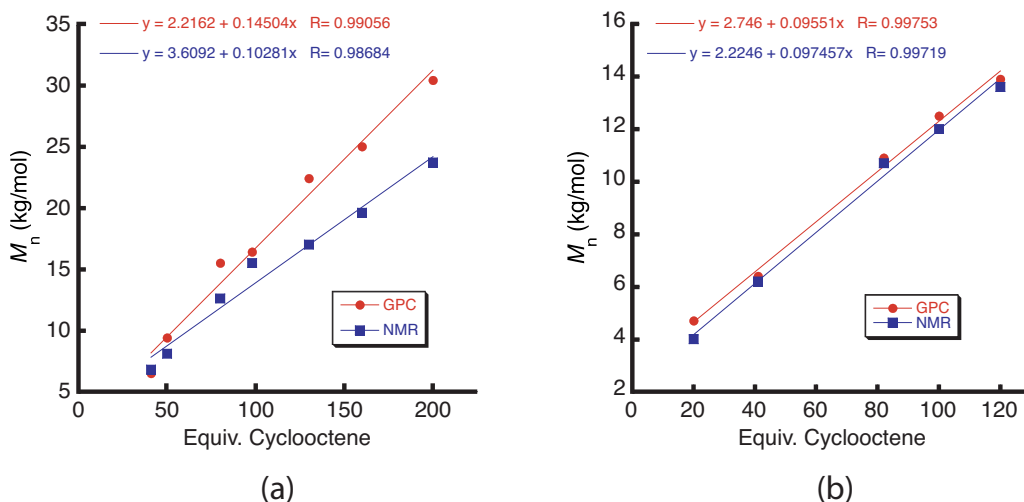


Figure 4.5: ROMP reactions using cyclooctene and (a) **12** or (b) **13** as PCTA. Yields for these reactions were typically 80–90%.

In contrast, only one main peak was observed in both the MALLS and UV signals for successful polymerizations involving PCTAs. The single peak indicates

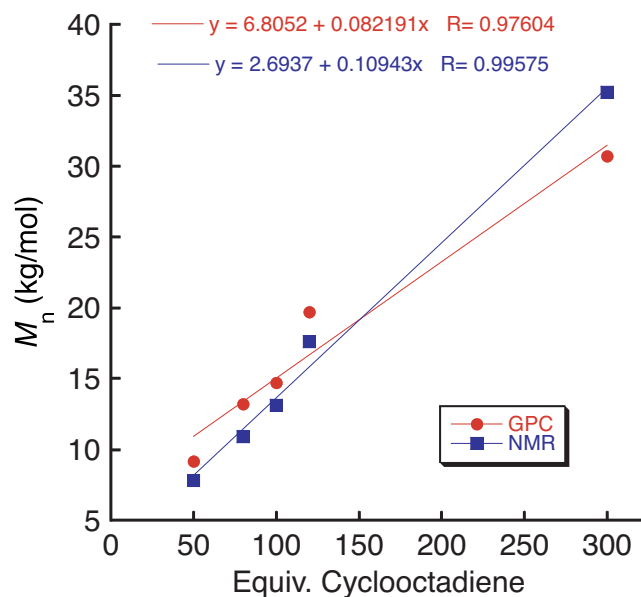


Figure 4.6: ROMP of cyclooctadiene with **12** as PCTA. Yields for these reactions were typically 80–90%.

that the product contains a single type of polymer – presumably, an ABA triblock copolymer with polystyrene A blocks and a polyoctenamer or polybutadiene B block. The presence of a minor peak, corresponding to approximately half of the molecular weight of the PCTA, was also observed. This is likely due to a small amount of inert polystyrene, formed by termination with water in the preparation of the PCTA.

The progress of a ROMP reaction with a PCTA can often be monitored qualitatively based on the viscosity of the reaction. The PCTA is first dissolved in a solution of the monomer and solvent at room temperature, followed by subsequent addition of the catalyst. No change is observed until shortly after the reaction vessel is heated (typically to 55 °C), at which time the solution becomes a gel. Some time later (typically 5-15 minutes, depending upon the molecular weight and concentration of the PCTA present) the gel is broken and the viscosity of the reaction decreases. These observations indicate that ROMP of the monomer occurs

initially in an uncontrolled manner. The resulting high molecular weight polymer is then slowly broken into smaller fragments by cross metathesis reactions with the PCTA.

A variety of monomers have been investigated in ROMP reactions with PCTAs, and less sterically crowded olefins seem to be ideal for these reactions. Thus, cyclooctene and cyclooctadiene work quite well in ROMP reactions with symmetric polystyrene PCTAs. Norbornene, in contrast, presents considerably more resistance toward molecular weight control with PCTAs. Although it may be possible to find reaction conditions which improve this situation (e.g., specific solvents, higher temperature, or longer reaction time), it is evident that reactions with PCTAs are particularly sensitive toward the steric environment of the monomer.

In addition to the identity of the monomer, several factors were observed to have dramatic influence on the efficiency of reactions involving PCTAs. In particular, chain transfer was not effective unless the reaction was carried out above a minimum monomer concentration. In addition, this minimum concentration was dependent upon the molecular weight of the PCTA. Thus, in the case of polystyrene PCTA and cyclooctene monomer, initial monomer concentrations of 1.8 M and 0.9 M were required for PCTAs with molecular weight of $4,600 \text{ g mol}^{-1}$ (**11**) and $2,500 \text{ g mol}^{-1}$ (**12**), respectively.[‡] This seems to indicate that the polymer portion of the PCTA acts to dilute the reaction. The backbiting and cross metathesis reactions necessary for chain transfer are only successful if the olefin of the PCTA is present in sufficient concentration. This has important implications on the scope of feasible PCTAs. If the molecular weight of the PCTA is increased, and the concentration of ROMP reactions involving that PCTA must be correspondingly increased, viscosity of the reaction medium at some point renders the reaction impracticable. This is especially true for monomers which are solids (such as norbornene).

[‡]Reactions involving cyclooctadiene required an even greater initial monomer concentration, and were typically carried out at 2.7 M.

Other factors that were investigated include reaction time and solvent. Using cyclooctadiene and **12**, no difference was observed between the polymer obtained after 48 hours of reaction time and the polymer obtained from an aliquot of the same polymerization reaction taken after 24 hours of reaction time. In addition, both toluene and benzene solvent yielded similar results for polystyrene PCTAs. It is expected, however, that the identity of the solvent may play an important role by determining the accessibility of the PCTA olefin. Polymeric CTAs may coil more tightly in poor solvents, decreasing the accessibility of their centrally-located olefin and the efficacy of chain transfer. Further investigations into the role of solvent in these reactions are ongoing.

The chemical environment immediately surrounding the olefin of the PCTA was briefly investigated. Using **8** and **9** as the terminating agents in the preparation of the PCTAs, variations were obtained in the steric environment of the PCTA olefin due to the proximity of the attached polystyrene groups. These variations had little or no effect upon the reactivity of the PCTAs, as **12** and **13** behaved quite similarly. In all PCTAs prepared, at least one methylene group was present between the olefin and the nearest styrene unit. Thus, significant variations in the electronic environment of the PCTA olefins were not obtained.

If PCTAs operate analogously with small molecule CTAs, then a ROMP reaction with 200 equivalents of PCTA relative to the catalyst should produce a uniform ABA triblock copolymer wherein the A blocks originate from the PCTA and the B block originates from the monomer. Proving the existence of a triblock structure is most conveniently done by degradation of the central block. In the case of polybutadiene (derived from cyclooctadiene monomer), this can be accomplished using osmium tetroxide. This process should result in a polymer product that is half of the molecular weight of the original PCTA, and contains no olefin groups. Indeed, when the polymer product from a reaction involving **11** and cyclooctadiene is subjected to osmium tetroxide and hydrogen peroxide, the resulting polymer displays no olefinic protons in the ^1H NMR spectrum. The molecular weight of the product, however, is $3,500 \text{ g mol}^{-1}$, which is higher

than expected. The reason for this anomaly is under investigation; possible explanations include coupling of the terminal aldehyde groups that result from the oxidative degradation.

4.4 Conclusions

Symmetric PCTAs have been investigated as a means of controlling molecular weight in ROMP reactions. Molecular weight control is afforded for PCTAs as long as certain requirements are met. In particular, the initial monomer concentration must be above a critical value which is determined by the molecular weight of the PCTA and by the identity of the monomer. Higher molecular weight PCTAs require higher initial monomer concentrations. Because of the corresponding increase in solution viscosity, reactions generally become impracticable with higher molecular weight PCTAs. Our results thus far indicate that this method is suitable for PCTAs with a molecular weight of less than $10,000 \text{ g mol}^{-1}$. Monomers that work best in ROMP reactions with PCTAs include cyclooctene, cyclooctadiene, and possibly derivatives of these molecules in which there is little steric crowding of the olefin. The ability to control the molecular weight of the product decreases with increasing substitution around the olefin in the monomer. Finally, unambiguous determination of the triblock structure of products from ROMP reactions with PCTAs is underway.

Reactions involving asymmetric PCTAs have not yet been thoroughly investigated, although it is evident from preliminary studies that they are considerably less dependent upon reaction conditions compared with reactions involving symmetric PCTAs. By locating the metathesis active site (i.e., the olefin) at the terminus of the PCTA, its accessibility and reactivity appears to be dramatically enhanced. It is therefore expected that the activity of asymmetric PCTAs will be less influenced by factors such as PCTA molecular weight and monomer concentration. Appendix B details the application of asymmetric PCTAs in the synthesis of polyacetylene block copolymers.

4.5 Experimental

General procedures and materials. See also Appendix B. Styrene (Aldrich) was distilled from CaH_2 and stored at $-78\text{ }^\circ\text{C}$ under an atmosphere of argon prior to use. Cyclooctene, 5-bromo-1-pentene and **8** (Aldrich) were degassed by purging with argon prior to use. Cyclooctadiene (Aldrich) was distilled from CaH_2 and stored under an atmosphere of argon prior to use. CH_2Cl_2 was purified by passage through a solvent column prior to use.

Preparation of 9. To an oven dried, 25 mL round bottom flask containing a stir bar was added 1.91 g 5-bromo-1-pentene. The flask was degassed by three freeze/pump/thaw cycles before adding 7 mL of dichloromethane by syringe. Solid catalyst **1** (87 mg) was added to the flask, which was subsequently heated to reflux while maintaining an atmosphere of argon. After 22 h, the reaction flask was cooled to room temperature and solvent was removed under reduced pressure. The product was purified by column chromatography on silica gel 60 (230-400 mesh, EM Science) using a mobile phase of 98% hexane and 2% ethyl acetate, yielding 0.96 g (56%) of a colorless oil.

Example procedure for the synthesis of a symmetrical PCTA. A flame dried, 500 mL flask containing a glass stir bar was cooled under static vacuum. To the flask was added 300 mL of dry, degassed tetrahydrofuran, followed by 1.2 mL of styrene via syringe. The flask was placed in a $-95\text{ }^\circ\text{C}$ hexane/ N_2 bath and then 1.0 mL *sec*BuLi was added by syringe, turning the contents of the flask orange. After 30 min, approximately 0.2 mL of **9** was added dropwise to the flask until the color completely disappeared. The flask was warmed to room temperature, concentrated under reduced pressure, and then precipitated into 300 mL of stirring MeOH. The resulting solid was isolated by filtration and dried under reduced pressure, yielding 1.27 g (68%) of a white powder.

Synthesis of block copolymers. In a typical procedure, the symmetric PCTA was added to a small vial containing a stir bar. The vial was purged with argon for 10 min, the monomer and solvent (either toluene or benzene) were added, and the

mixture was stirred to completely dissolve the polymer (1-2 min). Subsequently, an appropriate amount of a stock solution of the catalyst in solvent was added to the vial via syringe, the vial was placed in an oil bath maintained at 55 °C, and the reaction was stirred under an argon atmosphere for 24 h. The reaction mixture was then cooled to room temperature, precipitated in MeOH, and dried under reduced pressure.

References Cited

- [1] Benedicto, A. D.; Claverie, J. P.; Grubbs, R. H. *Macromolecules*, **1995**, *28*, 500–511.
- [2] Katayama, H.; Fukuse, Y.; Nobuto, Y.; Akamatsu, K.; Ozawa, F. *Macromolecules*, **2003**, *36*, 7020–7026.
- [3] Preishuber-Pflugl, P.; Buchacher, P.; Eder, E.; Schitter, R. M.; Stelzer, F. *J. Mol. Catal. A-Chem.*, **1998**, *133*, 151–158.
- [4] Crowe, W. E.; Mitchell, J. P.; Gibson, V. C.; Schrock, R. R. *Macromolecules*, **1990**, *23*, 3534–3536.
- [5] Bielawski, C. W.; Grubbs, R. H. *Angew. Chem.-Int. Edit.*, **2000**, *39*, 2903–2906.
- [6] Bielawski, C. W.; Benitez, D.; Morita, T.; Grubbs, R. H. *Macromolecules*, **2001**, *34*, 8610–8618.
- [7] Dawkins, J.V.; Houseman, J.H.; Slark, A.T. *Polym. Prep. (Am. Chem. Soc., Div. Polym. Chem.)*, **1999**, *40*, 167–168.
- [8] Moraes, M. A. R.; Moreira, A. C. F.; Barbosa, R. V.; Soares, B. G. *Macromolecules*, **1996**, *29*, 416–422.
- [9] Gluckman, M. S.; Kampf, M. J.; O'Brien, J. L.; Fox, T. G.; Graham, R. K. *J. Polym. Sci.*, **1959**, *37*, 411–423.
- [10] Sill, K.; Emrick, T. *Polym. Prep. (Am. Chem. Soc., Div. Polym. Chem.)*, **2003**, *44*, 823–824.
- [11] Suzuki, N.; Yamaguchi, Y.; Fries, A.; Mise, T. *Macromolecules*, **2000**, *33*, 4602–4606.
- [12] Brintzinger, H. H.; Fischer, D.; Mulhaupt, R.; Rieger, B.; Waymouth, R. M. *Angew. Chem.-Int. Edit. Engl.*, **1995**, *34*, 1143–1170.
- [13] Finne, A.; Albertsson, A. C. *J. Polym. Sci. Pol. Chem.*, **2004**, *42*, 444–452.
- [14] Ryner, M.; Finne, A.; Albertsson, A. C.; Kricheldorf, H. R. *Macromolecules*, **2001**, *34*, 7281–7287.
- [15] Kricheldorf, H. R.; Stricker, A.; Langanke, D. *Macromol. Chem. Phys.*, **2001**, *202*, 2525–2534.
- [16] Yuan, J. Y.; Zheng, Q.; Tao, L.; Pan, C. Y. *Chin. J. Chem.*, **2001**, *19*, 881–884.
- [17] Matyjaszewski, K.; Xia, J. H. *Chem. Rev.*, **2001**, *101*, 2921–2990.
- [18] Jagur-Grodzinski, J. *J. Polym. Sci. Pol. Chem.*, **2002**, *40*, 2116–2133.
- [19] Evans, A. G.; George, D. B. *J. Chem. Soc.*, **1961**, pp 4653–4659.
- [20] Morton, A. A.; Wohlers, H. C. *J. Am. Chem. Soc.*, **1947**, *69*, 167–172.
- [21] Power-Billard, K. N.; Wieland, P.; Schafer, M.; Nuyken, O.; Manners, I. *Macromolecules*, **2004**, *37*, 2090–2095.

- [22] Ueda, K.; Hirao, A.; Nakahama, S. *Macromolecules*, **1990**, *23*, 939–945.
- [23] Quirk, R. P.; Lee, Y. *J. Polym. Sci. Pol. Chem.*, **2000**, *38*, 145–151.
- [24] Smith, M.B.; March, J. *March's Advanced Organic Chemistry*. Wiley, New York, NY, 5th edition, 2001.

Chapter 5

Patterned Polymer Layers Using Surface-Initiated Ring-Opening Metathesis Polymerization

5.1 Abstract

Optimization of reaction conditions for surface-initiated ring-opening metathesis polymerization (SI-ROMP) is reported for a variety of metathesis substrates and catalysts. The combination of SI-ROMP with microcontact printing (μ CP) and dip pen nanolithography (DPN) generated patterned polymer layers on the micrometer and nanometer scale, respectively. The use of SI-ROMP and 1,3,5,7-cyclooctatetraene, along with μ CP or DPN, has been investigated with the goals of forming electrode junctions and patterned molecular wires.

5.2 Introduction

The fixation of polymers to surfaces is vitally important to the study of polymer coatings. The nature of the bonding force between polymer and surface is an important factor in determining the properties and stability of the polymer coating. Bonding forces can be relatively weak, which is often the case with adsorbed polymer films, or relatively strong, as in the case of covalently attached polymers. In general, highly robust polymer coatings that are stable toward solvent, temperature, or other environmental factors are best obtained using covalent attachment methodologies. As a result, much research has recently been directed toward improving the synthesis of surface-grafted polymer (i.e., polymer brush) layers.¹

Two approaches are common for forming polymer brushes.² In the first method, known as *grafting to*, functionalized polymers are reacted with, and thereby attached to a surface. The second method, known as *grafting from*, involves the direct growth of polymers from a surface using a surface-attached initiator species. The latter method has received more attention due to its ability to form brush layers with a higher density of attached polymer molecules. Recently, the versatility of the *grafting from* methodology has been extended by the development of surface-initiated ring-opening metathesis polymerization (SI-ROMP).³⁻⁶ Mild

reaction conditions, short reaction times, and the availability of a diverse group of monomers allow SI-ROMP to claim many benefits over other surface-initiated polymerization methods.

Incorporation of polymer materials into electronic devices such as capacitors and field effect transistors (FETs) is desirable due to the lower weight, easier processability, and lower cost of these materials relative to traditional inorganic materials.^{7,8} Polymer films comprising each of the component layers in FETs have been studied, and, as such, play an important role in determining device performance. The performance of thin-film transistors (TFTs) is most commonly quantified by measuring and comparing two values: field-effect mobility (μ), and on/off ratio.⁹ Mobility is a measure of the average charge carrier drift velocity per unit electric field and is greatly affected by the quality of the semiconductor layer. Example characteristic current-voltage (I/V) data for a top-contact FET (as described in Chapter 1) is shown in Figure 5.1. Mobility as well as on/off ratio (i.e., the ratio between the highest and lowest saturation currents in the I/V plot), can be calculated from these plots and the equation

$$I_{DS} = \frac{WC_i}{2L} \mu (V_G - V_0)^2$$

where I_{DS} is the current between the drain and source electrodes, W is the width between the drain and source electrodes (i.e., channel width), L is the channel length, C_i is the capacitance per unit area of the insulating dielectric layer, V_G is the applied voltage between the gate and source electrodes, and V_0 is the threshold voltage, which is calculated from the plot of $(I_{DS})^{1/2}$ versus gate voltage (see inset of Figure 5.1).

For applications such as the dielectric layer in TFTs, it is important for polymer films to be homogeneously smooth and free of pinholes.¹⁰ Excessive surface roughness can lead to diminished device performance, as it interferes with the interface between the dielectric and the overlying semiconductor layer.

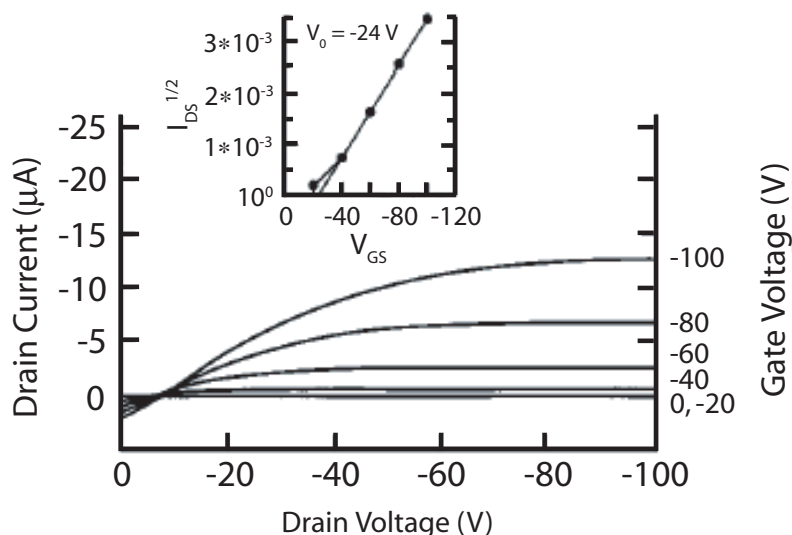


Figure 5.1: Example I/V diagrams for an FET. The large graph shows drain current versus drain voltage for five different gate voltages. The inset shows a plot of the square root of drain current versus gate voltage. Data reprinted from Katz and Bao.⁹

Furthermore, pinholes within the dielectric layer can result in significant current leakage and unacceptable on/off characteristics of the transistor.

Although SI-ROMP with a variety of monomers and conditions has been reported in the literature, only recently has the method been incorporated into the construction of working electronic devices. The first reported preparation of functional FETs utilizing SI-ROMP for the production of the dielectric layer is reprinted in Appendix C. We report here additional results that have been obtained using SI-ROMP and catalysts **1** and **2**.

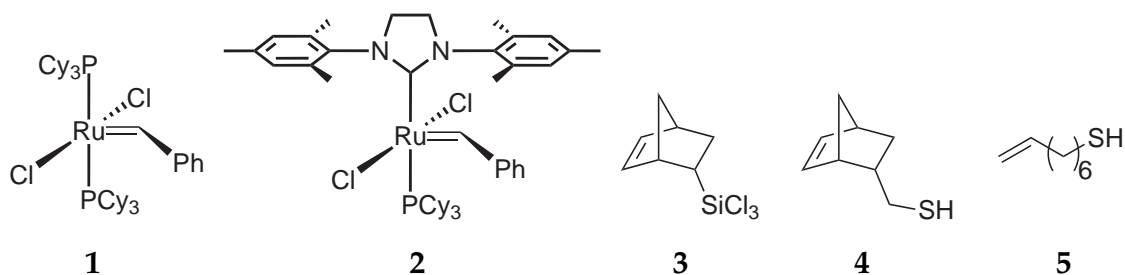


Figure 5.2: Catalysts and linking molecules employed in SI-ROMP.

As described in Appendix C, polymer brush layers were covalently attached to metal and metal oxide surfaces using a *grafting from* approach. The surfaces were first functionalized with self-assembled monolayers (SAMs) of olefin-containing linking molecules such as **3**, **4** or **5**. An olefin metathesis catalyst (**1** or **2**) was then allowed to react with and attach to the surfaces. Exposure of the catalyst-functionalized surfaces to a solution of cyclic olefin monomer afforded the desired polymer brush layers. Each step in the process was followed by extensive solvent washings to remove unbound linker, catalyst, or polymer molecules. The resulting films were characterized by atomic force microscopy (AFM), ellipsometry, profilometry, and optical microscopy. Thin-film transistors were prepared using the polymer brushes as the dielectric layer (see Appendix C). The electronic properties of these FETs were characterized and compared to devices prepared using inorganic dielectrics. In addition, patterns of polymer brush layers were prepared using microcontact printing and dip pen nanolithography.

5.3 Results and Discussion

5.3.1 Electronic Devices Using SI-ROMP

Many factors were determined to influence SI-ROMP reactions and the resulting polymer layers. These include environmental factors such as reaction conditions, chemical factors such as the reactivity of the linking species, catalyst, and monomer, and procedural factors such as post-polymerization heat treatment.

Before any of these variables could be investigated, however, it was first discovered that (as in many other cases) the purity of the reagents can be a determining factor in the success of SI-ROMP. Two examples illustrate this point. In the first example, all initial SI-ROMP reactions involving norbornene monomer and 1,2-dichloroethane (DCE) solvent, regardless of reaction conditions and the identity of the catalyst or linking species, yielded poor to moderate results. Polymer film thicknesses rarely exceeded 100 nm, and were often significantly

lower. This problem was eliminated simply by filtering the DCE through a short column of neutral alumina before use. Treatment of the polymerization solvent in this manner significantly improved results, allowing the production of the thick polymer films (up to 3 μm) that are discussed below. The difficulty in using untreated DCE solvent is thought to be due to the presence of a small amount of HCl, an impurity that is generated by the decomposition of DCE. This impurity is apparently able to significantly decrease the reactivity of the surface-attached catalyst. In support of this hypothesis, a series of SI-ROMP reactions were attempted using DCE solutions of norbornene monomer. If the monomer solution is used immediately upon preparation, the resulting polymer film has a thickness of approximately 10 nm. Addition of a small amount of triethylamine to the monomer solution affords a polymer film over 100 nm thick. Alternatively, allowing a solution of the monomer to sit for 8-12 hours at room temperature before use yields a polymer film greater than 800 nm thick. Finally, preparing a new monomer solution using alumina-filtered DCE affords a polymer film in excess of 1.5 μm thick. Presumably in these experiments, the HCl impurity is removed, either by neutralization with triethylamine, by slow reaction with the olefin of norbornene, or by filtration with alumina.

In the second example, initial attempts at using dicyclopentadiene (DCPD) as the monomer in SI-ROMP reactions yielded no polymer films whatsoever. However, purification of the DCPD solution (most conveniently by filtration through a short plug of alumina) allowed the preparation of polymer films with thickness in excess of 1.5 μm . It is likely that a small amount of cyclopentadiene, which is known to inhibit catalysts **1** and **2**, is present as an impurity in the DCPD. Interestingly, alumina treatment of the monomer solution works only for **2**; conditions for the successful SI-ROMP of DCPD with **1** have yet to be determined.

These examples show the sensitivity of SI-ROMP toward trace impurities in the reagents. Furthermore, they indicate that unsuccessful SI-ROMP reactions may be a result of insufficient purification methods, rather than an inherent inability of the monomer to polymerize from surface attached catalysts.

Application of SI-ROMP in the area of electronic devices requires the ability to produce uniform polymer films of controlled thickness. Previous reports have demonstrated control of polymer layer thicknesses up to approximately 100 nm.⁵ In agreement with these reports, we have found that monomer solution concentration is a convenient way in which to control the thickness of the resulting polymer film. Using catalyst **1** and norbornene monomer, polymer film thickness was found to depend (approximately linearly) upon the concentration of the monomer solution (Figure 5.3a).

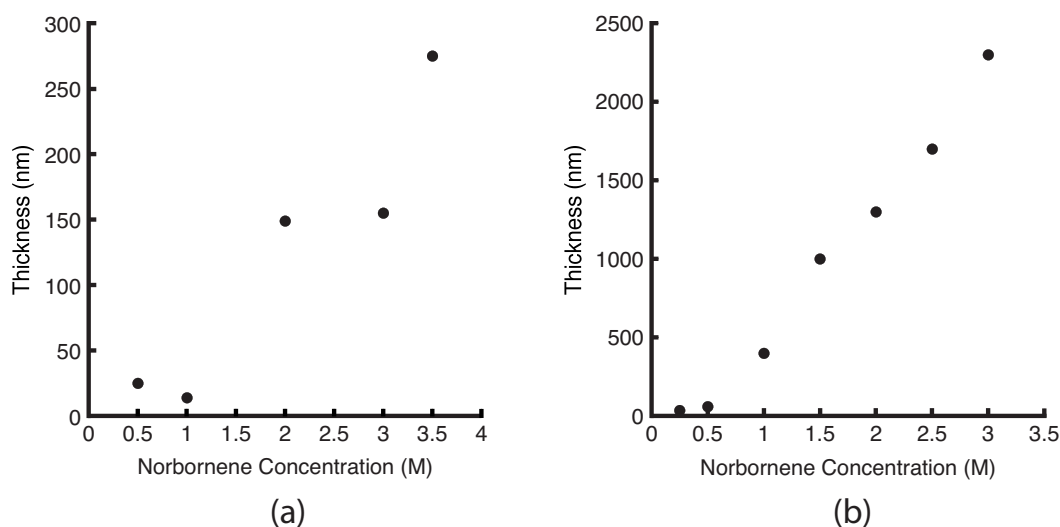


Figure 5.3: Variation in polynorbornene film thickness with monomer solution concentration using (a) catalyst **1**; (b) catalyst **2**. Note the different y-axis scales. For both graphs, polymerizations were carried out at room temperature for 15 minutes.

Unfortunately, SI-ROMP reactions involving **1** produced a practicable upper limit in polymer layer thickness of approximately 300 nm. These polymer films were found to suffer from unacceptable leakage current when utilized as the dielectric layer of FET devices. One possible approach toward addressing this problem is through the use of thicker polymer films, which might be obtained using a more active metathesis catalyst. Catalyst **2** is known to be much more highly active than catalyst **1** in solution-based ROMP reactions. This was also

found to be the case for SI-ROMP reactions. As shown in Figure 5.3b, polymer layers in excess of 2 μm were easily obtained using mild reaction conditions and short reaction times.

In the SI-ROMP reactions that produced the results shown in Figure 5.3, polymerization times (i.e., the duration of time in which the catalyst-functionalized surfaces were submerged in the monomer solution) were limited to 15 min, and reaction temperatures were maintained at room temperature. These conditions were determined to be optimal for producing the thickest possible polymer brush layers. The polymer layer remains relatively constant in thickness between 15 min and 1 h of polymerization time. For polymerization times greater than 1 h, the resulting polymer layer begins to decrease in thickness. Polymerizations allowed to continue for 24 h or more result in virtually no surface attached polymer layers whatsoever.* It seems likely that secondary metathesis reactions are occurring between active polymer chain ends and the backbone olefins of adjacent surface attached polymer chains. Alternatively, surface-attached catalyst which does not immediately initiate polymer growth may be reacting with the polymer molecules that form nearby. These "backbiting" reactions, as shown in Figure 5.4, would result in polymeric fragments that are no longer attached to the surface. This process would decrease the thickness of the final polymer layer. Furthermore, secondary metathesis reactions are known to occur more slowly than ROMP,¹¹ which seems to account for the time dependency of this phenomenon.

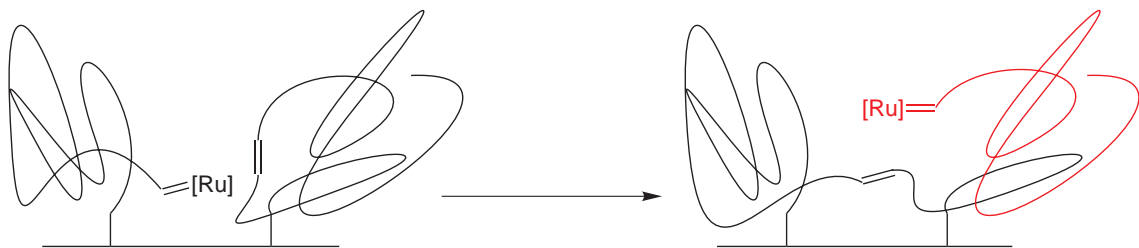


Figure 5.4: Secondary metathesis reaction producing non-surface-bound polymer.

*The same trend has been observed by increasing the polymerization temperature, although further studies are necessary to confirm this result.

Although short reaction times are a highly attractive aspect of SI-ROMP, the optimization of reaction times that is required to obtain a polymer film of desired thickness is inconvenient. Stability of the polymer layer toward long reaction times can be achieved by attaching each polymer molecule to the surface in multiple locations. This is most conveniently achieved by cross-linking the polymer film, for example by using a multifunctional monomer. Dicyclopentadiene (DCPD), the product of a Diels-Alder reaction between two cyclopentadiene molecules, is well studied for its ability to crosslink in ROMP reactions with metathesis catalysts.¹² As expected, SI-ROMP reactions involving DCPD monomer produced films that were stable toward long reaction times (Figure 5.5). While secondary metathesis reactions are still possible, they apparently do not lead to fragments of free (i.e., not surface-bound) polymer chains. The thickness of these polymer films is nearly independent of polymerization time (given sufficient reaction time for film formation - i.e., 15-30 min), yet remains highly dependent upon the monomer solution concentration.

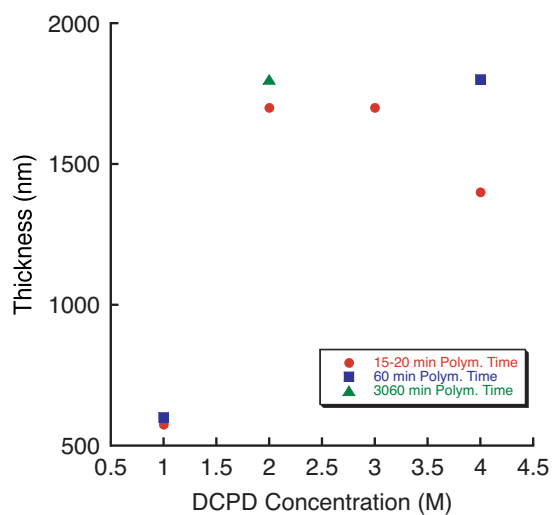


Figure 5.5: Variation in poly(DCPD) film thickness with monomer solution concentration and polymerization time.

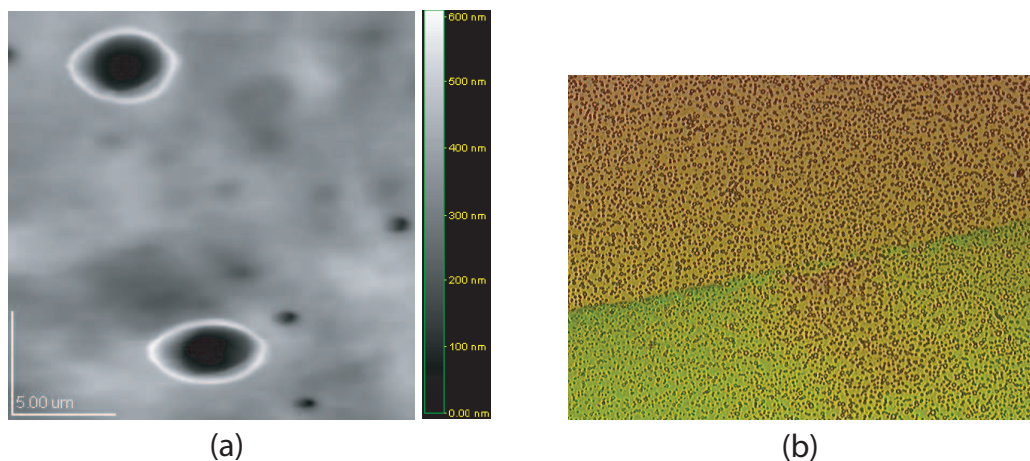


Figure 5.6: (a) AFM image of a polynorbornene film. (b) Optical micrograph (20x magnification) of a polynorbornene film.

Polynorbornene films were characterized immediately after their formation. Both optical microscopy and AFM indicated that numerous pinholes of various sizes were present (see, for example, Figure 5.6), and TFTs using these films suffered from significant leakage current. In an effort to eliminate these pinholes, the polynorbornene films were annealed at 135 °C for 15-60 min. This temperature, which is significantly above the glass transition temperature of the polymer, allows the polymer chains to reorient themselves and fill any voids on the surface. Characterization of the annealed films indicated that the pinholes were significantly reduced in size and number (Figure 5.7). Indeed, annealed polynorbornene films displayed significantly less leakage current, and when used as the dielectric layer in TFTs provided a large improvement in on/off ratios.

As with polynorbornene films, polymer films produced from SI-ROMP of DCPD also showed large numbers of pinholes. Annealing the DCPD films, however, did not lead to a reduction in their size or number. This is further evidence that the DCPD films undergo crosslinking reactions, as it is likely that crosslinked polymers would not possess the mobility that is present in non-crosslinked films. The DCPD films are thus not able to undergo the reorientation that reduces the presence of pinholes in polynorbornene films.

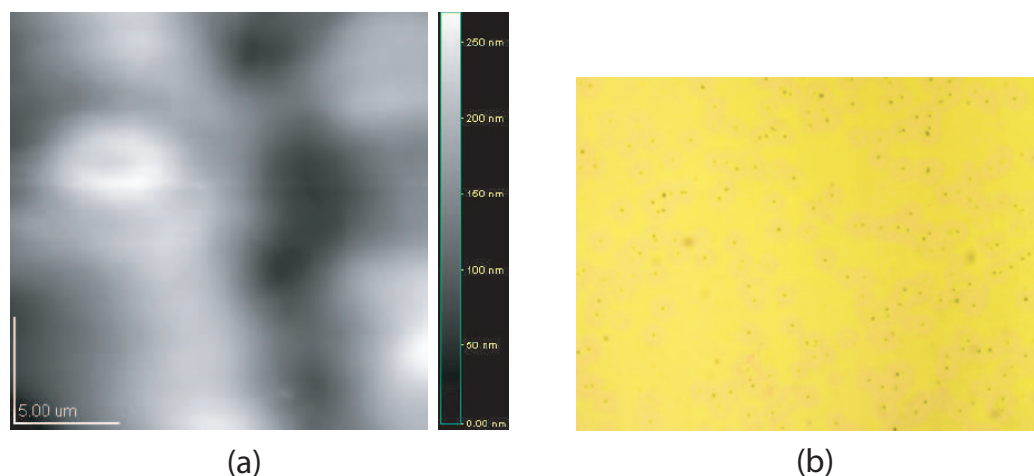


Figure 5.7: (a) AFM image of an annealed polynorbornene film. (b) Optical micrograph (200x magnification) of an annealed polynorbornene film.

The source of the pinholes observed in SI-ROMP films is not yet clearly understood, although it is likely that incomplete catalyst coverage is one source. Surface measurements (described in Appendix C) indicate that the density of ruthenium on catalyst-functionalized surfaces (i.e., before the polymerization step) is very low. This could result from the catalyst reacting with multiple linker molecules, in effect forming polymers of **4** or **3** on the surface. It could also indicate that steric crowding or low reactivity is preventing the formation of a high density of surface-attached catalyst molecules (as might be expected using linker **5**). Previous efforts to overcome these complications have involved mixed monolayers of metathesis active and metathesis inactive thiols. Investigations with different linking molecules, as well as mixed monolayers, are currently underway in an effort to produce more uniform SI-ROMP polymer layers.

With the goal of developing TFTs constructed solely from organic molecules, pentacene semiconducting layers were employed. The mobility of TFTs utilizing pentacene as the semiconductor is highly dependent upon the quality and grain size of the pentacene film.⁹ Surface roughness of SI-ROMP polynorbornene films was characterized using AFM. Despite the presence of pinholes, images such as those in Figures 5.6 and 5.7 indicate that the films are relatively smooth:

surface roughness does not typically exceed about 10% of the film thickness. Nevertheless, the mobilities reported in Appendix C are lower than those from traditional TFTs constructed with inorganic dielectric layers. The crystalline domains in the pentacene layers of the TFTs reported here must therefore be smaller, indicating that the interface between the dielectric layer and the pentacene layer is inferior to traditional devices (i.e., those prepared by spin coating the dielectric layer). This may result from the harsh conditions that are employed for vapor deposition of the pentacene layer, which could potentially be damaging the polynorbornene film. Indeed, TFTs formed using the lamination method (which avoids vapor deposition of the semiconductor over the dielectric) result in significantly improved mobilities.

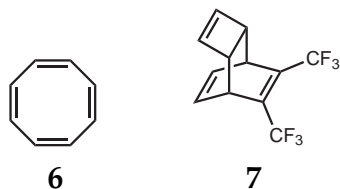
The results presented in Appendix C indicate that SI-ROMP polymer films are well suited for applications in electronic devices. Further optimization of the reaction conditions, with the goal of improving film quality and reproducibility, is currently underway. In addition, TFTs that utilize multiple SI-ROMP layers (in particular, the dielectric and semiconducting layers) which are covalently attached at their interface are also under investigation.

5.3.2 Patterning of SI-ROMP Layers

The construction of TFTs requires an ability to pattern at least one of the component layers. For example, in the TFTs described in Chapter 1, the source and drain electrodes are present in a regular pattern of discrete lines. The dimensions and spacing between the electrodes are important factors in calculating device mobility. For the long-term goal of applying SI-ROMP in the production of all-organic TFTs, two capabilities are required: the ability to deposit conducting polymers, and the ability to pattern the deposited polymer layers.

Conducting polymers have gained considerable attention in recent years, and are discussed at length in Appendix B. As numerous reports have shown, monomers such as 1,3,5,7-cyclooctatetraene (COT, **6**) and **7** allow the preparation of

conducting polymers using ROMP. These monomers have been used in our initial attempts to address the requirements listed above.



Depending upon the length scale required, several methods have recently been developed for patterning a variety of materials on surfaces. Among those methods, microcontact printing (μ CP)¹³ and dip pen nanolithography (DPN)¹⁴ are excellent methods for preparing patterned thiols on gold substrates at the micrometer and nanometer scales, respectively. Both methods have been applied to SI-ROMP, although for μ CP, only silicon substrates have so far been employed.^{5, 15, 16} Using thiols such as **4** and **5**, as well as monomers **6** and **7** we have begun to investigate the preparation of patterned, conducting polymer layers using SI-ROMP and either μ CP or DPN.[†]

A stamp suitable for μ CP was prepared by molding a poly(dimethylsiloxane) (PDMS) resin onto an AFM calibration grating. The resulting negative image displayed a well defined grating with a step height of 1040 nm and a 3 μ m pitch. Using this stamp, gold surfaces were modified with patterned SAMs of **4**. Relative to forming unpatterned SAMs from thiol solutions, the stamping process is very rapid, requiring less than 1 min of exposure of the gold surface to the thiol-coated stamp. The resulting patterned surfaces were exposed to catalyst and monomer solutions as described for unpatterned surfaces.

In many cases, evidence of patterned polymer growth could be visually observed on the gold surfaces. The surfaces were further characterized by optical microscopy and AFM. All patterned SI-ROMP polymers displayed appropriate pitch (i.e., spacing), with an average value of 3.0 μ m and a range of 2.5–3.5 μ m.

[†]The portion of this research involving DPN was carried out largely by Xiaogang Liu under the direction of Chad Mirkin at Northwestern University.

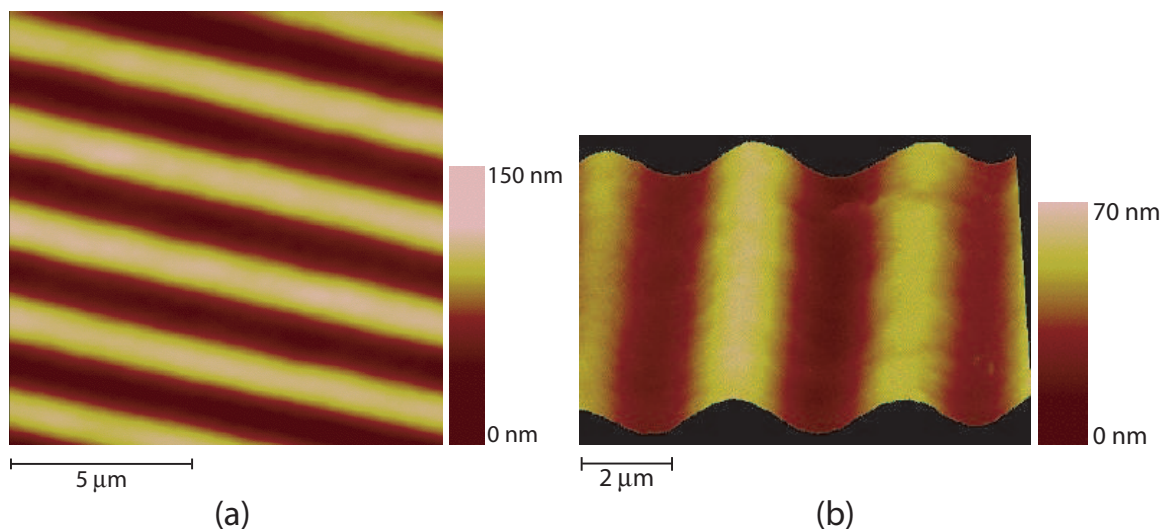


Figure 5.8: AFM images of patterned polynorbornene layers produced by μ CP: (a) top view; (b) edge view. The images were obtained using different samples.

In the case of patterned polynorbornene, step heights were difficult to discern, as the polymer patterns did not typically display well-defined edges. This indicates that the polymer is growing in all directions, and although the catalyst is confined to specific areas on the surfaces, the growth of polymer lessens the resolution of these areas (Figure 5.8). Thus, rather than step heights, peak-to-trough heights were measured by AFM. Preliminary results indicate that control over polymer growth can be very roughly obtained using the monomer solution concentration. Neither the concentration of the thiol solution, nor the time of exposure of the gold surface to the thiol-coated PDMS stamp seem to have significant influence on the resulting polymer layer. As seen previously, long polymerization times yield reduced film thickness: using 1.5 M norbornene, 20 min polymerization time yields 145 nm thick patterns, while 325 min polymerization time yields only 95 nm thick patterns. Many more studies remain to be done in order to claim a thorough understanding of this method. In particular, the purity and identity of the linking molecule appears to be highly influential in determining polymer film thicknesses. It seems likely that slightly diluted SAMs of the linking molecule (e.g., mixed SAMs using a second, metathesis inactive thiol) lead to an

increased density of catalyst that is covalently bound to the surface, and hence to thicker polymer layers.

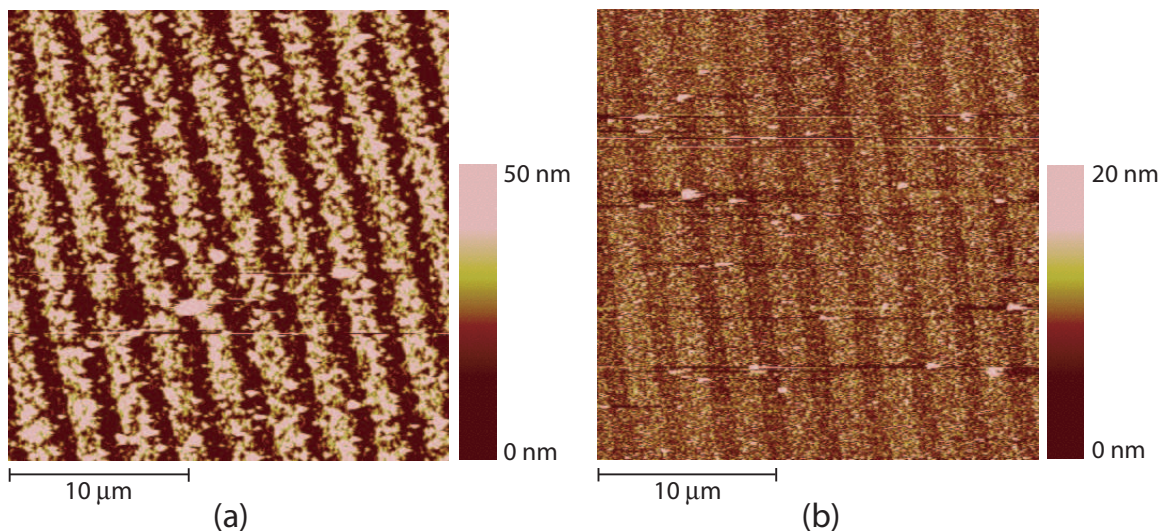
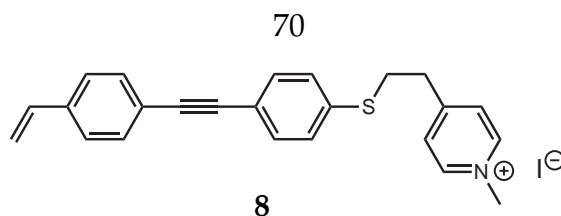


Figure 5.9: AFM images of polymer patterns produced by μ CP: (a) Poly(DCPD); (b) Poly(COT).

In addition to norbornene, both DCPD and COT have been investigated in SI-ROMP reactions using μ CP. As shown in Figure 5.9a, reactions involving DCPD produce patterned polymer layers of significant surface roughness. Thicknesses of the poly(DCPD) layers are also substantially lower than those for polynorbornene, given identical reaction conditions. In the case of COT, even in the absence of solvent (i.e., neat monomer), only minimal polymerization is observed (Figure 5.9b). It is possible that the ROMP of COT, which is very nearly thermodynamically neutral, requires a catalyst density greater than that which is presented by the catalyst-functionalized surfaces.[‡] Preliminary work using dip pen nanolithography (DPN) indicates that SAMs produced using different linking molecules, such as **8**, can lead to increased efficiency and yield in SI-ROMP reactions with COT.

[‡]Alternatively, ring-closing metathesis reactions (forming benzene) may be favorable in SI-ROMP experiments with COT.



The polymer layers that are formed using COT are highly non-uniform in thickness. Indeed, AFM images of the products from these reactions show the formation of pillars, rather than films (Figure 5.10). This may be a result of the highly rigid nature of poly(COT). Because of tip effects, the width of these pillars is difficult to determine from AFM images. However, the observed variation in width may indicate that each pillar is composed of numerous poly(COT) chains oriented normal to the substrate and aligned side by side. This sort of behaviour has also been seen in block copolymers containing poly(COT), as described in Appendix B.

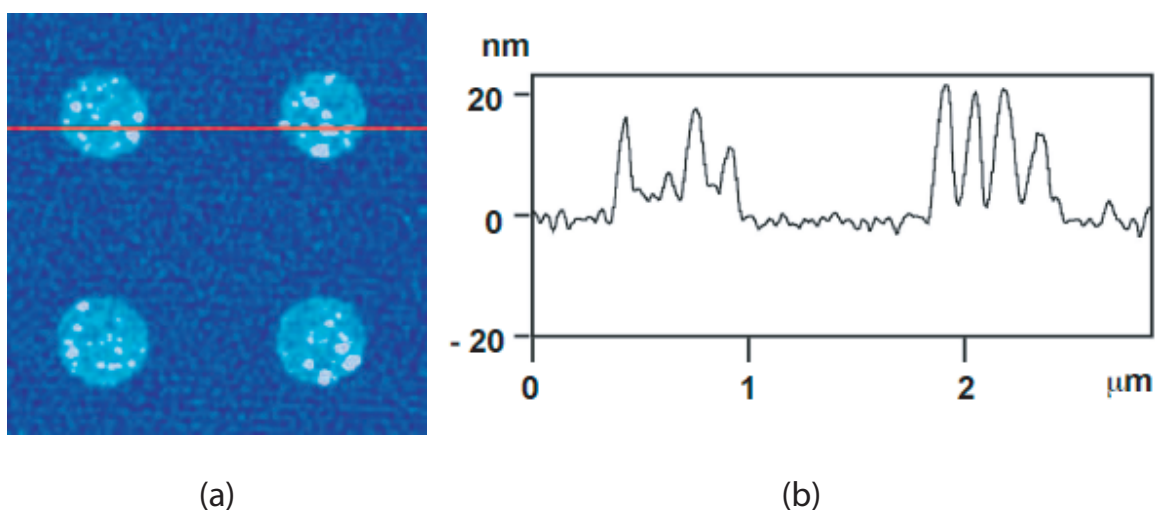


Figure 5.10: AFM images of poly(COT) patterns produced by DPN: (a) top view; (b) profile of red line in (a).

Alternative procedural methods for patterning polymer layers are possible, and remain to be investigated. For example, unpatterned SAMs could be exposed to a PDMS stamp coated with the catalyst. It may also be possible to form a patterned polymer layer by exposing an unpatterned, catalyst-functionalized SAM to a PDMS stamp coated with a ROMP monomer, although this procedure would

most likely provide polymer layers of only limited thickness. Finally, negative images of the PDMS stamp may be possible by pressing and holding the stamp against a catalyst-functionalized surface while introducing the monomer solution or a vapor of the monomer. Polymerization would then be expected to occur only in the areas not covered by the PDMS stamp. This process has been investigated in the case of non-covalently attached catalyst,¹⁷ and is expected to work equally well for SI-ROMP experiments.

5.4 Conclusions

Development of SI-ROMP is ongoing, in particular as it relates to the production of component layers in electronic devices. We have shown that SI-ROMP is possible with both norbornene and DCPD, using a variety of solvents and linking molecules. Polynorbornene layers are unstable over time in the presence of catalyst, presumably due to secondary metathesis reactions that create non-surface bound polymer fragments. This drawback can be overcome by using a crosslinkable monomer such as DCPD. We have also shown that SI-ROMP can be used in conjunction with patterning techniques such as μ CP and dip pen nanolithography in order to form patterned layers of surface attached polymers. We are currently working toward the production of surface-attached conducting polymers using SI-ROMP, μ CP or DPN, and monomers such as COT. Current goals of this research include the formation of semiconducting layers for TFTs and poly(COT) electrode junctions.

5.5 Experimental Section

Materials. Acetone, isopropyl alcohol, ethanol, 8-bromo-1-octene, tetrahydrofuran (anhydrous), hexamethyldisilathiane, tetrabutylammoniumfluoride (1.0 M in THF with 5% H₂O), and bicyclo[2.2.1]hept-2-ene (norbornene) were used as received from Aldrich. Dichloromethane (Aldrich, anhydrous) was degassed prior

to use by sparging with argon. 1,2-dichloroethane (Aldrich, anhydrous) was first filtered through a plug of neutral alumina (Brockman Grade I; this procedure is necessary in order to have film growth), and then degassed by sparging with argon. 5-(Bicycloheptenyl)trichlorosilane (**3**) was purchased from Gelest, Inc., and used as received. Bicyclo[2.2.1]hept-5-ene-2-methanethiol (**4**) was prepared as described in the literature.¹⁸ Catalysts **1**¹⁹ and **2**²⁰ were prepared as described in the literature. 7-Octene-1-thiol (**5**) was prepared according to a literature procedure,²¹ with 8-bromo-1-octene as starting material.

Substrate preparation and metal/organic semiconductor deposition. Silicon wafers containing a 3000 Å thermally grown oxide layer were obtained from Silicon Quest International. Gold substrates (typically composed of a 500 or 1000 Å layer of gold over a 50 or 100 Å layer of titanium, both vacuum deposited in an e-beam evaporator) were prepared on silicon wafers containing a native oxide layer (Silicon Quest International). Substrates were cut into 1 cm² squares, individually cleaned by sequential washings with acetone, deionized water, and *i*PrOH, and dried in a stream of dry nitrogen (N₂). The substrates were then soaked in a boiling solution of H₂O/H₂O₂/NH₄OH (5:1:1) for 30 min, washed with water and *i*PrOH, and dried with dry N₂.

Surface functionalization. In a typical procedure using gold substrates, self-assembled monolayers (SAMs) were formed by submerging freshly cleaned substrate squares in a filtered solution of thiol in absolute EtOH (typically 0.5 or 0.75 mM) for 24 h. The squares were then removed and washed, first with EtOH, then with *i*PrOH before being dried in a stream of dry N₂. Using Si/SiO₂ substrates, freshly cleaned squares were submerged for 6 h in a 0.5 wt% solution of trichlorosilane in pentane in a N₂ glovebox. The squares were then removed, sonicated for 5 min each in toluene (2 times), 50/50 toluene/acetone, and acetone, and dried in a stream of dry N₂.

Reaction of the olefin-functionalized substrates with catalyst was done in dichloromethane solutions of catalyst **1** or **2** (typically 13 or 25 mM) at room temperature (rt) or 40 °C. After the prescribed length of time, the squares were

removed from solution, washed thoroughly with dichloromethane, and dried under N₂. They were then immediately placed in a fresh, filtered solution of norbornene in 1,2-dichloroethane or toluene and allowed to react for a prescribed length of time at rt or 40 °C. The squares were then washed thoroughly with dichloromethane and dried under vacuum.

Device construction. For the FETs using a gold strip as the gate electrode deposited on SiO₂ (both lamination and direct deposition methods), linker **4** and catalyst **2** were used. Catalyst attachment and norbornene polymerization were done at rt for 10 min and 15 min, respectively. The thickness of the polynorbornene film was 1.2 μm for the lamination devices, and ranged from 800 to 1100 nm for the direct deposition samples. In mobility calculations, a width (W) of 2–3 mm and length (L) of 1 mm were used for the laminated devices. A width of 940 μm and length of 240 μm were used for the direct deposition devices.

For the FETs using Si/SiO₂ as gate electrode, catalyst attachment was done with dichloromethane solutions of catalyst **1** or **2** at rt for 10 min, and the polymerizations were carried out with 1,2-dichloroethane solutions of norbornene (between 2 and 4 M) at rt, times varying between 15 and 40 min. The thickness of the polynorbornene films, which were very smooth and did not require annealing, ranged between 230 and 800 nm, but only those films thicker than 600 nm were used to make TFTs.

The organic semiconducting layer of pentacene (Aldrich) was deposited by thermal evaporation under vacuum (typically to a thickness of 300 Å). Gold overlayers were deposited in an e-beam evaporator under vacuum.

Microcontact printing. An Ultrasharp AFM calibration grid (silicon grating TGZ04, MikroMasch) was placed in a small petri dish. Poly(dimethylsiloxane) resin (Sylguard 184, Dow Corning) was added to the dish and allowed to cure according to the manufacturer's specifications. The resulting mold was cut into a small, 1 cm³ cube to produce a stamp suitable for μCP. A patterned SAM was prepared by first placing a small amount of a solution of thiol in absolute EtOH (typically 0.5 or 0.75 mM) onto the PDMS stamp using a cotton applicator tip.

After allowing the stamp to dry for approximately 1 min in air, the stamp was lightly pressed onto a clean gold surface and held in place for approximately 20 sec. The stamp was removed and the gold surface was washed with EtOH. Catalyst attachment and polymerization reactions using the patterned SAM were performed as detailed above.

Characterization. Ellipsometric measurements were performed on a Rudolph Ellipsometer AutoEL. Profilometric measurements were measured using a Dektak 3030. Current-voltage characteristics were obtained with a Hewlett-Packard (HP) 4155A semiconductor parameter analyzer. AFM Tapping Mode data was acquired on a JEOL JSPM-4210 scanning probe microscope in a nitrogen environment. "NONCONTACT ULTRASHARP" silicon cantilevers were purchased from NT-MDT, Ltd. Rutherford backscattering spectroscopy (RBS) and medium energy ion scattering (MEIS, a low energy ultrahigh resolution variant of RBS) were performed at the Rutgers University ion scattering facility. 1.5 MeV He ions (in RBS) and 100 keV protons (in MEIS) were used to quantify film composition and thickness.

References Cited

- [1] Zhao, B.; Brittain, W. J. *Prog. Polym. Sci.*, **2000**, *25*, 677–710.
- [2] Edmondson, S.; Osborne, V. L.; Huck, W. T. S. *Chem. Soc. Rev.*, **2004**, *33*, 14–22.
- [3] Weck, M.; Jackiw, J. J.; Rossi, R. R.; Weiss, P. S.; Grubbs, R. H. *J. Am. Chem. Soc.*, **1999**, *121*, 4088–4089.
- [4] Watson, K. J.; Zhu, J.; Nguyen, S. T.; Mirkin, C. A. *J. Am. Chem. Soc.*, **1999**, *121*, 462–463.
- [5] Kim, N. Y.; Jeon, N. L.; Choi, I. S.; Takami, S.; Harada, Y.; Finnie, K. R.; Girolami, G. S.; Nuzzo, R. G.; Whitesides, G. M.; Laibinis, P. E. *Macromolecules*, **2000**, *33*, 2793–2795.
- [6] Juang, A.; Scherman, O. A.; Grubbs, R. H.; Lewis, N. S. *Langmuir*, **2001**, *17*, 1321–1323.
- [7] Drury, C. J.; Mutsaers, C. M. J.; Hart, C. M.; Matters, M.; de Leeuw, D. M. *Appl. Phys. Lett.*, **1998**, *73*, 108–110.
- [8] Garnier, F.; Hajlaoui, R.; Yassar, A.; Srivastava, P. *Science*, **1994**, *265*, 1684–1686.
- [9] Katz, H. E.; Bao, Z. *J. Phys. Chem. B*, **2000**, *104*, 671–678.
- [10] Bao, Z. N. *Adv. Mater.*, **2000**, *12*, 227–230.
- [11] Choi, T. L.; Grubbs, R. H. *Angew. Chem.-Int. Edit.*, **2003**, *42*, 1743–1746.
- [12] Rule, J. D.; Moore, J. S. *Macromolecules*, **2002**, *35*, 7878–7882.
- [13] Smith, R.K.; Lewis, P.A.; Weiss, P. S. *Prog. Surf. Sci.*, **2004**, *75*, 1–68.
- [14] Ginger, D. S.; Zhang, H.; Mirkin, C. A. *Angew. Chem.-Int. Edit.*, **2004**, *43*, 30–45.
- [15] Liu, X. G.; Guo, S. W.; Mirkin, C. A. *Angew. Chem.-Int. Edit.*, **2003**, *42*, 4785–4789.
- [16] Harada, Y.; Girolami, G. S.; Nuzzo, R. G. *Langmuir*, **2003**, *19*, 5104–5114.
- [17] Gu, H. W.; Fu, D.; Weng, L. T.; Xie, J.; Xu, B. *Adv. Funct. Mater.*, **2004**, *14*, 492–500.
- [18] Inokuma, S.; Sugie, A.; Moriguchi, K.; Shimomura, H.; Katsube, J. *Heterocycles*, **1982**, *19*, 1909–1913.
- [19] Schwab, P.; Grubbs, R. H.; Ziller, J. W. *J. Am. Chem. Soc.*, **1996**, *118*, 100–110.
- [20] Sanford, M. S.; Ulman, M.; Grubbs, R. H. *J. Am. Chem. Soc.*, **2001**, *123*, 749–750.
- [21] Hu, J.; Fox, M. A. *J. Org. Chem.*, **1999**, *64*, 4959–4961.

Appendix A

Synthesis of A,B-Alternating Copolymers by Ring-Opening-Insertion Metathesis Polymerization

This has previously appeared as: Choi, T.-L.; Rutenberg, I.M.; Grubbs, R.H.
Angewandte Chemie, International Edition, **2002**, *41*, 3839–3841.

A.1 Abstract

Ring-opening-insertion metathesis polymerization (ROIMP), a new approach for generating A,B-alternating copolymers via metathesis polymerization, is reported. The ring-opening metathesis polymerization of cyclic olefins, initially generating a polymer containing internal olefins along the backbone, is followed by insertion of acyclic, bis(α,β -unsaturated carbonyl) terminal olefins using a highly active ruthenium-based olefin metathesis catalyst. The generality of ROIMP is demonstrated by the polymerization of several cyclic and acyclic monomer combinations, each generating A,B-alternating copolymers in high yield and with degrees of alternation greater than 95%.

A.2 Introduction

Alternating copolymers are normally formed by step growth polymerization of AA-BB monomers and in some special chain growth reactions.^{1,2} Although recent developments in ring opening metathesis polymerization (ROMP)³⁻⁵ and acyclic diene metathesis polymerization (ADMET)⁶ have extended the versatility of both chain growth and step growth reactions, these metathesis polymerizations have not provided a general solution to alternating copolymerization. Examples of alternating copolymers by ROMP are rare due to the difficulty of finding systems in which there is an alternation in the affinity of the propagating metal carbene for the monomers.⁷⁻⁹ Although ADMET is a step growth polymerization, examples of alternating copolymerization with two monomers by this mechanism have not been reported since most olefins studied have similar reactivity. Therefore, a general metathesis route toward A,B-alternating copolymers would open the way to the synthesis of new functional polymers.

Although well-defined olefin metathesis catalysts such as $((\text{CF}_3)_2\text{MeCO})_2(\text{ArN})\text{-Mo}=\text{CH}(t\text{-Bu})$ (**1**) and $\text{Cl}_2(\text{PCy}_3)_2\text{Ru}=\text{CHPh}$ (**2**) have proven useful for polymer synthesis, the highly active catalyst **1** suffers from sensitivity to some polar

functional groups¹⁰ and the highly functional group tolerant catalyst **2** shows decreased reactivity.¹¹ These disadvantages were recently addressed with the development of catalyst **3**, which exhibits high activity and remains tolerant of many functional groups.¹² Furthermore, catalyst **3** promotes ring-closing metathesis and selective cross metathesis of α,β -unsaturated carbonyl olefins with high conversions,^{13–18} thereby expanding the scope of olefin metathesis in organic synthesis. This suggests that catalyst **3** should be able to produce polymers from α,β -unsaturated carbonyl olefins. Also, if the coupling between internal olefins and α,β -unsaturated carbonyl olefins is selective, as is the case in cross metathesis, diacrylate monomers should be selectively inserted into ROMP polyolefins to yield alternating copolymers (Scheme A.1). Herein, we report the development of a new method for synthesizing A,B-alternating copolymers by ring opening insertion metathesis polymerization (ROIMP).

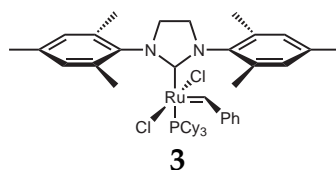
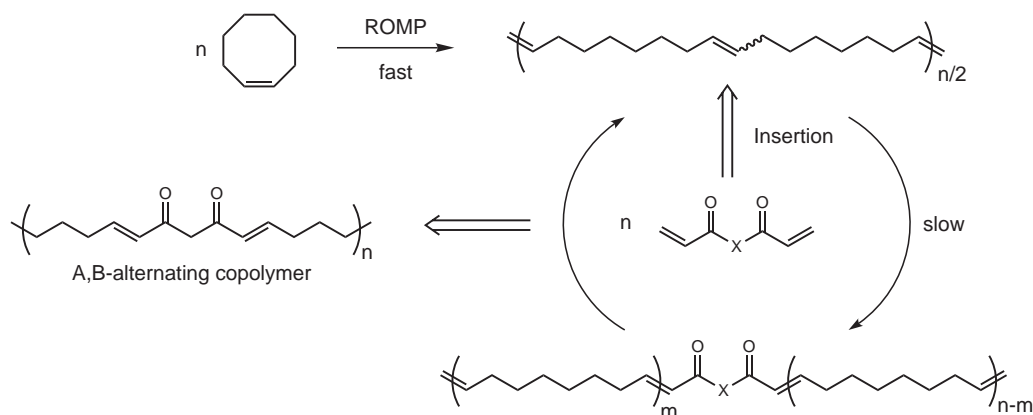


Figure A.1: Ruthenium olefin metathesis catalyst.

Scheme A.1: Proposed mechanism for ROIMP.



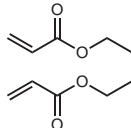
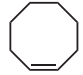

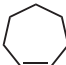
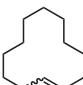
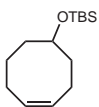
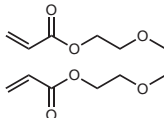
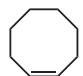
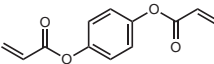
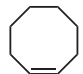
A.3 Results and Discussion

Treatment of a 1:1 mixture of monomers A (diacrylates) and B (cycloalkenes) with catalyst **3**, indeed, yielded highly A,B-alternating copolymers in high isolated yields. Examples of A,B-alternating copolymers from a variety of diacrylates and cycloalkenes are shown in Table A.1. For example, using a total monomer to catalyst ratio of just 290:1, a 1:1 mixture of 1,4-butanediol diacrylate and cyclooctene gave a copolymer with up to 99% A,B-alternation and a molecular weight of 90,100 g mol⁻¹ (entry 1). It is important to match the stoichiometry of cyclooctene because any excess of cyclooctene results in oligocyclooctene blocks, lowering A,B-alternation.

The extent of A,B-alternation could be easily determined by ¹H NMR, since olefinic protons for A,B-alternating units have a distinct chemical shift from the starting materials and homo-coupled units. E-Acrylate dimers produce a sharp singlet at 6.9 ppm (Figure A.2a), while polycycloalkenes display a multiplet at 5.4 ppm (Figure A.2c). On the other hand, A,B-alternating units produce a doublet of triplets at 7.0 ppm and a doublet at 5.8 ppm (Figure A.2b). Therefore, the extent of A,B-alternation can be easily calculated by integrating these peaks. The sharp coupling patterns demonstrate a highly uniform polymer structure with E olefin isomer ($J = 15.9$ Hz). ¹³C NMR also shows high A,B-alternation, displaying only two olefinic carbon peaks for carbons α and β to the carbonyl group (Figure A.2d).

In support of the mechanism shown in Scheme A.1, independently prepared polyoctenamer was treated with diacrylate and catalyst **3**, yielding A,B-alternating copolymer similar to the product of entry 1 in Table A.1. In addition, monitoring the reaction by ¹H NMR showed rapid and complete ROMP of cyclooctene followed by gradual appearance of peaks corresponding to A,B-alternating units. Furthermore, when a ROIMP reaction was terminated after 20 minutes, a polymer enriched in homo-polycycloalkene olefin units was obtained. These results strongly suggest a mechanism whereby ROMP of the cycloalkene initially pro-

Table A.1: Examples of ROIMP products, their A,B-alternations, molecular weights, and distributions.

Entry	Acyclic Diene	Cycloalkene ^a	$\frac{[M]}{[C]}$ ^b	conc. ^c (M)	yield ^d (%)	A,B-alt. ^e (%)	M_n (PDI) ^f ($\frac{g}{mol} * 10^{-3}$)
1			290	0.2	84	99	90.0(1.73)
2			125	0.4	75	96	20.3(1.58)
3			125	0.4	93	97	14.0(1.80)
4			200	0.5	91	94	26.1(1.71)
5			250	0.4	69	94.5	21.4(1.43)
6			200	0.2	99	98.5	26.5(1.80)
7			100	0.1	98	97	25.2(2.06)

^a1.0 eq. of cycloalkene was used except cyclopentene (1.3 eq.) ^bRatio of total monomer to catalyst ^cConcentration with respect to acyclic diene ^dIsolated yields after precipitation into hexane or methanol ^eDetermined by ¹H NMR ^fDetermined by CH₂Cl₂ GPC relative to polystyrene standards.

duces an unsaturated polymer scaffold to which subsequent insertion of the diacrylate forms the final A,B-alternating structure.

Other cycloalkenes were also viable for ROIMP and yielded highly A,B-alternating polymers (entries 2–4). However, substrates with particularly low ring strain, such as cyclopentene and cycloheptene, required a lower monomer to catalyst ratio of 125:1 due to the slow rate of ROMP.¹⁹ In order to obtain a high A,B-alternation (96%) with volatile cyclopentene (bp 44 °C), a slight excess of 1.3 equiv. of the cycloalkene relative to the diacrylate was used. Even with 2.0 equiv. of cyclopentene, a polymer with higher than 85% A,B-alternation was

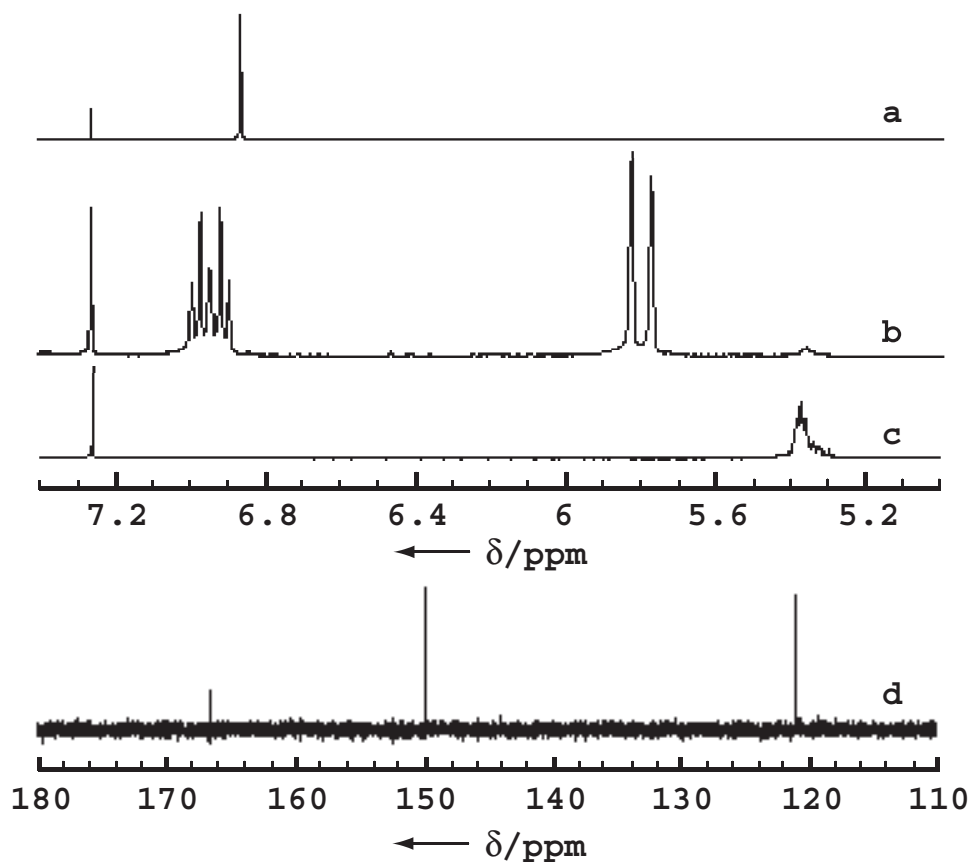


Figure A.2: NMR data for a ROIMP product (Table A.1, entry 1).

obtained. Also, treating an isolated polymer of lower A,B-alternation with catalyst **3** yielded a final polymer with higher A,B-alternation. These results suggest that the equilibrium for cyclopentene lies toward the cyclic form at 40 °C; excess homo-polycyclopentene units are degraded back to cyclopentene and lost from the system by evaporation.²⁰

Notably, various functional groups can be incorporated into ROIMP copolymers. 5-*t*-Butyldimethylsilyloxycyclooctene proved to be a viable monomer, comparable to the parent cyclooctene (entry 5). In this way, free alcohol groups could be installed into alternating monomer units upon simple deprotection. Further variations such as ethylene glycol and phenyl groups can be substituted into diacrylate units as shown in entries 6 and 7. These results demonstrate that the regioselective incorporation of functional groups is possible by the appropriate

choice of monomers A and B, thus opening up a new class of polymers that can be synthesized by ROIMP.

ROIMP exhibits remarkable conversion and selectivity. Compared to ADMET, where high vacuum and elevated temperature are required to drive the polymerization to high conversion by removal of ethylene gas,⁶ ROIMP gives high conversion under gentle reflux conditions for two reasons. First, ROMP of monomer B is efficient in making the initial homo-polycycloalkene chains. Second, the formation of 1,2-disubstituted α,β -unsaturated carbonyl compounds is thermodynamically favored by more than 3 kcal mol⁻¹ per bond.* These enthalpic factors, combined with the loss of ethylene, drive the reaction to high conversion. In addition, the unfavorable oligomerization of diacrylates, where the intermediate is an unstable enoic carbene, leads to high A,B-alternation.²¹ Therefore, ROIMP has benefits of both chain-growth and step-growth polymerization, leading to high molecular weight and high selectivity.

To optimize conversion, other polymerization conditions were investigated. It was found that 0.1–0.5 M solutions in CH₂Cl₂ at 40 °C yield the best results. In contrast to ROMP, increasing the concentration beyond 0.5 M resulted in lower conversion. Switching to toluene or 1,2-dichloroethane as solvent also gave lower conversion, at either 40 °C or 60 °C. While there is precedence for CH₂Cl₂ being the best solvent for cross metathesis of functionalized olefins,²¹ the concentration dependence for ROIMP is somewhat surprising, since concentrations of 0.1–0.5 M are considered dilute conditions for conventional step growth polymerization reactions. Controlling the molecular weight of polymers is a very important issue since polymers with different molecular weights often exhibit different properties. For alternating copolymers produced by ROIMP, molecular weight can be roughly controlled by changing the relative stoichiometry of the two monomers. For example, using 0.96 equiv. of cyclooctene to 1.0 equiv. of hydroquinone diacrylate gave 17,800 g mol⁻¹ with 98% A,B-alternation (PDI = 1.64), whereas a copolymer of 45,200 g mol⁻¹ and 95.5% A,B-alternation (PDI = 1.69) was obtained by increasing

*This value was obtained by AM1 calculation from Spartan v. 1.1, Wavefunction.

to 1.06 equiv. of cyclooctene. These results show that, compared with the 1:1 case (entry 7, Table A.1), using an excess of hydroquinone diacrylate shortens the polymer chain, but an excess of cyclooctene gives higher molecular weight due to the oligomeric blocks of polycyclooctene.

A.4 Conclusion

In conclusion, we have demonstrated a new, general method for synthesizing highly alternating copolymers by olefin metathesis. The high conversion and degree of alternation arise from the thermodynamically driven selective bond formation between diacrylates and cycloalkenes.

A.5 Experimental

General Experimental Section. NMR spectra were recorded on Varian-300 NMR. Chemical shifts are reported in parts per million (ppm) downfield from tetramethylsilane (TMS) with reference to internal solvent. Multiplicities are abbreviated as follows: singlet (s), doublet (d), triplet (t), quartet (q), quintet (quint), and multiplet (m). The reported ^1H NMR data refer to the major olefin isomer unless stated otherwise. The reported ^{13}C NMR data include all peaks observed and no peak assignments were made. High-resolution mass spectra (EI and FAB) were provided by the UCLA Mass Spectrometry Facility (University of California, Los Angeles).

Analytical thin-layer chromatography (TLC) was performed using silica gel 60 F254 precoated plates (0.25 mm thickness) with a fluorescent indicator. Flash column chromatography was performed using silica gel 60 (230-400 mesh) from EM Science. All other chemicals were purchased from the Aldrich, Strem, or Nova Biochem Chemical Companies, and used as delivered unless noted otherwise. CH_2Cl_2 was purified by passage through a solvent column prior to use.

Procedure for entry 1: To a flask charged with 1,4-butanediol diacrylate (90 mg, 0.45 mmol) in 2 ml of CH₂Cl₂, catalyst **3** (2.7 mg) and cyclooctene (65 μl, 0.45 mmol) were added. Quick degassing by dynamic vacuum was conducted and the flask was fitted with a condenser and refluxed under argon for 6 hours. The product (108 mg, 84%) was precipitated into methanol. ¹H NMR (300MHz, CDCl₃, ppm): δ 6.93 (1H, dt, *J*=7.2, 15.9 Hz), 5.77 (1H, d, *J*=15.9 Hz), 4.13 (2H, broad), 2.12 (2H, m), 1.73 (2H, m), 1.43 (2H, m), 1.30 (2H, m). ¹³C NMR (75 MHz, CDCl₃, ppm), δ 166.8, 149.6, 121.3, 64.0, 32.5, 29.3, 28.2, 25.8.

Procedure for entry 2: To a flask charged with 1,4-butanediol diacrylate (34 mg, 0.15 mmol) in 0.4 ml of CH₂Cl₂, catalyst **3** (2.3 mg) and cyclopentene (20 μl, 0.15 mmol) were added. Quick degassing by dynamic vacuum was conducted and the flask was fitted with a condenser and refluxed under argon for 6 hours. The product (37 mg, 75%) was precipitated into hexane. ¹H NMR (300MHz, CDCl₃, ppm): δ 6.85 (1H, dt, *J*=7.2, 15.9 Hz), 5.82 (1H, d, *J*=15.9 Hz), 4.10 (2H, broad), 2.22 (2H, m), 1.60-1.75 (3H, m). ¹³C NMR (75 MHz, CDCl₃, ppm): δ 166.5, 148.4, 121.9, 64.0, 31.7, 30.7, 26.6, 25.6.

Procedure for entry 3: To a flask charged with 1,4-butanediol diacrylate (60 mg, 0.30 mmol) in 0.8 ml of CH₂Cl₂, catalyst **3** (4.1 mg) and cycloheptene (35.5 μl, 0.30 mmol) were added. Quick degassing by dynamic vacuum was conducted and the flask was fitted with a condenser and refluxed under argon for 6 hours. The product (74 mg, 93%) was precipitated into hexane. ¹H NMR (300MHz, CDCl₃, ppm): δ 6.93 (1H, dt, *J*=6.9, 15.3 Hz), 5.78 (1H, dt, *J*=1.5, 17.0 Hz), 4.13 (2H, broad), 2.17 (2H, m), 1.72 (2H, m), 1.30- 1.42 (3H, m). ¹³C NMR (75 MHz, CDCl₃, ppm): δ 166.8, 149.5, 121.4, 64.0, 32.4, 29.0, 28.1, 25.8.

Procedure for entry 4: To a flask charged with 1,4-butanediol diacrylate (60 mg, 0.30 mmol) in 0.6 ml of CH₂Cl₂, catalyst **3** (2.6 mg) and cyclododecene (58 μl, 0.30 mmol) were added. Quick degassing by dynamic vacuum was conducted and the flask was fitted with a condenser and refluxed under argon for 6 hours. The product (92 mg, 91%) was precipitated into methanol. ¹H NMR (300MHz, CDCl₃, ppm): δ 6.94 (1H, dt, *J*=7.2, 15.3 Hz), 5.80 (1H, dt, *J*=1.5, 15.9 Hz), 4.13 (2H, t, *J*=5.1

Hz), 2.16 (2H, dt, $J=6.9, 6.6$ Hz), 1.73 (2H, t, $J=3.0$ Hz), 1.42 (2H, m), 1.24 (7H, m). ^{13}C NMR (75 MHz, CDCl_3 , ppm): δ 166.9, 149.9, 121.2, 64.0, 32.6, 29.9, 29.8, 29.5, 28.4, 25.8.

Procedure for entry 5: To a flask charged with 1,4-butanediol diacrylate (40 mg, 0.20 mmol) in 0.5 ml of CH_2Cl_2 , catalyst **3** (1.4 mg) and cyclododecene (54 mg, 0.20 mmol) were added. Quick degassing by dynamic vacuum was conducted and the flask was fitted with a condenser and refluxed under argon for 6 hours. The product (60 mg, 69%) was precipitated into methanol. ^1H NMR (300MHz, CDCl_3 , ppm): δ 6.96 (1H, dt, $J=6.6, 16.2$ Hz), 5.80 (1H, d, $J=15.9$ Hz), 4.16 (2H, broad), 3.69 (1H, m), 2.20 (2H, m), 1.75 (2H, broad), 1.58 (1H, m) 1.46 (2H, m), 0.90(9H, s), 0.03(6H, s). ^{13}C NMR (75 MHz, CDCl_3 , ppm): δ 166.7, 149.6, 149.3, 121.5, 121.2, 71.4, 64.0, 36.7, 35.5, 21.7, 28.3, 26.2, 25.8, 24.0, 18.4, -3.9, -4.0.

Procedure for entry 6: To a flask charged with tri(ethylene glycol) diacrylate (53 mg, 0.21 mmol) in 1 ml of CH_2Cl_2 , catalyst **3** (1.8 mg) and cyclooctene (28 μl , 0.21 mmol) were added. Quick degassing by dynamic vacuum was conducted and the flask was fitted with a condenser and refluxed under argon for 6 hours. The product (68 mg, 99%) was precipitated into hexane. ^1H NMR (300MHz, CDCl_3 , ppm): δ 6.95 (1H, dt, $J=6.9, 15.9$ Hz), 5.82 (1H, d, $J=15.9$ Hz), 4.26 (2H, t, $J=4.8$ Hz), 3.70 (2H, t, $J=5.1$ Hz), 3.64 (2H, s), 2.16 (2H, dt, $J=6.6, 6.6$ Hz), 1.42 (2H, m) 1.29 (2H, m). ^{13}C NMR (75 MHz, CDCl_3 , ppm): δ 166.7, 150.0, 121.2, 70.8, 69.6, 63.6, 32.5, 29.3, 28.2.

Procedure for entry 7: To a flask charged with hydroquinone diacrylate (44 mg, 0.21 mmol) in 1 ml of CH_2Cl_2 , catalyst **3** (3.5 mg) and cyclooctene (27.5 μl , 0.21 mmol) were added. Quick degassing by dynamic vacuum was conducted and the flask was fitted with a condenser and refluxed under argon for 6 hours. The product (60 mg, 98%) was precipitated by hexane. ^1H NMR (300MHz, CDCl_3 , ppm): δ 7.11- 7.20 (3H, m), 6.00 (1H, d, $J=15.3$ Hz), 2.27 (2H, dt, $J=6.9, 6.3$ Hz), 1.52 (2H, broad), 1.37 (2H, broad). ^{13}C NMR (75 MHz, CDCl_3 , ppm): δ 165.0, 152.0, 148.2, 122.6, 120.7, 32.7, 29.3, 28.2.

References Cited

- [1] Odian, G. *Principles of Polymerizations*. Wiley, New York, 1991.
- [2] Drent, E.; Budzelaar, P. H. M. *Chem. Rev.*, **1996**, *96*, 663–681.
- [3] Ivin, K. J.; Mol, J. C. *Olefin Metathesis and Metathesis Polymerization*. Academic Press, San Diego, CA, 1997.
- [4] Grubbs, R. H.; Khosravi, E. *Mater. Sci. Technol.*, **1999**, *20*, 65–104.
- [5] Buchmeiser, M. R. *Chem. Rev.*, **2000**, *100*, 1565–1604.
- [6] Lehman, S. E.; Wagener, K. B. *Macromolecules*, **2002**, *35*, 48–53.
- [7] AlSamak, B.; Carvill, A. G.; Hamilton, J. G.; Rooney, J. J.; Thompson, J. M. *Chem. Commun.*, **1997**, pp 2057–2058.
- [8] Al Samak, B.; Amir-Ebrahimi, V.; Corry, D. G.; Hamilton, J. G.; Rigby, S.; Rooney, J. J.; Thompson, J. M. *J. Mol. Catal. A-Chem.*, **2000**, *160*, 13–21.
- [9] Ilker, M. F.; Coughlin, E. B. *Macromolecules*, **2002**, *35*, 54–58.
- [10] Schrock, R. R. *Acc. Chem. Res.*, **1990**, *23*, 158–165.
- [11] Schwab, P.; Grubbs, R. H.; Ziller, J. W. *J. Am. Chem. Soc.*, **1996**, *118*, 100–110.
- [12] Scholl, M.; Ding, S.; Lee, C. W.; Grubbs, R. H. *Org. Lett.*, **1999**, *1*, 953–956.
- [13] Chatterjee, A. K.; Grubbs, R. H. *Org. Lett.*, **1999**, *1*, 1751–1753.
- [14] Chatterjee, A. K.; Morgan, J. P.; Scholl, M.; Grubbs, R. H. *J. Am. Chem. Soc.*, **2000**, *122*, 3783–3784.
- [15] Choi, T. L.; Chatterjee, A. K.; Grubbs, R. H. *Angew. Chem.-Int. Edit.*, **2001**, *40*, 1277–1279.
- [16] Chatterjee, A. K.; Choi, T. L.; Grubbs, R. H. *Synlett*, **2001**, pp 1034–1037.
- [17] Choi, T. L.; Grubbs, R. H. *Chem. Commun.*, **2001**, pp 2648–2649.
- [18] Lee, C. W.; Choi, T. L.; Grubbs, R. H. *J. Am. Chem. Soc.*, **2002**, *124*, 3224–3225.
- [19] Bielawski, C. W.; Grubbs, R. H. *Angew. Chem.-Int. Edit.*, **2000**, *39*, 2903–2906.
- [20] Schrock, R. R.; Yap, K. B.; Yang, D. C.; Sitzmann, H.; Sita, L. R.; Bazan, G. C. *Macromolecules*, **1989**, *22*, 3191–3200.
- [21] Choi, T. L.; Lee, C. W.; Chatterjee, A. K.; Grubbs, R. H. *J. Am. Chem. Soc.*, **2001**, *123*, 10417–10418.

Appendix B

Direct Synthesis of Soluble, End-Functionalized Polyenes and Polyacetylene Block Copolymers

This has previously appeared as: Scherman, O. A.; Rutenberg, I. M.; Grubbs, R. H.
Journal of the American Chemical Society, **2003**, *125*, 8515–8522.

B.1 Abstract

The ring-opening metathesis polymerization (ROMP) of 1,3,5,7-cyclooctatetraene (COT) in the presence of a chain transfer agent (CTA) with a highly active ruthenium olefin metathesis catalyst resulted in the formation of soluble polyenes. Small molecule CTAs containing an internal olefin and a variety of functional groups resulted in soluble telechelic polyenes with up to 20 double bonds. Use of polymeric CTAs with an olefin terminus resulted in polyacetylene block copolymers. These materials were subjected to a variety of solution and solid phase characterization techniques including ^1H NMR, UV/vis, and FT-IR spectroscopies, as well as MALDI-TOF MS and AFM.

B.2 Introduction

Intrinsically conducting polymers (ICP)s are of great interest due to their potential use in a wide variety of applications such as polymer light-emitting diodes (PLED)s, electrostatic dissipation (ESD) materials, and charge storage devices. As a consequence of their rigidity, most ICPs are insoluble materials, preventing thorough characterization and thereby slowing the development of this field. Moreover, the inherent instability of ICPs and associated processing difficulties create a large barrier for commercialization. In an effort to overcome these obstacles, the development of a practical synthesis of relatively stable and soluble conducting polymers with a controlled architecture is important.

The field of conducting polymers was founded upon the discovery of polyacetylene (PA), the simplest ICP, in the 1970s.¹⁻⁵ There have since been numerous accounts on the synthesis of PA including the Ziegler-Natta polymerization of acetylene,⁶ the synthesis of precursor polymers followed by thermal evolution of a small molecule,^{7,8} and the ring-opening metathesis polymerization (ROMP) of 1,3,5,7-cyclooctatetraene (COT).⁹⁻¹² Despite these developments, applications of PA remain particularly elusive. Unlike PA, however, three decades of research

involving other ICPs such as polyaniline, poly(1,4-phenylenevinylene) (PPV), polypyrrole (PPy), and polythiophene (PTh) has resulted in their commercialization in applications such as anti-fouling coatings¹³ and electrodes in batteries and capacitors.¹⁴

Since most ICPs are completely insoluble in organic solvents, several strategies have been employed to address this problem. One common approach is to add substitution along the polymer backbone thereby disturbing alignment between polymer chains and allowing for the penetration of solvating molecules. This approach has worked well for improving the solubilities of PPV and PTh in the forms of poly[2-(2-ethylhexyloxy)-5-methoxy-1,4-phenylenevinylene](MEH-PPV),¹⁵ ester-substituted PPVs,¹⁶ and poly(3-alkylthiophene).¹⁷ While the materials' solubilities are greatly enhanced, they also maintain a suitable level of conductivity; unfortunately, this strategy is not amenable to PA. Both alkyl- and aryl-acetylene (R-acetylenes) derivatives have been polymerized to produce the corresponding soluble poly(R-acetylene)s. Although the disorder stemming from the substituents aids in solubilizing the R-PA, it simultaneously disrupts the π -conjugation along the polymer backbone. As a result, these materials exhibit substantially decreased conductivities in comparison to the parent PA.

Another synthetic method used to solubilize ICPs is to produce copolymers by introducing a second monomer with good solubility properties. Typically, in order to keep the conductive characteristics of the ICP, block copolymers are necessary. PA block copolymers have been previously synthesized via two approaches. In the first approach, using sequential addition of monomers, a soluble PA-precursor polymer such as poly(phenyl vinyl sulfoxide) is prepared as one of the blocks.¹⁸ Upon heating, an elimination reaction converts the precursor polymer to PA. This method has been adapted both to anionic polymerization and, through the Durham route, to ROMP.⁷ The second approach involves sequential addition copolymerization of COT and another ROMP-active monomer.¹⁹ In both approaches, however, block copolymer composition is limited because both monomers must be polymerizable by the same method.

As many of the desirable characteristics of ICPs and PA are realized with a relatively small number of repeat units, several groups have endeavored to produce soluble polyenes with up to 20 double bonds.^{20,21} Furthermore, the areas of natural product synthesis²² and network polymer formation²³ would benefit if functional end groups were built into these soluble polyenes. It has been demonstrated that heating of a ROMP polymer, prepared from a Durham precursor monomer using highly active molybdenum and tungsten olefin metathesis catalysts, leads to polyenes with alkyl end groups.^{19, 21, 24, 25} For polyenes with less than 16 double bonds, these alkyl groups enhance solubility and allow for more detailed characterization.²⁰ One drawback to producing polyenes via the Durham route is the need for a subsequent deprotection step.

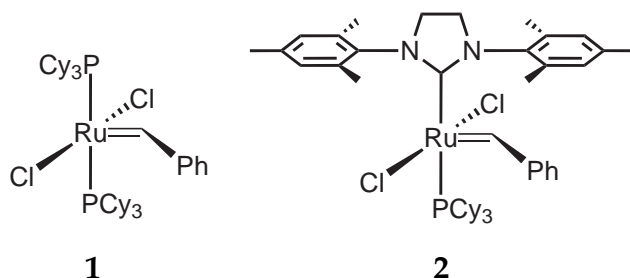


Figure B.1: Ruthenium olefin metathesis catalysts.

Recently, we reported the direct synthesis of PA via the ROMP of COT with the highly active ruthenium catalyst **2**.¹² This reaction is not possible with the less active catalyst **1** as the ring strain of COT (2.5 kcal/mol) is extremely low.²⁶ Catalyst **2** has also been shown to form telechelic polymers with a variety of functional end groups when utilized in conjunction with a chain transfer agent (CTA)*.^{27, 28} Building upon this work, we report herein a method of forming telechelic polyenes by the ROMP of COT in the presence of a CTA. Furthermore, these polyenes are soluble in common organic solvents allowing for extensive solution-phase characterization. We also describe here the ROMP of COT in the presence of an

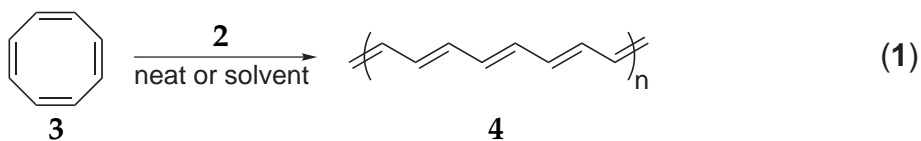
*The higher reaction temperatures required for chain transfer with catalysts **1** and **2** preclude the ROMP of Durham monomers due to the instability of the PA precursor.

olefin-terminated polymer, which allows PA block copolymers to be formed with a variety of commodity polymers such as polystyrene (PS), poly(methyl methacrylate) (PMMA), and poly(ethylene glycol) (PEG). Indeed, nearly any monomer that is polymerizable by living anionic or controlled radical techniques can be used as the solubilizing block. Furthermore, no elimination step is necessary in forming the PA block, thus reducing synthetic complexity and material waste. Since the ROMP of COT forms PA directly without the need for deprotection steps,^{11, 12} and olefin-terminated polymers are commercially available, this represents the first one-step synthesis of PA-containing block copolymers from commercially available materials.

B.3 Results and Discussion

B.3.1 Synthesis of Soluble Polyenes

We recently published a report detailing the ROMP of COT (**3**) to form PA with catalyst **2** (Equation 1).¹² The characteristics of the PA produced by **2** proved to



be very similar to PA produced by previous synthetic routes.¹² Unfortunately, the characteristic insolubility of PA was also observed. The functional group tolerance of catalyst **2**, however, suggests the possibility of placing solubilizing functional groups at the chain ends by utilizing a chain transfer agent (CTA). It has been previously shown that the use of a CTA with **2** can produce telechelic oligomers and polymers from CTAs containing functional groups such as alcohols, halides, and esters.^{27, 28} The same strategy can now be applied for the direct formation of telechelic PA. Furthermore, if the PA chain length can be controlled by this method, it would provide for the direct formation of soluble polyenes as outlined in Equation 2.

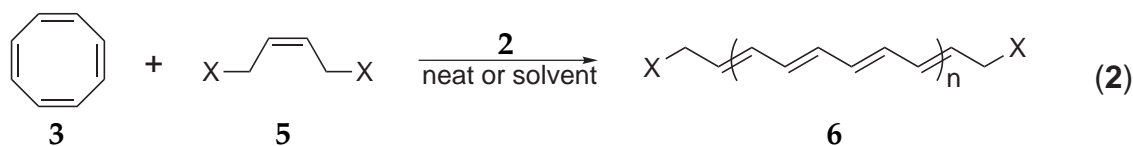


Table B.1: Effects of Monomer/CTA and Monomer/Catalyst Ratio on Yield of Polyenes

Entry	CTA	[COT]/ [CTA]	[COT]/[2]	% yield
1 ^a	5a	1	500	76
2 ^a	5a	2	500	83
3 ^b	5a	1	540	78
4 ^b	5a	2	480	69
5 ^b	5a	3	520	49
6 ^b	5a	1	980	40
7 ^b	5a	3	1050	9
8 ^c	5b	2	490	5
9 ^c	5b	4	490	18
10 ^d	5c	4	800	12
11 ^a	5d	1	5000	0
12 ^e	5e	1	500	0

^aReaction carried out in 1 mL of CH₂Cl₂. ^bReaction carried out neat.
^cReaction carried out in 1 mL of toluene. ^dReaction carried out in 3 mL of toluene. ^eReaction carried out in 1 mL of THF.

The synthesis of telechelic PA was successfully carried out both neat and in solution via the ROMP of COT with a CTA using catalyst **2** (see Table B.1). Upon addition of **2**, the yellow COT solution turned light orange and then became progressively darker over the next 5 min depending on the ratio of COT to CTA. After 24 h, only a small amount of solid was observed to precipitate on the container walls. This result was visibly different from the large amount of solid (metallic in appearance) produced when a CTA was omitted from the reaction. After isolation, the resulting polymer was completely soluble in common organic solvents, enabling characterization by ¹H NMR, UV-vis, and FT-IR spectroscopies, as well as MALDI-TOF MS.

Attempts to use CTAs such as **5d** and **5e** were not successful (Figure B.2). While no solids precipitated during the ROMP of COT with CTA **5d**, ¹H NMR spectroscopy of the crude reaction mixture showed very little polyene and no

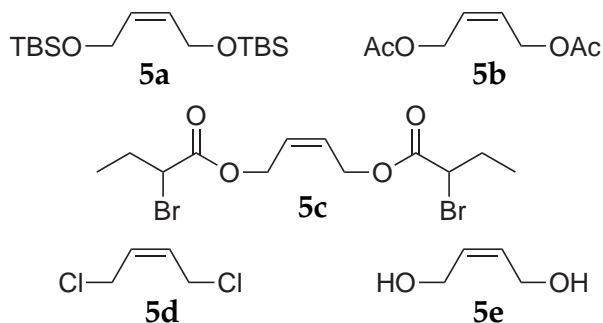


Figure B.2: CTAs **5a–e**.

material could be isolated (entry 11). Immiscibility of COT and **5e** prevented neat polymerization and required solvents such as THF for ROMP in solution. Unfortunately, THF has been shown to dramatically decrease the rate of ROMP,¹¹ and no desired polyene product was observed in the ¹H NMR spectrum of the crude reaction mixture (entry 12).

As a consequence of the loss of material at each stage of preparation, obtaining the polyenes in high yield was somewhat difficult. Some polyene product was simply lost upon repetitive centrifuge/decant/wash cycles, while shorter polyene chains were most likely soluble in the MeOH washes. Entries 1 and 2 in Table B.1 show that for ROMP carried out in solution, increasing the amount of COT relative to CTA **5a** has a very minimal effect on the yield of polyene **6a**. When the corresponding reactions are carried out neat (entries 3-5, Table B.1), a decrease in yield of **6a** is observed with a decrease in the amount of CTA **5a**. This trend is likely due to insoluble PA chains precipitating out of solution when too few chain transfer groups are present to attenuate the molecular weight. When the amount of COT relative to catalyst **2** is increased to 1000:1 (entries 6 and 7, Table B.1), the yields decrease substantially. This observation is likely due to the incomplete initiation of catalyst **2**²⁹ which would result in a “true” monomer to catalyst ratio far in excess of 1000. Finally, although it does not lead to chain termination, backbiting of catalyst **2** onto the growing polyene chain has previously been shown to eliminate benzene.¹² As benzene is not metathesis active, backbiting essentially removes monomer from the reaction.

B.3.1.1 Characterization of Soluble Polyenes

The loss of monomer over the course of the reaction because of backbiting also evidently hinders our attempt to control the molecular weight of the polyenes by adjusting the ratio of COT to CTA. Previous reports of ROMP reactions with catalyst **2** and a CTA have shown that molecular weight is dictated by the ratio of [monomer]:[CTA] if the reaction is allowed to reach thermodynamic equilibrium.^{27, 28, 30} This result was not found to be the case for COT. While accurate molecular weights and distributions could not be obtained for the polyenes, ¹H NMR spectroscopy as well as MALDI-TOF MS data indicated average chain lengths of around 10–13 double bonds for all reactions and did not vary with the ratio of COT:CTA. The average chain length of the isolated polyenes, however, may be misleading. When a higher COT to CTA ratio is employed, more polyene chains reach lengths that render them insoluble. For lower ratios, shorter, MeOH-soluble polyene chains are favored. As a result of likely fractionation of smaller and longer chains during workup, regardless of the starting COT to CTA ratio, the isolated polyene chains are heavily weighted to an average of 10–13 double bonds. Of course, the backbiting of **2** might be attenuated by decreasing the reaction temperature; however, if the polymerization of COT occurred without significant backbiting with a CTA molecule, an insoluble PA chain would result. Hence, in the direct synthesis of polyenes **6** with catalyst **2**, the ability to control molecular weight is limited.

The solution phase ¹H NMR spectrum of polyene **6a** (Figure B.3) clearly shows signals corresponding to the backbone protons of the telechelic polyene between $\delta=6-7$ ppm, which are characteristically shifted downfield due to the highly conjugated segment of olefins. The allylic CH₂ protons give rise to peaks around $\delta=4.2$ ppm and the *tert*-butyl and methyl protons of the silane protecting group (from CTA **5a**) correspond to singlets at $\delta=0.9$ and 0.05 ppm, respectively. The absence of a singlet at $\delta=5.79$ ppm suggests that all of the unreacted COT was successfully removed from the polyene product. Integration of the methylene and

polyene backbone peaks suggests an average of 10 double bonds for the sample, which is consistent with the MALDI-TOF MS data presented below.

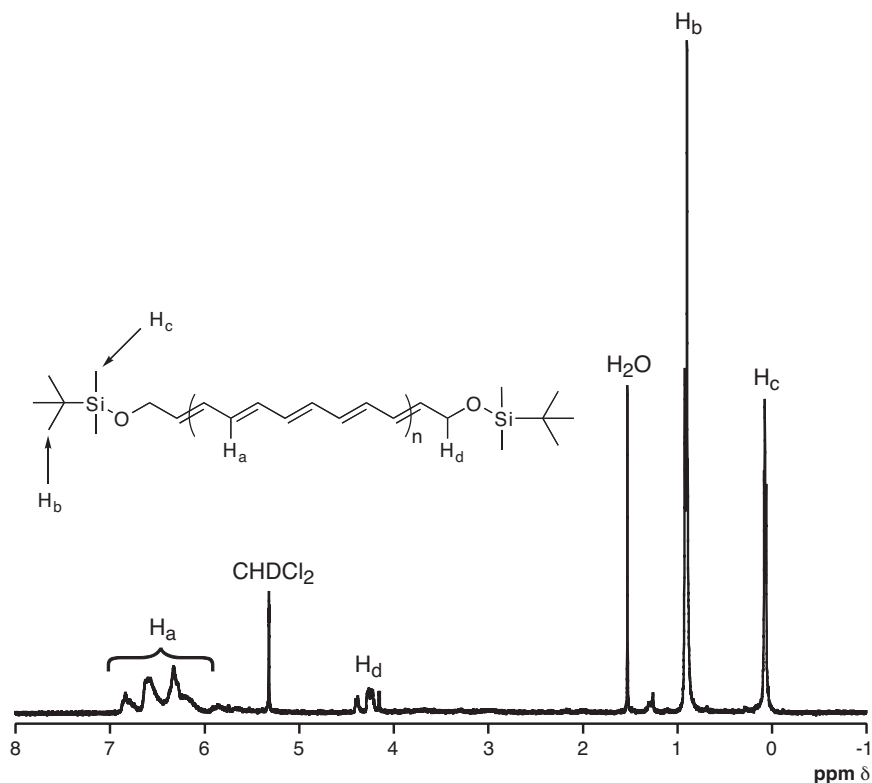


Figure B.3: ^1H NMR spectrum of telechelic polyene **6a** in CD_2Cl_2 .

Previous reports have provided very detailed UV-vis spectroscopy data on soluble polyenes containing up to 15 double bonds.^{20,21} As the number of conjugated double bonds increases, the absorption shifts to longer wavelengths and some detail of the higher energy transitions is lost. UV-Vis spectroscopy was carried out on polyene **6a** in both THF and CH_2Cl_2 . Figure B.4 shows the UV-vis spectrum in CH_2Cl_2 with 4 distinct transitions between 355 and 450 nm and a smooth absorption profile extending past 500 nm. These transitions are consistent with a polyene composed of 10 to 20 double bonds.²⁰

Infrared spectroscopy was also carried out on telechelic polyenes **6a** and **6b**. Figure B.5 displays the FT-IR spectra for both telechelic polyenes. The bands at 745, 773, and 1011 cm^{-1} are visible in both polyene spectra and are conserved from the IR spectrum of poly(COT).¹² The peak at 743 cm^{-1} can be attributed to the *cis*

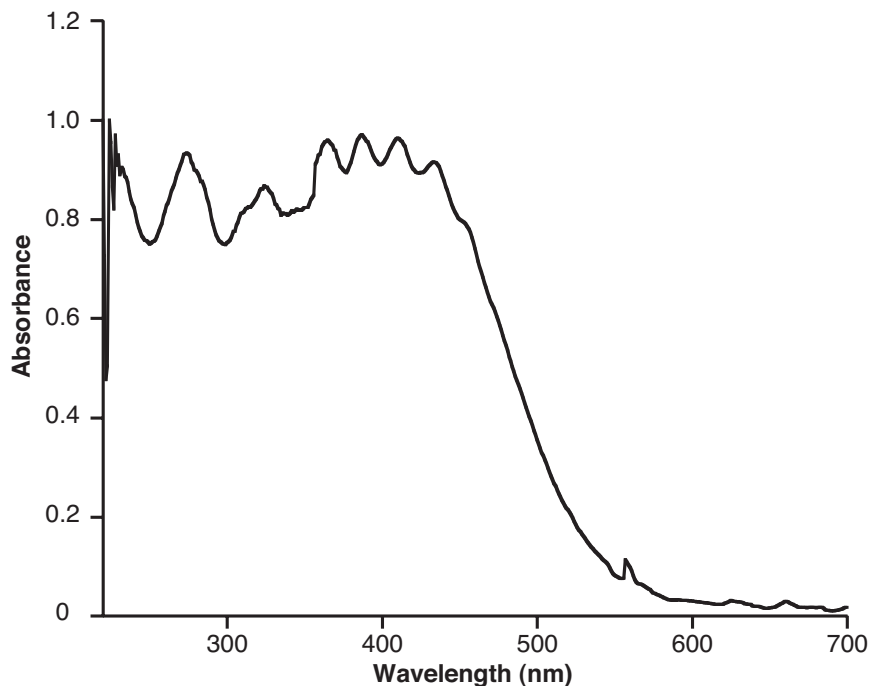


Figure B.4: UV-Vis spectrum of telechelic polyene **6a** in CH_2Cl_2 .

C-H out-of-plane vibrational mode while the peak 1011 cm^{-1} is due to the *trans* C-H mode.³¹ The presence of a much larger *trans* peak at 1011 cm^{-1} supports the mechanism of *trans*-selective catalyst **2** backbiting into the polymer chain to attach the endgroups and form telechelic polymers or to simply isomerize *cis* olefins to their *trans* counterparts.

Finally, mass spectrometry was carried out on the telechelic polyenes. Figure B.6 shows the MALDI-TOF spectrum for **6a** acquired from a dithranol matrix. The first labeled peak with a mass of 628.9 Da corresponds exactly to telechelic polyene **6a** with 13 double bonds. There is a difference of 26.0 amu between each peak in the series corresponding to a C_2H_2 unit. The series is easily visible out to a mass peak of 811.0 amu, corresponding to a species with 20 double bonds. Furthermore, no other series with 26.0 amu mass differences are observed suggesting that all of the polyene chains are capped at *both* ends.

These data provide evidence for the formation of a telechelic polyene with the CTA functionality successfully placed onto both ends of each polyene chain. It also shows that catalyst **2** is capable of backbiting into a growing polyene

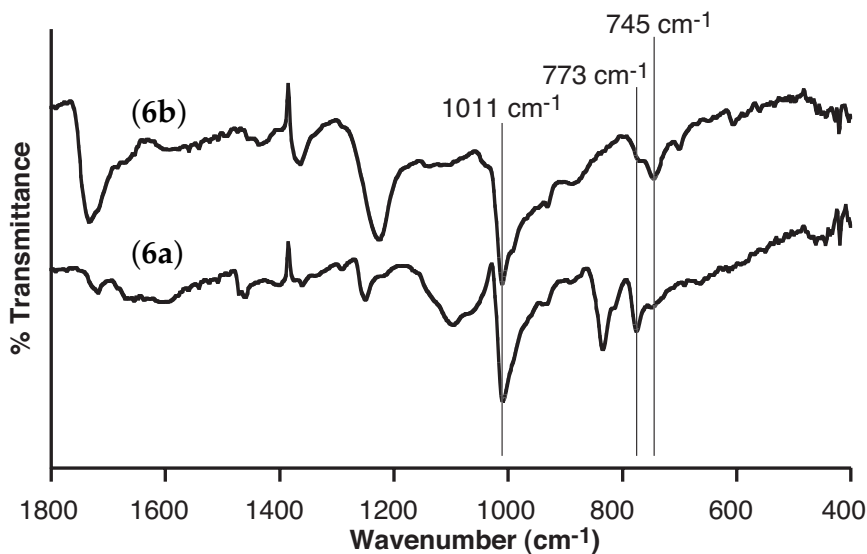


Figure B.5: FT-IR % transmittance spectra of polyenes **6a** and **6b** in KBr pellets.

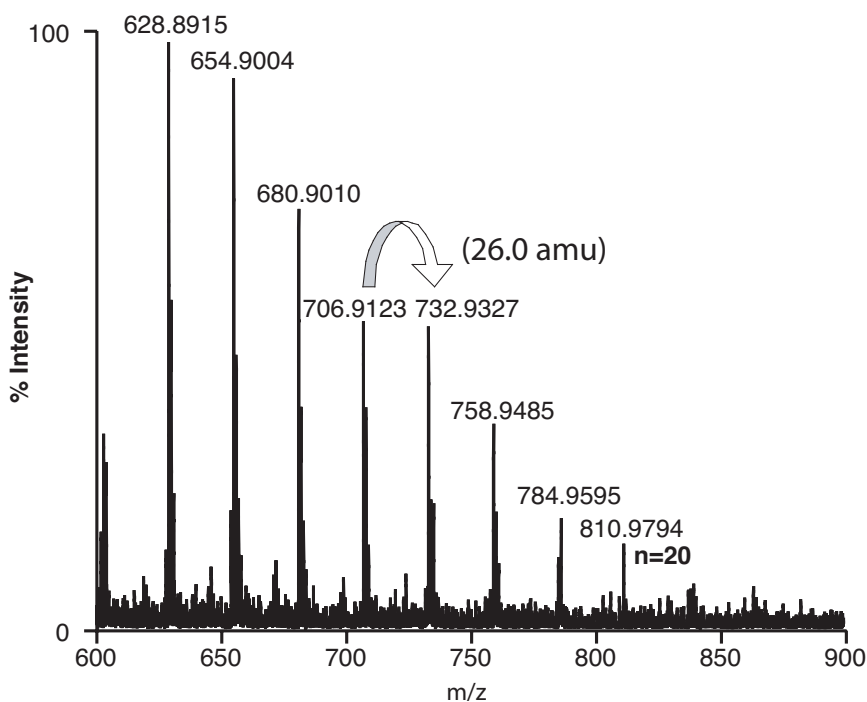


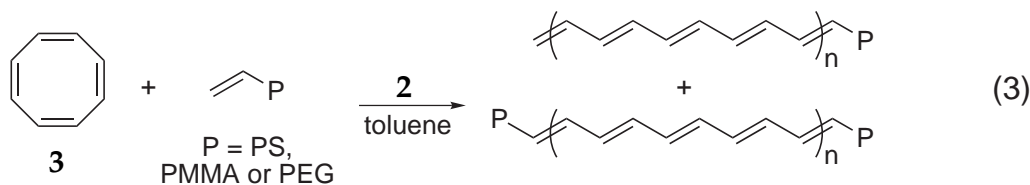
Figure B.6: MALDI-TOF MS of polyene **6a** ionized from a dithranol matrix.

chain in order to mediate chain transfer. Furthermore, the materials produced are completely soluble in common organic solvents and allow for much more detailed characterization of polyenes. These results encouraged us to further explore the use of CTAs as a method for producing soluble and processable

PA-based materials. We anticipated difficulties, however, using telechelic PA as macroinitiators (e.g. entry 10, Table B.1). An alternative route to PA block copolymers was therefore sought.

B.3.2 Synthesis of PA-containing Block Copolymers

CTAs containing terminal olefins have been previously used with catalyst **2** to form mixtures of monofunctionalized and difunctionalized (i.e., telechelic) polymers.²⁸ Furthermore, only difunctional materials result when a large excess of a CTA containing an internal olefin is used. Extending this concept, olefin-terminated *polymers* were found to control the ROMP of COT by forming block copolymers containing PA as one of the blocks (see Equation 3). As in the case with small molecule CTAs, a polymer with an olefin in the middle of the chain should lead exclusively to triblock copolymers containing PA as the middle block. We are currently investigating this possibility, but due to difficulties in obtaining *absolutely* pure polymers containing an internal olefin, we have limited this report to include only end-functionalized polymers.



The use of olefin-terminated polymers as CTAs allows for a wide variety of block copolymer compositions, as polymers containing olefin endgroups can be prepared using numerous techniques.³²⁻³⁵ Atom transfer radical polymerization (ATRP) was chosen for this work principally for its synthetic ease. Recent advances in ATRP allow these reactions to be performed without the exclusion of oxygen, and with monomers that have not been rigorously purified.³⁶ Allyl bromide and 5-bromo-1-pentene were convenient ATRP initiators for forming PMMA and PS functionalized with a terminal olefin.³³ ¹H NMR spectroscopic and MALDI-TOF MS analysis of the polymers confirmed the presence of olefin endgroups, and molecular weights were determined by GPC and NMR. As with previous

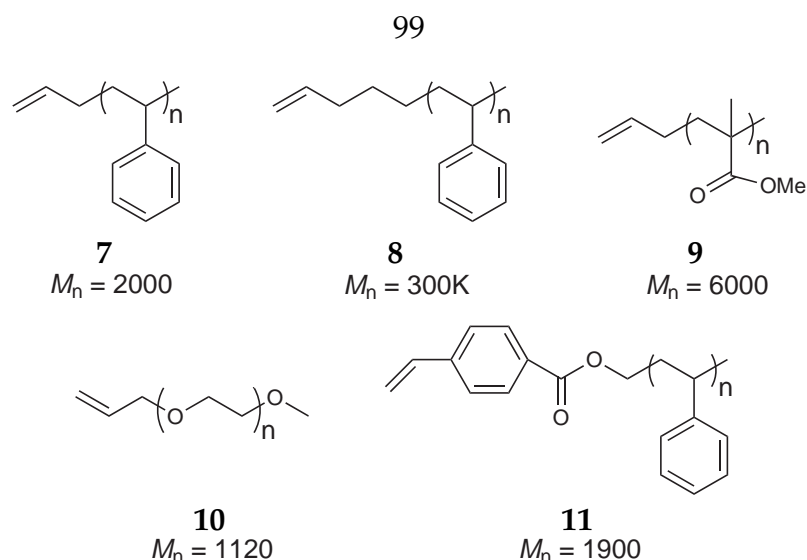


Figure B.7: Olefin-terminated polymers.

reports in the literature, mass spectral analysis showed that the halogen endgroups were replaced by hydrogen atoms for many of the polymer chains after long polymerization times.^{37,38} Since ruthenium-based catalysts have been shown to successfully catalyze ATRP,³⁹ however, the loss of the halogen endgroup was considered advantageous, reducing the possibility of unwanted side reactions during the subsequent ROMP step. Indeed, no reaction was observed when the olefin-terminated polymer was subjected to ATRP conditions in the presence of COT.

Formation of PA block copolymers was accomplished via the ROMP of COT in the presence of olefin-terminated polymers 7–11.[†] Typically, the amount of solvent was adjusted to ensure an initial monomer concentration, $[COT]_0$, of approximately 0.2 M. When large amounts of olefin-terminated polymer were used, however, additional solvent was added to ensure complete dissolution. Monomer-to-catalyst ratios were typically maintained at 1000:1, although ratios of up to 21000:1 were found to be viable. After completely dissolving the olefin-terminated polymers in toluene, COT was added, followed by the catalyst (either in solid form or from a stock solution). Within minutes, a color appeared

[†]It is evident from the characterization data that the products of these reactions contain a significant portion of unmodified polymer; however, the amount of PA that is incorporated is clearly sufficient to affect the material properties.

that varied depending on the relative proportions of COT and olefin-terminated polymer, as well as the molecular weight of the latter. For low proportions of COT, the color of the reaction was light orange, while for medium proportions it was deep orange or red and for high proportions it was deep red or black. This color was maintained throughout the reaction. Isolation of the block copolymer product was accomplished by precipitation in a non-solvent for the olefin-terminated polymer such as MeOH or hexanes. Table B.2 shows the colors of the final polymer products from various reactions. A solution of product polymer, when left on the benchtop, became clear over the period of many weeks, indicating eventual decomposition of the conjugated structure. However, the solid polymers maintain their color for months if protected from light and oxygen.

Table B.2: Variation in composition of PA block copolymers.

CTA	[COT]/[CTA]	[COT]/[2]	product color	% yield ^a	polymer ^b
7	4	900	orange	18	7a
7	20	4000	dark rust	26	7b
7	100	21000	brown/black	13	7c^c
8	200	800	dark grey	82	8a^d
8	1000	4000	faded black	71	8b
9	2	1000	light orange	44	9a^d
9	5	1000	orange	20	9b
9	20	1000	deep red	58	9c
9	40	1000	black	52	9d
10	1	500	dark red	62	10a
10	4	1600	brown/black	39	10b
10	7	1400	brown/black	28	10c
10	20	4000	brown/black	22	10d
11	20	4000	brown	36	11a

^aCalculated based on total mass of reactants and recovered product. ^bAll reactions were carried out in toluene with [COT]₀=0.2 M unless otherwise noted. ^c[COT]₀=1.1 M. ^d[COT]₀=0.03 M.

For most block copolymer compositions, solubility of the final product was identical to that of the olefin-terminated polymer. All of the entries in Table B.2 yielded completely soluble block copolymers. When very large amounts of COT were used in conjunction with a low molecular weight non-conjugated block (for

example, samples **7c**, **9d** and **10d**), some solid product was deposited on the walls of the reaction flask. This material was redissolved upon sonication, indicating that the solubilizing effect of the nonconjugated block is sufficient to keep the block copolymers soluble, even in cases where significant crystallization of the PA blocks is possible.

Yields of the block copolymer products varied widely depending on the proportions of COT and olefin-terminated polymer, as well as the molecular weight of the latter (see Table B.2). Yields exceeded 80% when higher molecular weight olefin-terminated polymers were used, or if lower proportions of COT were used. As the proportion of COT was increased, however, a corresponding increase in the ratio of [COT]/[**2**] led to decreased yields (see, for example, sample **7c**). Thus, as described for small molecule CTAs, the generally low yields reported in Table B.2 are likely due to incomplete incorporation of COT. This observation is further supported by the ^1H NMR spectra of the block copolymers (*vide infra*).

B.3.2.1 Characterization of Block Copolymers

Characterization of the block copolymers by UV-vis spectroscopy provided the clearest evidence for the presence of extended PA blocks. Figure B.8 shows the UV spectra for three types of block copolymers—PS-*b*-PA, PMMA-*b*-PA, and PEG-*b*-PA. For comparison, the absorption spectra of the homopolymers (i.e., the olefin-terminated polymer) are also shown. The absorbance bands previously seen for polyenes containing 10–15 double bonds²⁰ were observed in block copolymers made from small amounts of COT (e.g., sample **9a**). These details are lost, however, when larger amounts of COT are used. The smooth spectra that result indicate the presence of a wide range of conjugation lengths. In addition, as the proportion of COT is increased, the absorption region corresponding to the PA block shifts to longer wavelengths, while the absorption due to the nonconjugated block remains unchanged. These data indicate that increasing the amount of COT in the reaction produces PA blocks with longer conjugation lengths.

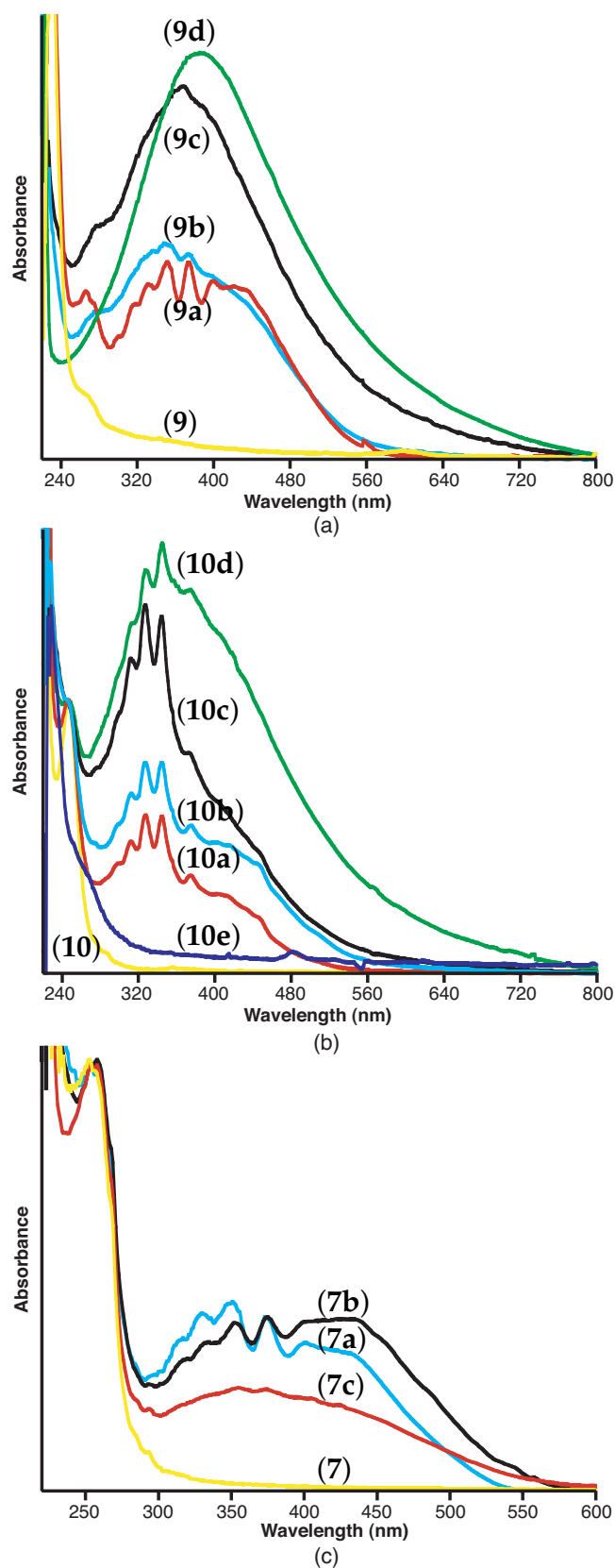


Figure B.8: UV-vis spectra of PA-containing block copolymers in CH_2Cl_2 solution. (a) PMMA (9), PMMA-*b*-PA (9a-d). (b) PEG (10), PEG-*b*-PA (10a-d), bis(hydroxy)-terminated PEG reaction product (10e). (c) PS (7), PS-*b*-PA (7a-c).

To show that PA is covalently attached to the olefin terminated polymers in these reactions, the ROMP of COT was carried out in the presence of a bis(hydroxy)-terminated PEG. A significant amount of insoluble, black solid formed during the reaction. This solid was removed by filtration, and the remaining polymer product (white) was isolated by precipitation. The UV-vis spectrum of the resulting polymer is shown in Figure B.8b (sample 10e). The lack of absorbance above 320 nm indicates that no PA was present in the product.

Characteristic IR absorption bands of polyCOT produced with catalyst 2 include 1010, 992, 930, 773, and 745 cm^{-1} .¹² Unfortunately, absorption from the nonconjugated polymer segments often obscured these absorption bands in the PA block copolymers. For PMMA-*b*-PA, however, absorption of the PA segment at 1012 cm^{-1} is clearly visible and overlays with the absorption spectra of the olefin-terminated homopolymer (see Figure B.9).

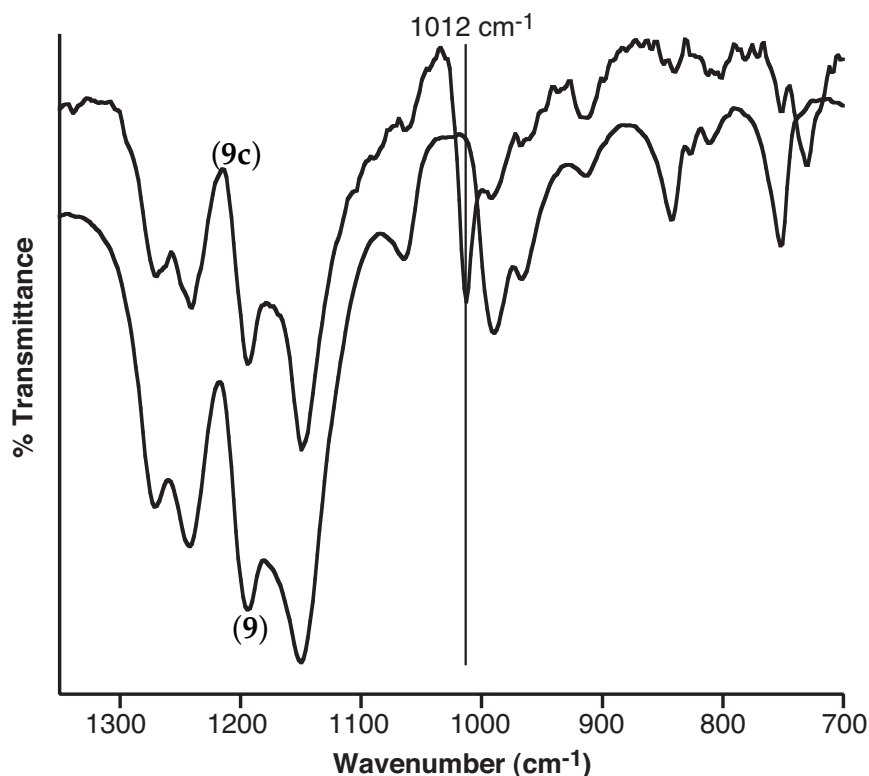


Figure B.9: FT-IR spectra of 9 and 9c.

For samples of PMMA-*b*-PA and PEG-*b*-PA, it was possible to observe characteristic peaks in the polyene region of the ^1H NMR spectra that appeared very similar to the peaks shown in Figure B.3.[‡] In general, integration of the polyene region indicated far smaller PA blocks than would be expected from the ratio of COT to olefin-terminated polymer. For example, integration for sample **9b** showed an average of four or fewer ($-\text{C}=\text{C}-$) units per polymer chain, whereas 20 ($-\text{C}=\text{C}-$) units would be expected from the initial reactant ratio. As discussed previously, this low incorporation can be attributed to two likely sources: the ROMP of COT does not reach completion, and/or benzene formed from backbiting leads to an effective loss of monomer. In all NMR spectra, however, a significant amount of unreacted olefin endgroups remained visible after block copolymer formation, indicating that some polymer chains have no attached PA blocks. This observation makes it very difficult to speculate on the average conjugation length of the PA blocks.

Along with the trends observed in UV-vis spectra, AFM afforded a method for observing changes in the relative sizes of conjugated segments between samples. Phase separation in PA-containing block copolymers has been observed previously.^{19, 40–42} Tapping Mode (TM) AFM images of PS-*b*-PA films show a phase separated morphology consisting of isolated domains against a uniform background. These domains, which were absent in films formed from the olefin-terminated homopolymer, were randomly distributed in space, but fairly regular in size and shape. Furthermore, the sizes of the domains exhibited a dependency on the relative proportions of COT and olefin-terminated polymer used in the preparation of the block copolymers. Figure B.10 shows TM AFM height images of films made by spin coating 0.4 wt% toluene solutions of **8a** and **8b**. Clearly, the domains (appearing as white spots) are larger for **8b** which contains a greater percentage of conjugated material, implying that the white spots in Figure B.10 represent PA domains. As shown by the side views of these images (Figure B.10b

[‡]Observance of these peaks was impossible for PS-*b*-PA samples due to the intense resonances from the phenyl protons of polystyrene.

and d), the domains appear to be directed perpendicular to the film surface. These domains are highly stable: annealing the polymer films under vacuum at 130 °C for 24+ hours only reduced their height and spatial density. Furthermore, the domains could also be observed using contact mode.[§] We believe that these images, the UV spectra of the two copolymers, and the fact that the solution of **8b** was darker in color than that of **8a** are evidence for a variation in the conjugation length of the PA blocks that relates to the relative amount of COT used in the polymerizations. It should be reiterated, however, that these polymers remained completely soluble in common organic solvents.

[§]This morphology is possibly a result of the fast evaporation of solvent that occurs when the films are made. With films that were formed by slowly evaporating the solvent (i.e., not spin coating), the spiked morphology was not observed. Rather, a highly disordered morphology with large, randomly placed crystal-like structures was seen.

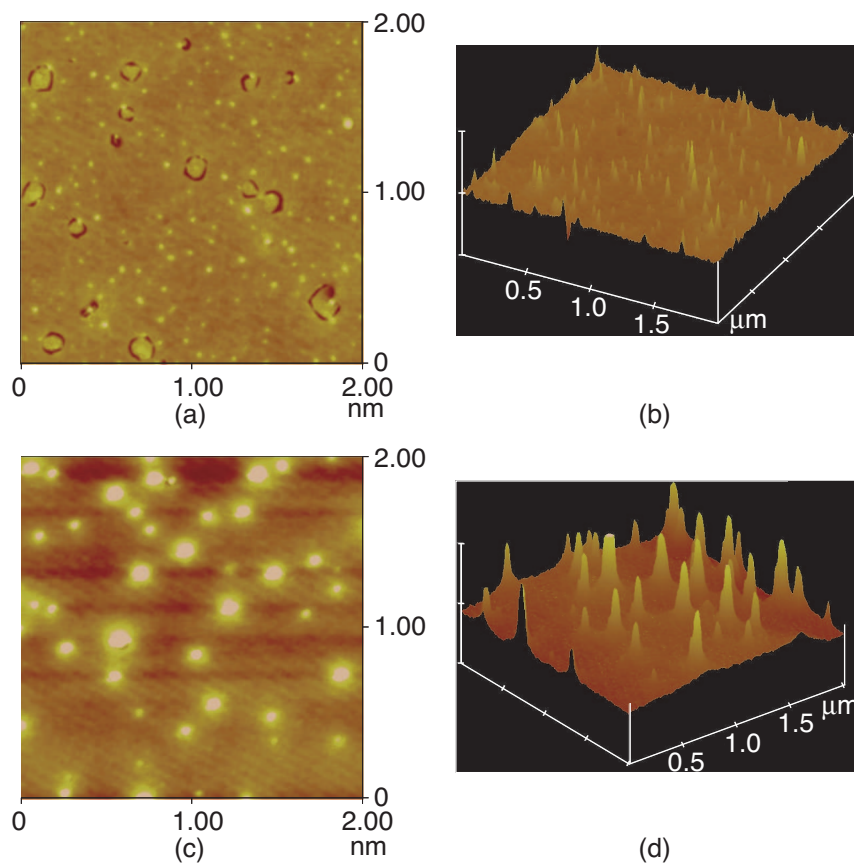


Figure B.10: TM AFM height images. (a, b) Sample **8a**, produced from **8** and 200 equivalents of COT. (c, d) Sample **8b**, produced from **8** and 1000 equivalents of COT. In (a), (b), and (c) the same height scale applies (0–15 nm), while in (d) the height scale is 0–20 nm.

B.4 Conclusions

The synthesis of telechelic polyenes via the direct ROMP of COT in the presence of a CTA with catalyst **2** has been demonstrated. The telechelic polyenes remained completely soluble in common organic solvents and were characterized in detail using solution and solid-state spectroscopic methods. Furthermore, PA block copolymers were synthesized in one step from olefin-functionalized commodity polymers. As a consequence of their solubility, all of these block copolymers were amenable to spin coating and subsequent AFM investigation. We hope that

the tunability and improved processability of these materials may soon lead to their commercialization; investigations of their electronic properties are currently underway.

B.5 Experimental Section

General Procedures. NMR spectra were recorded on a Varian Mercury 300 (300 MHz for ^1H and 75 MHz for ^{13}C). All NMR spectra were recorded in CD_2Cl_2 or CDCl_3 and referenced to residual proteo species. Gel permeation chromatography (GPC) was carried out on three AM GPC Gel columns, 15 μm pore size, (American Polymer Standards Corp.) connected in series with a Type 188 differential refractometer (Knauer). Molecular weights were calculated relative to polystyrene standards. MALDI-TOF mass spectra were recorded using an Applied Biosystems (ABI) Voyager DE-PRO time-of-flight mass spectrometer. A 20 Hz nitrogen laser (337 nm, 3 ns pulse width) was used to desorb the sample ions that were prepared in a dithranol matrix. Mass spectra were recorded in linear (or reflector) delayed extraction mode with an accelerating voltage of 20 kV and a delay time of 100 ns. The low mass cut-off gate was set to 500 Da to prevent the lower mass matrix ions from saturating the detector. Calibration was external using a peptide mixture provided by the instrument manufacturer covering the mass range of interest. Raw spectra were acquired with an internal 2 GHz ACQIRIS digitizer and treated with Data Explorer software provided by ABI. Tapping Mode atomic force microscopy images were obtained in air using a Nanoscope IIIa AFM (Digital Instruments, Santa Barbara, CA) with silicon cantilever probes (Veeco Metrology, Santa Barbara, CA). To improve image quality, height and amplitude images were flattened using commercial software (also from Digital Instruments). AFM samples were prepared using dilute solutions of polymer (either 0.4 or 1 wt/wt %) in either toluene or CH_2Cl_2 . A 35 μL aliquot of the solution was spin coated onto freshly cleaved mica substrates (1 cm^2) at 3000 rpm. FT-IR Spectra (KBr pellet) were recorded on a Perkin-Elmer Paragon 1000 or on a Bio-Rad Excalibur FTS 3000 spectrometer

controlled by Win-IR Pro software. UV-Vis spectra were obtained on a Beckman DU 640 Spectrophotometer in either THF or CH₂Cl₂.

Materials. Toluene and CH₂Cl₂ were dried by passage through solvent purification columns.⁴³ 1,3,5,7-Cyclooctatetraene (COT) (**3**) (generously donated by BASF) was dried over CaH₂ and distilled prior to use. Cis-1,4-diacetoxy-2-butene (96%) (**5b**) (Aldrich) was dried over CaH₂ and distilled prior to use. Cis-2-butene-1,4-diol (95%) (**5d**) (Aldrich) was distilled prior to use. Cis-Cyclooctene (Aldrich) was degassed by freeze/pump/thaw cycles before use. Vinyl-terminated PS (**11**) ($M_n = 1900$, $M_w/M_n = 1.11$), and vinyl terminated PEG (**10**) ($M_n = 1120$, $M_w/M_n = 1.17$) were purchased from Polymer Source, Inc. (PCy₃)₂(Cl)₂Ru=CHPh (**1**)⁴⁴ and (IMesH₂)(PCy₃)(Cl)₂Ru=CHPh (**2**)⁴⁵ [Mes = 2,4,6-trimethylbenzene] as well as CTAs **5a**⁴⁶ and **5c**⁴⁷ were synthesized according to literature procedure. All other materials were used as received.

Procedure for the ROMP of COT (3**) with CTA **5a** (in solution).** A stir bar was placed in an oven-dried small vial with a teflon screw cap. Under an argon atmosphere, 0.5 mL (4.44 mmol) of COT and 1.6 mL (4.34 mmol) of CTA **5a** were added by syringe. Subsequently 1.0 mL (8.84×10^{-3} mmol) of a 7.5 mg/mL solution of **2** in CH₂Cl₂ was added by syringe. The vial was placed in a 55 °C oil bath. The yellow solution turned dark orange within 5 min. After 24 h, the reaction vial was removed from the heating bath and the solution was precipitated into 100 mL of stirring MeOH and filtered through a Büchner funnel to yield a red solid. The solid was dried under reduced pressure, yielding 91 mg of polymer (20%). Alternatively, the precipitate in MeOH solution was placed in centrifuge tubes and a number of centrifuge-decant-wash with MeOH cycles were performed until the decanted liquid was colorless. The red solid was then dissolved in CH₂Cl₂, transferred to an amber vial, and the solvent was removed under reduced pressure.

Procedure for the ROMP of COT with CTA **5a (neat).** An oven-dried small vial with a teflon screw cap was charged with a stirbar and 7.3 mg (8.61×10^{-3} mmol) of catalyst **2**. Under an argon atmosphere, 0.5 mL (4.44 mmol) of COT and 0.55 mL (1.49 mmol) of the CTA **5a** were added by syringe. The vial was placed in an

aluminum heating block set to 55 °C. The yellow solution immediately turned dark reddish-orange. After 24 h, the solution was removed from the heating block and dissolved in CH₂Cl₂. The solution was precipitated into 100 mL of stirring MeOH and filtered through a Büchner funnel to yield a purple solid. The solid was then dried under reduced pressure, yielding 124 mg of polymer (27%).

Synthesis of vinyl-terminated polystyrene (7). To a small round bottom flask containing a stirbar was added 0.365 g (4.62 mmol) 2,2'-dipyridyl, 0.299 g (4.70 mmol) copper powder, 0.114 g (0.511 mmol) CuBr₂, 0.4 mL (4.62 mmol) allyl bromide, and 3.0 mL (44.6 mmol) styrene. The flask was sealed with a rubber septum, purged with argon for 5 min, and heated to 110 °C. After 15 min, the reaction mixture turned bright green. The reaction was terminated after 24 h by cooling down to room temperature, dissolving the mixture in THF, and precipitating in MeOH. The resulting solid was isolated by filtration, dissolved in THF, and passed through a plug of alumina before reprecipitating in MeOH. The isolated white product was dried in vacuo.

Synthesis of vinyl-terminated polystyrene (8). As for 7, but with 5-bromo-1-pentene as initiator.

Synthesis of vinyl-terminated polymethylmethacrylate (9). As for 7. To maintain lower reaction viscosity, however, an amount of diphenylether equivalent to the amount of methyl methacrylate monomer (by mass) was added.

Synthesis of PA block copolymers. In a typical procedure, the olefin terminated polymer chain transfer agent was added to a small vial containing a stirbar. The vial was purged with argon for 10–15 min, toluene was added, and the mixture was stirred to completely dissolve the polymer. COT was then added, followed by the appropriate amount of a stock solution of catalyst in toluene. The solution was heated up to 55 °C and left stirring under an argon atmosphere for 24 h. The reaction mixture was cooled down to room temperature and precipitated in a nonsolvent such as MeOH or hexane. The resulting solid was isolated by filtration, dried under reduced pressure, and stored in an amber vial under an atmosphere of argon.

B.6 Acknowledgements

MALDI-TOF analysis was carried out in a multi-user MS lab funded in part by the MRSEC. The authors thank Dr. Mona Shahgholi for assistance with MALDI analysis of the polyenes, and Dr. Brian Connell, Dr. Stuart J. Cantrill, and Daniel P. Sanders for critical reading of this manuscript. O.A.S. thanks the National Science Foundation for a graduate fellowship.

References Cited

- [1] Shirakawa, H. *Angew. Chem. Int. Ed.*, **2001**, *40*, 2575–2580.
- [2] MacDiarmid, A. G. *Angew. Chem. Int. Ed.*, **2001**, *40*, 2581–2590.
- [3] Heeger, A. J. *Angew. Chem. Int. Ed.*, **2001**, *40*, 2591–2611.
- [4] Shirakawa, H. *Synth. Met.*, **2001**, *125*, 3–10.
- [5] Berets, D. J.; Smith, D. S. *Trans. Faraday Soc.*, **1968**, *64*, 823–828.
- [6] Shirakawa, H.; Ikeda, S. *Polym. J.*, **1971**, *2*, 231.
- [7] Edwards, J. H.; Feast, W. J. *Polymer*, **1980**, *21*, 595–596.
- [8] Swager, T. M.; Dougherty, D. A.; Grubbs, R. H. *J. Am. Chem. Soc.*, **1988**, *110*, 2973–2974.
- [9] Korshak, Y. V.; Korshak, V. V.; Kanischka, G.; Hocker, H. *Makromol. Chem., Rapid Commun.*, **1985**, *6*, 685–692.
- [10] Klavetter, F. L.; Grubbs, R. H. *Synth. Met.*, **1989**, *28*, D99–D104.
- [11] Klavetter, F. L.; Grubbs, R. H. *J. Am. Chem. Soc.*, **1988**, *110*, 7807–7813.
- [12] Scherman, O. A.; Grubbs, R. H. *Synth. Met.*, **2001**, *124*, 431–434.
- [13] Wang, X. H.; Li, J.; Zhang, J. Y.; Sun, Z. C.; Yu, L.; Jing, X. B.; Wang, F. S.; Sun, Z. X.; Ye, Z. J. *Synth. Met.*, **1999**, *102*, 1377–1380.
- [14] Lessner, P.; Su, T.; Melody, B.; Kinard, J.; Rajasekaran, V. Solid electrolytic capacitor having conductive polymer counter electrode, US Patent 6391379, 2000.
- [15] Voss, K. F.; Foster, C. M.; Smilowitz, L.; Mihailovic, D.; Askari, S.; Srdanov, G.; Ni, Z.; Shi, S.; Heeger, A. J.; Wudl, F. *Phys. Rev. B*, **1991**, *43*, 5109–5118.
- [16] Wagaman, M. W.; Grubbs, R. H. *Macromolecules*, **1997**, *30*, 3978–3985.
- [17] Elsenbaumer, R. L.; Jen, K. Y.; Miller, G. G.; Shacklette, L. W. *Synth. Met.*, **1987**, *18*, 277–282.
- [18] Leung, Louis M.; Tan, K. H.; Lam, T. S.; He, WeiDong. *React. Funct. Polym.*, **2002**, *50*, 173–179.
- [19] Stelzer, F.; Grubbs, R. H.; Leising, G. *Polymer*, **1991**, *32*, 1851–1856.
- [20] Knoll, K.; Schrock, R. R. *J. Am. Chem. Soc.*, **1989**, *111*, 7989–8004.
- [21] Dounis, Panagiotis; Feast, W. James; Widawski, Gilles. *J. Mol. Catal. A: Chem.*, **1997**, *115*, 51–60.
- [22] Rychnovsky, S. D. *Chem. Rev.*, **1995**, *95*, 2021–2040.
- [23] Jerome, R.; Henrioulleganville, M.; Boutevin, B.; Robin, J. J. *Prog. Polym. Sci.*, **1991**, *16*, 837–906.
- [24] Cacialli, F.; Daik, R.; Dounis, P.; Feast, W. J.; Friend, R. H.; Haylett, N. D.; Jarrett, C. P.; Schoenenberger, C.; Stephens, J. A.; Widawski, G. *Philos. Trans.*

- R. Soc. Lond. Ser. A: Math. Phys. Eng. Sci.*, **1997**, *355*, 707–713.
- [25] Schrock, R. R.; Krouse, S. A.; Knoll, K.; Feldman, J.; Murdzek, J. S.; Yang, D. C. *J. Mol. Catal.*, **1988**, *46*, 243–253.
- [26] Schleyer, P. v. R.; Williams, J. E.; Blanchard, K.R. *J. Am. Chem. Soc.*, **1970**, *92*, 2377–2386.
- [27] Bielawski, C. W.; Scherman, O. A.; Grubbs, R. H. *Polymer*, **2001**, *42*, 4939–4945.
- [28] Bielawski, C. W.; Benitez, D.; Morita, T.; Grubbs, R. H. *Macromolecules*, **2001**, *34*, 8610–8618.
- [29] Sanford, M. S.; Love, J. A.; Grubbs, R. H. *J. Am. Chem. Soc.*, **2001**, *123*, 6543–6554.
- [30] Scherman, O. A.; Kim, H. M.; Grubbs, R. H. *Macromolecules*, **2002**, *35*, 5366–5371.
- [31] Shibahara, S.; Yamane, M.; Ishikawa, K.; Takezoe, H. *Macromolecules*, **1998**, *31*, 3756–3758.
- [32] Shiono, T.; Kang, K. K.; Hagihara, H.; Ikeda, T. *Macromolecules*, **1997**, *30*, 5997–6000.
- [33] Nakagawa, Y.; Matyjaszewski, K. *Polym. J.*, **1998**, *30*, 138–141.
- [34] Manring, L. E. *Macromolecules*, **1989**, *22*, 2673–2677.
- [35] Kurosawa, H.; Shiono, T.; Soga, K. *Macromol. Chem. Phys.*, **1994**, *195*, 1381–1388.
- [36] Matyjaszewski, K.; Coca, S.; Gaynor, S. G.; Wei, M. L.; Woodworth, B. E. *Macromolecules*, **1998**, *31*, 5967–5969.
- [37] Bednarek, M.; Biedron, T.; Kubisa, P. *Macromol. Chem. Phys.*, **2000**, *201*, 58–66.
- [38] Bednarek, M.; Biedron, T.; Kubisa, P. *Macromol. Rapid Commun.*, **1999**, *20*, 59–65.
- [39] Simal, F.; Demonceau, A.; Noels, A. F. *Angew. Chem. Int. Ed.*, **1999**, *38*, 538–540.
- [40] Aime, J. P.; Reibel, D.; Mathis, C. *Synth. Met.*, **1993**, *55*, 127–134.
- [41] Dai, L. M. *Synth. Met.*, **1997**, *84*, 957–960.
- [42] Stelzer, F.; Fischer, W.; Leising, G.; Heller, Ch. *Springer Ser. Solid-State Sci.*, **1992**, *107*(*Electron. Prop. Polym.*), 231–237.
- [43] Pangborn, A. B.; Giardello, M. A.; Grubbs, R. H.; Rosen, R. K.; Timmers, F. J. *Organometallics*, **1996**, *15*, 1518–1520.
- [44] Schwab, P.; Grubbs, R. H.; Ziller, J. W. *J. Am. Chem. Soc.*, **1996**, *118*, 100–110.
- [45] Sanford, M. S.; Ullman, M.; Grubbs, R. H. *J. Am. Chem. Soc.*, **2001**, *123*, 749–750.
- [46] Corey, E. J.; Venkates, A. *J. Am. Chem. Soc.*, **1972**, *94*, 6190–6191.
- [47] Asgarzadeh, F.; Ourdouillie, P.; Beyou, E.; Chaumont, P. *Macromolecules*, **1999**, *32*, 6996–7002.

Appendix C

Synthesis of Polymer Dielectric Layers for Organic Thin-Film Transistors via Surface-Initiated Ring-Opening Metathesis Polymerization

This has previously appeared as: Rutenberg, I. M.; Scherman, O.A.; Grubbs, R. H.; Jiang, W.; Garfunkel, E.; Bao, Z. *Journal of the American Chemical Society*, **2004**, *126*, 4062–4063.

C.1 Abstract

Polymer-based dielectric layers for use in electronic devices such as thin-film transistors (TFTs), capacitors, and other logic elements have attracted much attention for their low cost, processability, and tunable properties. Current methods for incorporating organic materials into these devices are either not ideal or not possible when applied to the deposition of polymer dielectric materials. The living ring-opening metathesis polymerization (ROMP) of strained, cyclic olefins can provide a method for growing organic polymers from a surface. ROMP would allow for pinhole-free dielectrics with controlled layer thickness and tunable electronic and surface properties by growing a covalently attached polymer from the surface. Furthermore, ROMP from surfaces is unique in its ability to polymerize monomers from either solution or vapor phase and can be performed under mild ambient conditions, afford polymer growth in minutes, and allow for flexibility in polymer structure and dielectric layer composition. We have shown the feasibility of producing TFTs and capacitors using surface attached ROMP polymers as a layer of dielectric material. Preliminary results indicate that this method will allow for highly tunable materials with desired properties. The ability to grow conformal polymer layers on any topology will be very important as device dimensions and applications change.

C.2 Introduction

The use of organic materials in electronic devices such as field effect transistors (FETs) and light emitting diodes (LEDs) has become an attractive approach toward decreasing weight and cost, simplifying production, and increasing versatility of these devices. Electronic devices containing polymer layers have been incorporated into applications such as active-matrix displays¹⁻³ and integrated circuits.^{4,5}

For optimal FET performance, a polymer dielectric layer should be chemically and electrically compatible, with the organic semiconductor facilitating a smooth

interface between adjacent layers.* Low leakage and tunable dielectric properties are also desirable. This requires that the layer be pinhole-free, with controlled thickness and composition.

Current methods for depositing polymer layers include spin-coating, ink-jet printing, and screen printing.⁷⁻⁹ Unlike these methods, surface-initiated polymerizations can produce densely packed, conformal layers over any surface topology. Compared with other surface-initiated polymerization methods, ring-opening metathesis polymerization (ROMP) allows mild conditions and short reaction times. Therefore, we have chosen to investigate surface-initiated ROMP (SI-ROMP) as a method for forming polymer dielectric layers.

SI-ROMP has been demonstrated from Au, Si, and Si/SiO₂ surfaces using catalyst **1** and a variety of linking molecules.¹⁰⁻¹² Conformal block copolymers grown on Au nanoparticles demonstrated the living nature of SI-ROMP with catalyst **1**.¹³ We report here that SI-ROMP polymer layers can be used as the dielectric layer in electronic devices, either alone or in tandem with an inorganic dielectric layer. We also report that, as with solution-phase ROMP,¹⁴ catalyst **2** is more active than catalyst **1** in SI-ROMP (Figure C.1).

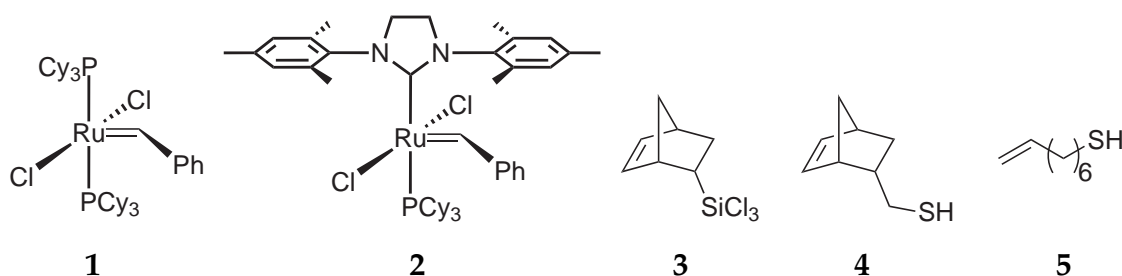


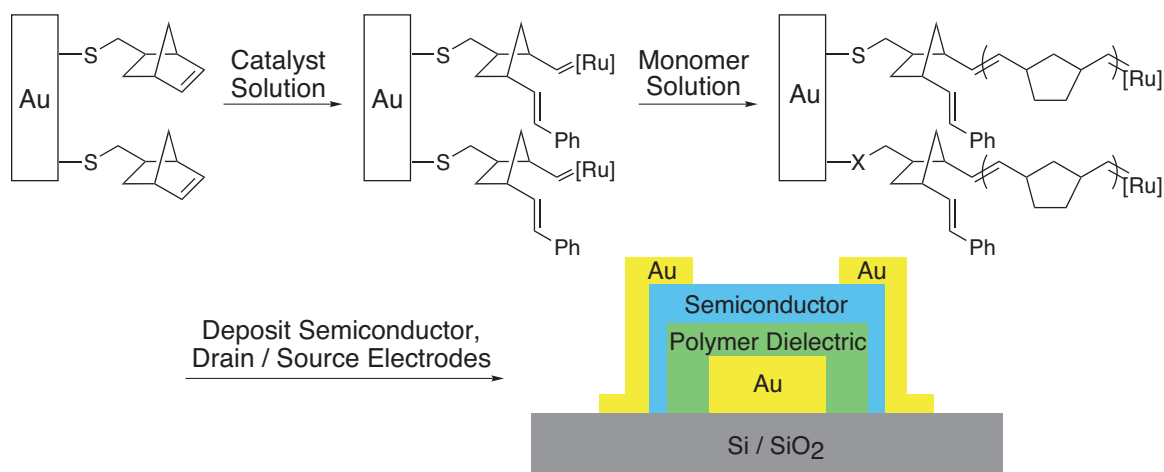
Figure C.1: Catalysts and linking molecules employed in SI-ROMP.

Polymer dielectric layers covalently attached to Au or Si/SiO₂ surfaces were formed via ROMP from surface-tethered metathesis catalysts (Scheme C.1). Exposure of a self-assembled monolayer (SAM) of a linking molecule (**3**, **4** or **5**)[†]

*Performance as measured by mobility and on/off ratio – see Katz and Bao.⁶

[†]In general, films produced with linker **4** were thicker than those produced with linker **5**. Catalyst attachment is likely more efficient with **4**; the reasons for this are currently under investigation.

Scheme C.1: Construction of an FET using a SI-ROMP polymer dielectric layer (**4** shown as example linker).



(Figure C.1) to a solution of catalyst (**1** or **2**), followed by subsequent exposure to a solution of monomer, generated the polymer film. Between each of these steps, the surfaces were extensively rinsed with solvent to remove chemically unbound material.

Many variables were found to significantly affect the thickness and uniformity of SI-ROMP polymer films. Most importantly, catalyst **2** is far more active than catalyst **1**. Given identical reaction conditions, films produced from catalyst **2** are up to 10 times thicker than those produced from catalyst **1**. For example, using **4** as the linker, films produced after 15 min of exposure to a 3 M solution of norbornene at room temperature (rt) are nearly 2.5 μm in thickness using catalyst **2**, versus 250 nm with catalyst **1**. Furthermore, catalyst **2** produces polymer films greater than 300 nm thick from 1 M monomer solutions, whereas catalyst **1** requires concentrations in excess of 3 M to produce equivalent films.

Polymerization conditions were also found to affect SI-ROMP films. Decreased thicknesses result for polymerizations conducted above rt, or for prolonged periods of time (> 1 h). Almost no film remains after 24 h of polymerization time, suggesting that, as in solution-phase ROMP, secondary metathesis (chain transfer) reactions are occurring between growing chains. Slower than ROMP, and

promoted by elevated temperature,¹⁵ secondary metathesis in SI-ROMP would lead to chain termination and generation of polymer fragments that are no longer covalently attached to the substrate.

Smooth, pinhole-free dielectric films are important, since the overlaying semiconductor layer of an FET must continuously bridge the source and drain contacts.¹⁶ Electrical shorting between the gate and drain and/or source electrodes was observed due to pinholes present in untreated SI-ROMP polynorbornene films. Annealing at 135 °C for 15 min densifies the films and significantly reduces the number of pinholes, resulting in relatively smooth, unshorted films.

Construction of FETs (as shown in Scheme C.1) was demonstrated using the lamination method.¹⁷ A SI-ROMP polymer dielectric layer was grown on a Au strip gate electrode (1000 Å thick, 1 mm wide) using linker **4**, catalyst **2**, and a 3 M norbornene solution. The thickness of the resulting polynorbornene film was 1.2 μm with a capacitance of 3 nF cm⁻² measured at 20 Hz. After annealing, a 400 Å layer of pentacene was vapor deposited over the polymer dielectric. This was pressed against a separate PDMS substrate containing parallel Au strips as drain and source electrodes spaced 240 μm apart. A representative current-voltage (I/V) diagram for the resulting FETs is shown in Figure C.2. Ranges for mobility and on/off ratio were 0.1–0.3 cm² V⁻¹ s⁻¹ and 10–100, respectively.⁶ Little to no hysteresis was observed for these devices (see inset of Figure C.2), indicating minimal charge buildup between the dielectric and semiconducting layers.

In addition to the lamination method, direct deposition of Au drain/source electrodes over the pentacene semiconducting layer also produced functioning FETs. Example I/V characteristics for these devices are shown in Figure C.3. As seen in previous studies, mobilities and on/off ratios (up to 10⁻² cm² V⁻¹ s⁻¹ and 100, respectively) were lower than those for the laminated devices due to partial degradation of the pentacene layer by the metal deposition.¹⁷ The capacitance of the SI-ROMP dielectric films for these devices was found to have no significant frequency dependence down to 20 Hz (see inset of Figure C.3).

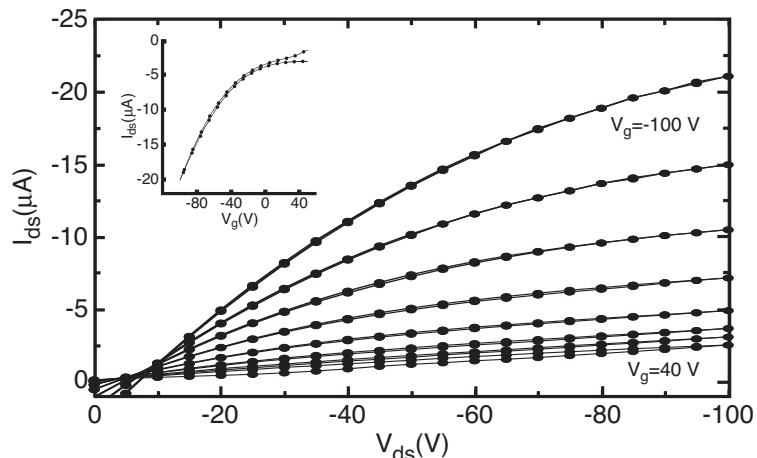


Figure C.2: Current-voltage characteristics of an FET produced by lamination, containing a SI-ROMP polynorbornene dielectric layer. The drain bias was swept from 0 to -100 V and back at gate biases between 40 and -100 V in 20 V steps. Inset shows drain current as gate voltage was swept from 40 to -100 V and back.

Finally, FETs were constructed using a SI-ROMP polymer dielectric layer covalently bound to a Si/SiO₂ (either native or thermally grown oxide) surface. Working devices were constructed using either catalyst (**1** or **2**), linker **3**, and 2 M norbornene solutions.

Apart from washing extensively with solvent, no effort was made to remove residual (covalently bound or imbedded) catalyst from the polymer films. Rutherford backscattering spectroscopy (RBS) and medium energy ion scattering (MEIS) measurements, however, indicated exceptionally low surface concentrations of Ru for catalyst-functionalized SAMs as well as the washed films. Increasing the concentration of ruthenium bonded to the SAM may result in denser films and less leakage.

These devices demonstrate that surface-initiated polymer dielectric layers are both chemically and electrically compatible with other FET component layers. In general, a high yield (> 90%) of working TFTs was obtained only with annealed dielectric films at least 1 μm thick. Further optimization of polymer growth conditions, yielding higher graft densities and reduced surface roughness, should

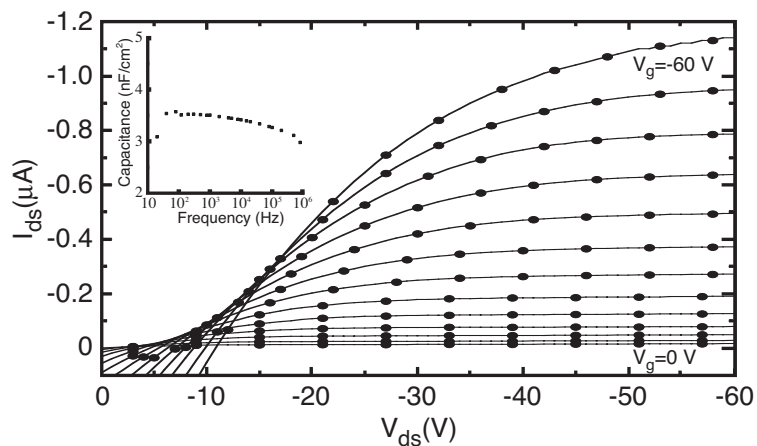


Figure C.3: Current-voltage characteristics of an FET produced by direct deposition of the semiconductor layer and Au drain/source electrodes over a SI-ROMP polynorborene dielectric layer grown from a Au gate electrode. The drain bias was swept from 0 to -60 V at gate biases between 0 and -60 V in 5 V steps. Inset shows capacitance of a polynorborene capacitor as a function of frequency. The leakage current is due to the unpatterned gate and organic semiconducting layers.

allow the use of thinner films as well as improve the compatibility between the polymer film and organic semiconductor.[‡]

For devices using patterned (e.g., striped Au) substrates, the SI-ROMP polymer grows conformally over the gate electrode, eliminating the need to pattern the dielectric. Furthermore, spin-coated dielectric layers tend to be thinner at the edges of the electrode, leading to a lower breakdown voltage. In contrast, the thickness of the surface-grown polymer layer can be about the same at the edges as for the flat surface, illustrating a clear advantage of SI-ROMP.

In conclusion, construction of FETs using SI-ROMP polymer dielectric layers has been demonstrated. Mild reaction conditions, short reaction times, and simple solution processing methods make SI-ROMP an attractive method for constructing polymer dielectric layers. Layer thicknesses ranging from below 100 nm to above 2 μm are accessible simply by varying the polymerization conditions. Research is underway in optimizing FET device characteristics, as well as incorporating SI-ROMP block copolymers into organic-based FETs.

[‡]Increased grain-size was observed when pentacene was deposited over SI-ROMP polymer layers that had been annealed.

C.3 Acknowledgements

The authors thank the National Science Foundation, Office of Naval Research, NJCOOE, and Lucent Technologies for financial support, and Dr. Brian Connell and Daniel P. Sanders for advice on this manuscript.

References Cited

- [1] Rogers, J. A.; Bao, Z. *J. Polym. Sci. Pol. Chem.*, **2002**, *40*, 3327–3334.
- [2] Sheraw, C. D.; Zhou, L.; Huang, J. R.; Gundlach, D. J.; Jackson, T. N.; Kane, M. G.; Hill, I. G.; Hammond, M. S.; Campi, J.; Greening, B. K.; Francl, J.; West, J. *Appl. Phys. Lett.*, **2002**, *80*, 1088–1090.
- [3] Huitema, H. E. A.; Gelinck, G. H.; van der Putten, Jbph; Kuijk, K. E.; Hart, C. M.; Cantatore, E.; Herwig, P. T.; van Breemen, Ajjm; de Leeuw, D. M. *Nature*, **2001**, *414*, 599–599.
- [4] Gelinck, G. H.; Geuns, T. C. T.; de Leeuw, D. M. *Appl. Phys. Lett.*, **2000**, *77*, 1487–1489.
- [5] Crone, B. K.; Dodabalapur, A.; Sarpeshkar, R.; Filas, R. W.; Lin, Y. Y.; Bao, Z.; O'Neill, J. H.; Li, W.; Katz, H. E. *J. Appl. Phys.*, **2001**, *89*, 5125–5132.
- [6] Katz, H. E.; Bao, Z. *J. Phys. Chem. B*, **2000**, *104*, 671–678.
- [7] Halik, M.; Klauk, H.; Zschieschang, U.; Schmid, G.; Radlik, W.; Weber, W. *Adv. Mater.*, **2002**, *14*, 1717–1722.
- [8] Bao, Z. N.; Feng, Y.; Dodabalapur, A.; Raju, V. R.; Lovinger, A. J. *Chem. Mat.*, **1997**, *9*, 1299–1301.
- [9] Kawase, T.; Sirringhaus, H.; Friend, R. H.; Shimoda, T. *Adv. Mater.*, **2001**, *13*, 1601–1605.
- [10] Weck, M.; Jackiw, J. J.; Rossi, R. R.; Weiss, P. S.; Grubbs, R. H. *J. Am. Chem. Soc.*, **1999**, *121*, 4088–4089.
- [11] Juang, A.; Scherman, O. A.; Grubbs, R. H.; Lewis, N. S. *Langmuir*, **2001**, *17*, 1321–1323.
- [12] Kim, N. Y.; Jeon, N. L.; Choi, I. S.; Takami, S.; Harada, Y.; Finnie, K. R.; Girolami, G. S.; Nuzzo, R. G.; Whitesides, G. M.; Laibinis, P. E. *Macromolecules*, **2000**, *33*, 2793–2795.
- [13] Watson, K. J.; Zhu, J.; Nguyen, S. T.; Mirkin, C. A. *J. Am. Chem. Soc.*, **1999**, *121*, 462–463.
- [14] Bielawski, C. W.; Grubbs, R. H. *Angew. Chem.-Int. Edit.*, **2000**, *39*, 2903–2906.
- [15] Choi, T. L.; Grubbs, R. H. *Angew. Chem.-Int. Edit.*, **2003**, *42*, 1743–1746.
- [16] Bao, Z. N.; Rogers, J. A.; Katz, H. E. *J. Mater. Chem.*, **1999**, *9*, 1895–1904.
- [17] Loo, Y. L.; Someya, T.; Baldwin, K. W.; Bao, Z. N.; Ho, P.; Dodabalapur, A.; Katz, H. E.; Rogers, J. A. *Proc. Natl. Acad. Sci. U. S. A.*, **2002**, *99*, 10252–10256.